Thrombomodulin ameliorates transforming growth factor-β1–mediated chronic kidney disease via the G-protein coupled receptor 15/Akt signal pathway

OPEN

Atsuro Takeshita[1,2,8], Taro Yasuma[1,2,8], Kota Nishihama[1], Corina N. D'Alessandro-Gabazza[2], Masaaki Toda[2], Toshiaki Totoki[4], Yuko Okano[1,2], Akihiro Uchida[1], Ryo Inoue[6], Liqiang Qin[7], Shujie Wang[5], Valeria Fridman D'Alessandro[2], Tetsu Kobayashi[3], Yoshiyuki Takei[4], Akira Mizoguchi[5], Yutaka Yano[1,9] and Esteban C. Gabazza[2,9]

[1]*Department of Diabetes, Metabolism, and Endocrinology, Mie University Graduate School of Medicine, Tsu-city, Mie, Japan;* [2]*Department of Immunology, Mie University Graduate School of Medicine, Tsu-city, Mie, Japan;* [3]*Department of Pulmonary and Critical Care Medicine, Mie University Graduate School of Medicine, Tsu-city, Mie, Japan;* [4]*Department of Gastroenterology and Hepatology, Mie University Graduate School of Medicine, Tsu-city, Mie, Japan;* [5]*Department of Neural Regeneration and Cell Communication, Mie University Graduate School of Medicine, Tsu-city, Mie, Japan;* [6]*Central Institute for Experimental Animals, Kawasaki-ku, Kawasaki, Japan; and* [7]*Department of Nephrology, Taizhou Hospital, Wenzhou Medical University, Lihai, Zhejiang Province, People's Republic of China*

Kidney fibrosis is the common consequence of chronic kidney diseases that inexorably progresses to end-stage kidney disease with organ failure treatable only with replacement therapy. Since transforming growth factor-β1 is the main player in the pathogenesis of kidney fibrosis, we posed the hypothesis that recombinant thrombomodulin can ameliorate transforming growth factor-β1–mediated progressive kidney fibrosis and failure. To interrogate our hypothesis, we generated a novel glomerulus-specific human transforming growth factor-β1 transgenic mouse to evaluate the therapeutic effect of recombinant thrombomodulin. This transgenic mouse developed progressive glomerular sclerosis and tubulointerstitial fibrosis with kidney failure. Therapy with recombinant thrombomodulin for four weeks significantly inhibited kidney fibrosis and improved organ function compared to untreated transgenic mice. Treatment with recombinant thrombomodulin significantly inhibited apoptosis and mesenchymal differentiation of podocytes by interacting with the G-protein coupled receptor 15 to activate the Akt signaling pathway and to upregulate the expression of anti-apoptotic proteins including survivin. Thus, our study strongly suggests the potential therapeutic efficacy of recombinant thrombomodulin for the treatment of chronic kidney disease and subsequent organ failure.

Correspondence: *Esteban C. Gabazza, Department of Immunology, Mie University School of Medicine, Edobashi 2-174, Tsu-city, Mie 514-8507, Japan. E-mail: gabazza@doc.medic.mie-u.ac.jp; or Yutaka Yano, Diabetes, Metabolism and Endocrinology, Mie University Graduate School of Medicine, Edobashi 2-174, Tsu-city, Mie 514-8507, Japan. E-mail: yanoyuta@clin.medic.mie-u.ac.jp*

[8]AT and TY contributed equally to this work.

[9]YY and ECG are co-senior authors.

Received 1 September 2019; revised 24 April 2020; accepted 7 May 2020

Kidney International (2020) ■, ■–■; https://doi.org/10.1016/j.kint.2020.05.041

KEYWORDS: apoptosis; chronic kidney disease; G-protein coupled receptor; recombinant human thrombomodulin; transforming growth factor β1

Translational Statement

Fibrosis and dysfunction of the kidneys is currently a major health problem worldwide. There is currently no antifibrotic drug approved for the treatment of renal fibrosis. Transforming growth factor β1 is the main and common driver of renal fibrogenesis in chronic kidney disease caused by many disorders. We found here that recombinant thrombomodulin, a drug approved in Japan to treat disseminated intravascular coagulation, suppresses the progression of glomerular sclerosis, tubulointerstitial fibrosis, and renal failure caused by overexpression of human transforming growth factor-β1, suggesting its potential therapeutic value for the treatment of chronic kidney diseases.

Chronic renal disease is a major public health problem associated with high morbidity and mortality that affects about 13% of the adult population in developed countries.[1] The World Health Organization reported that chronic kidney disease (CKD) was the cause of 1.5% of deaths worldwide in 2012.[1] Furthermore, recent epidemiological data indicate a global steady rise in the number of patients with CKD.[2,3] In most cases, the pathological process progressively evolves, leading ultimately to end-stage kidney failure, which is treatable solely with lifelong dialysis or renal transplantation.[4,5] Diabetes mellitus (DM) and arterial hypertension are the most frequent causes of CKD followed by ischemia, glomerulosclerosis of unknown etiology, urologic

obstructions, and chronic infections.[6] Regardless of the underlying disorder, the final and common pathological consequence of CKD is fibrosis of the kidneys.[7] Renal fibrosis is the aberrant healing and remodeling of parenchymal structures of the kidneys subjected to prolonged or repetitive injury characterized by the presence of tubulointerstitial fibrosis, glomerulosclerosis, and tubular atrophy.[8] The main driver of renal fibrogenesis is transforming growth factor (TGF)-β1.[8,9] TGFβ1 may promote fibrosis by stimulating the secretion of extracellular matrix proteins and chemotactic factors or proliferating factors of fibroblasts, by inhibiting metalloproteinases, and by promoting epithelial mesenchymal transition.[10] Apart from treating the underlying disease, an approved drug that targets specifically renal fibrosis is currently unavailable.[6]

Thrombomodulin (TM) is a transmembrane glycoprotein with multiple biological functions including modulation of the clotting system, the immune response, inflammatory reactions, and cell survival.[11] The molecular structure of TM contains a lectin-like domain, 6 epidermal growth factor-like domains, a serine/threonine-rich domain, a transmembrane portion, and a cytoplasmic tail.[12] Thrombin, a procoagulant factor generated during coagulation system activation, becomes an anticoagulant and antifibrinolytic factor after binding to TM.[13] The TM-thrombin complex increases the generation of activated protein C (APC), an anticoagulant with anti-inflammatory and cytoprotective activity, by activating protein C. In addition, TM alone can directly downregulate the inflammatory response by inhibiting the activity of high-mobility group protein B-1 (HMGB1), by suppressing immunogenic dendritic cells, eosinophils, mast cells, and the complement system.[13–18]

There are published results showing preventive effects of TM in diabetic renopathy and ischemia-reperfusion renal injury.[19–21] However, no study has assessed the effect of recombinant TM on progressive kidney fibrosis induced by TGFβ1, a common driver of renal fibrosis in several diseases causing CKD. We posed the hypothesis that TM can ameliorate TGFβ1-mediated kidney fibrosis and renal failure. To interrogate this hypothesis, we evaluated the therapeutic effect of recombinant TM in a newly developed glomerulus-specific TGFβ1 transgenic (TG) mouse that develops progressive kidney fibrosis and renal failure.

RESULTS

Increased circulating TM fragments correlate with renal dysfunction

TM, an endothelial cell membrane-bound glycoprotein, is cleaved in fragments, losing its protective functions during endothelial injury.[22] Diabetic nephropathy is associated with endothelial injury.[23,24] Patients with DM with nephropathy, compared with patients without nephropathy, showed significantly high circulating levels of TM (4.4 vs. 3.3 pg/ml) and active TGFβ1 (0.28 vs. 0.24 ng/ml) (Supplementary Table S1, Supplementary Figure S1A). TM significantly correlated with creatinine, active TGFβ1, and soluble podocin (Supplementary Figure S1B). These observations suggest that a loss of functional membrane-bound TM is associated with increased release of active TGFβ1 and kidney dysfunction.

TG mouse with glomerulus-specific expression of full-length human *TGFβ1* gene

We developed a TG mouse overexpressing the full-length human *TGFβ1* gene in podocytes. The mouse was generated by placing the human TGFβ1 under the control of the podocin promoter on a bacterial artificial chromosome (BAC) construct (Supplementary Figure S2; Supplementary Figure S3). We obtained 5 founder mice expressing 3 copies and 3 founder mice expressing 1 copy of the human *TGFβ1* transgene. The expression of the transgene was kidney-specific, and the offspring of the founders were viable (Supplementary Figure S3). Mice had full-term pregnancy and litters were of normal size. Mice were born in the expected Mendelian ratio.

To characterize the TG mice, we measured several renal parameters every 4 weeks for a period of 16 weeks (Supplementary Figure S4). The plasma and urine concentrations of TGFβ1 were significantly increased in the TGFβ1-TG mice compared with wild-type (WT) mice from early weeks after birth and then remained stable at high level (Figure 1a). TGFβ1-TG mice showed significant increase in the renal tissue content of hydroxyproline at the 20th week (190.5 vs. 96.0 μg/kidney), mesangial expansion from the 4th week (1.9 vs. 1.1 score), and in collagen deposition from the 12th week (0.9% vs. 0.1%) after birth compared to their WT counterparts (Figure 1a–f). Conventional optical microscopy showed widening of basement membrane of the Bowman capsule, thickening of glomerular basement membrane, increased collagen deposition in mesangial and interstitial spaces, and tubular atrophy (Figure 1b–d). Transmission electron microscopy showed glomerulosclerosis including microvillous transformation and foot process effacement of podocytes, decreased glomerular capillary endothelial fenestration, thickening of glomerular basement membrane and increased mesangial matrix deposition (Figure 2a–i). The urinary concentrations of the early markers of nephropathy L-fatty acid binding protein (185.1 vs. 87.0 pg/ml) and kidney injury molecule 1 (441.9 vs. 256.9 pg/ml) were significantly enhanced in TGFβ1-TG mice from the 4th and 8th weeks of age, respectively, compared with their age-matched WT mice (Supplementary Figure S5). Total proteinuria and the total protein-creatinine ratio in urine were significantly increased at 4th, 8th, 12th, 16th, and 20th weeks in TGFβ1-TG mice compared with in their WT counterparts (Figure 3a). The plasma level of blood urea nitrogen was significantly elevated from the 4th week (5.1 vs. 4.1 mg/dl) and the concentration of creatinine from the 8th week (1.1 vs. 0.4 mg/dl) in TGFβ1-TG mice compared with in their WT counterparts (Figure 3b).

rhTM inhibits glomerulosclerosis and tubulointerstitial fibrosis

When compared with TGFβ1-TG mice treated with saline (SAL) and WT mice treated with recombinant human (rh)

FLA 5.6.0 DTD ■ KINT2156_proof ■ 12 August 2020 ■ 9:15 pm ■ ce

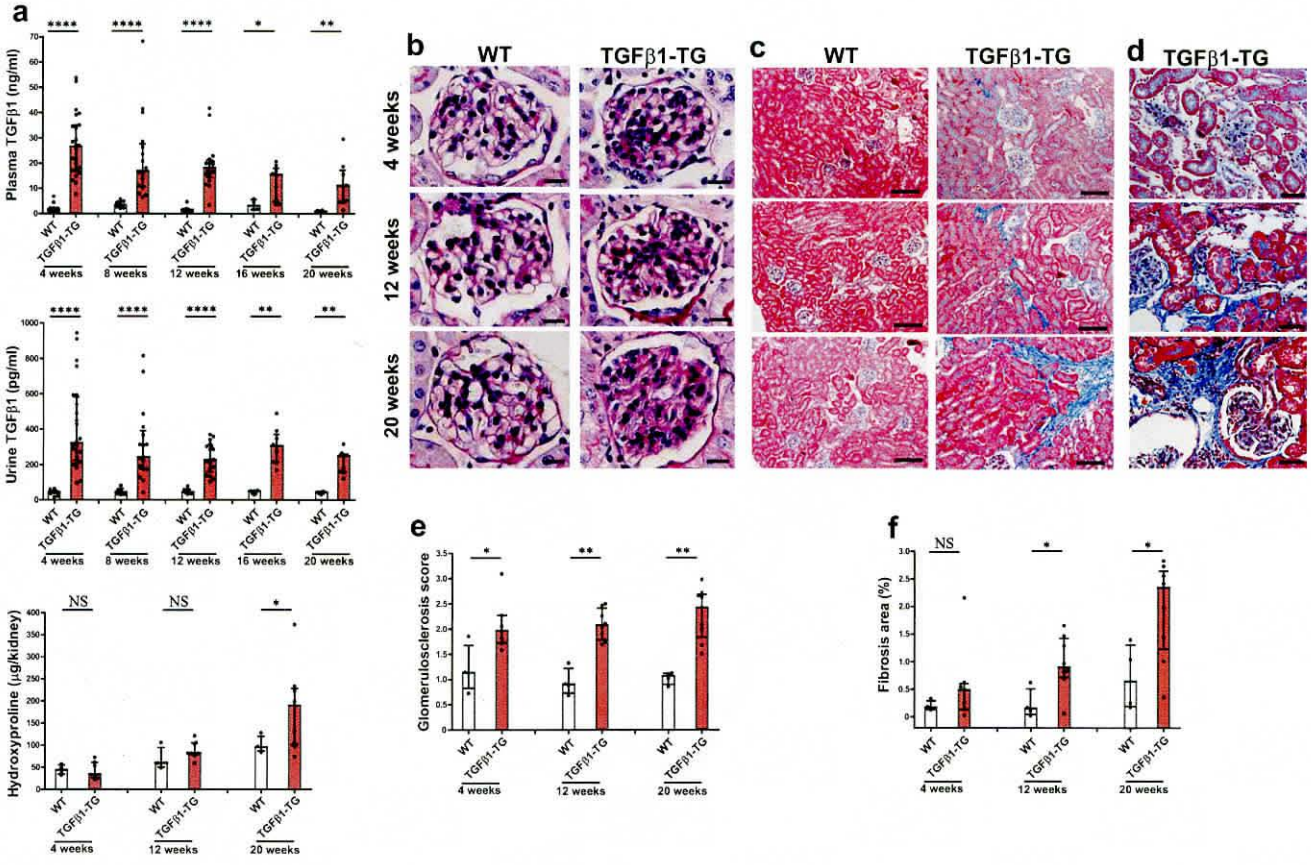

Figure 1 | The human transforming growth factor β1 (TGFβ1) transgenic (TG) mouse develops progressive kidney fibrosis. (**a**) The concentrations of TGFβ1 protein in plasma and urine were measured by enzyme immune assay and the tissue hydroxyproline content by a colorimetric assay. (**b–d**) Sections of renal tissue were stained with (**b**) periodic acid–Schiff (bars = 20 μm) and with (**c,d**) Masson trichrome (bars = 100 μm) and then (**e,f**) quantified using a scoring system or the WinROOF imaging software (Mitani Corporation, Tokyo, Japan). The number of mice for kidney tissue evaluation: for wild-type (WT) mice, $n = 4$ at 4, 12, and 20 weeks; for TG mice, $n = 7$ at 4 weeks, $n = 8$ at 16 weeks, and $n = 9$ at 20 week-olds. The number of mice for plasma and urine evaluation: for WT mice, $n = 12$ at 4 weeks, $n = 8$ at 8-weeks, $n = 7$ at 12 weeks, and $n = 4$ at 16 and 20 weeks; for TG mice, $n = 24$ at 4 weeks, $n = 17$ at 8 and 12 weeks, and $n = 9$ at 16 and 20 weeks. Data are expressed as median ± interquartile range. Statistical analysis by Mann-Whitney *U* test. $^*P < 0.05$, $^{**}P < 0.01$, $^{****}P < 0.0001$. NS, not significant. To optimize viewing of this image, please see the online version of this article at www.kidney-international.org. Q1

TM or SAL, TGFβ1-TG mice treated with rhTM showed significantly reduced mesangial expansion/cellularity (1.3 vs. 3.0 score) and significantly low tubulointerstitial collagen deposition and glomerulosclerosis (121.3% vs. 139.7%) (Figure 4a–e). Consistent with these observations, the hydroxyproline content (11.7 vs. 19.9 μg/g), the kidney tissue concentrations of collagen I (101.3 vs. 196.7 ng/mg/protein) and periostin (21.7 vs. 40.8 ng/mg/protein), and the relative mRNA expression of collagen I were significantly decreased in renal tissues from TGFβ1-TG mice treated with rhTM compared with in renal tissues from control mice (Figure 4f, Supplementary Tables S2 and S3). The transmission electron microscopy showed a significant reduction of foot process effacement of podocytes and thickening of glomerular basement membrane in mice treated with rhTM compared with in mice treated with SAL alone (Supplementary Figure S6AB and B). In addition, the kidney tissue concentrations of the profibrotic cytokines monocyte chemoattractant protein-1 (45.0 vs. 76.1 pg/mg/protein), interleukin-13 (612.1 vs. 1002.0 pg/mg/protein), and active TGFβ1 (131.0 vs. 151.5 pg/mg/protein) were significantly reduced in TGFβ1-TG mice treated with rhTM compared with in control mice (Supplementary Figure S7). The kidney tissue concentration of HMGB1 was also significantly decreased in renal tissues from TGFβ1-TG mice treated with rhTM compared with in renal tissues from control mice (Supplementary Figure S7). The plasma concentration of thrombin antithrombin complex was significantly increased in the TGFβ1-TG/SAL group compared to the WT/SAL group but no difference was found between the TGFβ1-TG/rhTM and WT/rhTM groups (Supplementary Figure S8A). As expected, there was high concentration of TM in plasma of TGFβ1-TG and WT mice treated with rhTM. The plasma concentration of the APC/α-antitrypsin complex was significantly decreased in the TGFβ1-TG/SAL group compared with in the WT/SAL and TGFβ1-TG/rhTM groups (280.5 vs. 384.6 pg/ml), and there

FLA 5.6.0 DTD ■ KINT2156_proof ■ 12 August 2020 ■ 9:15 pm ■ ce

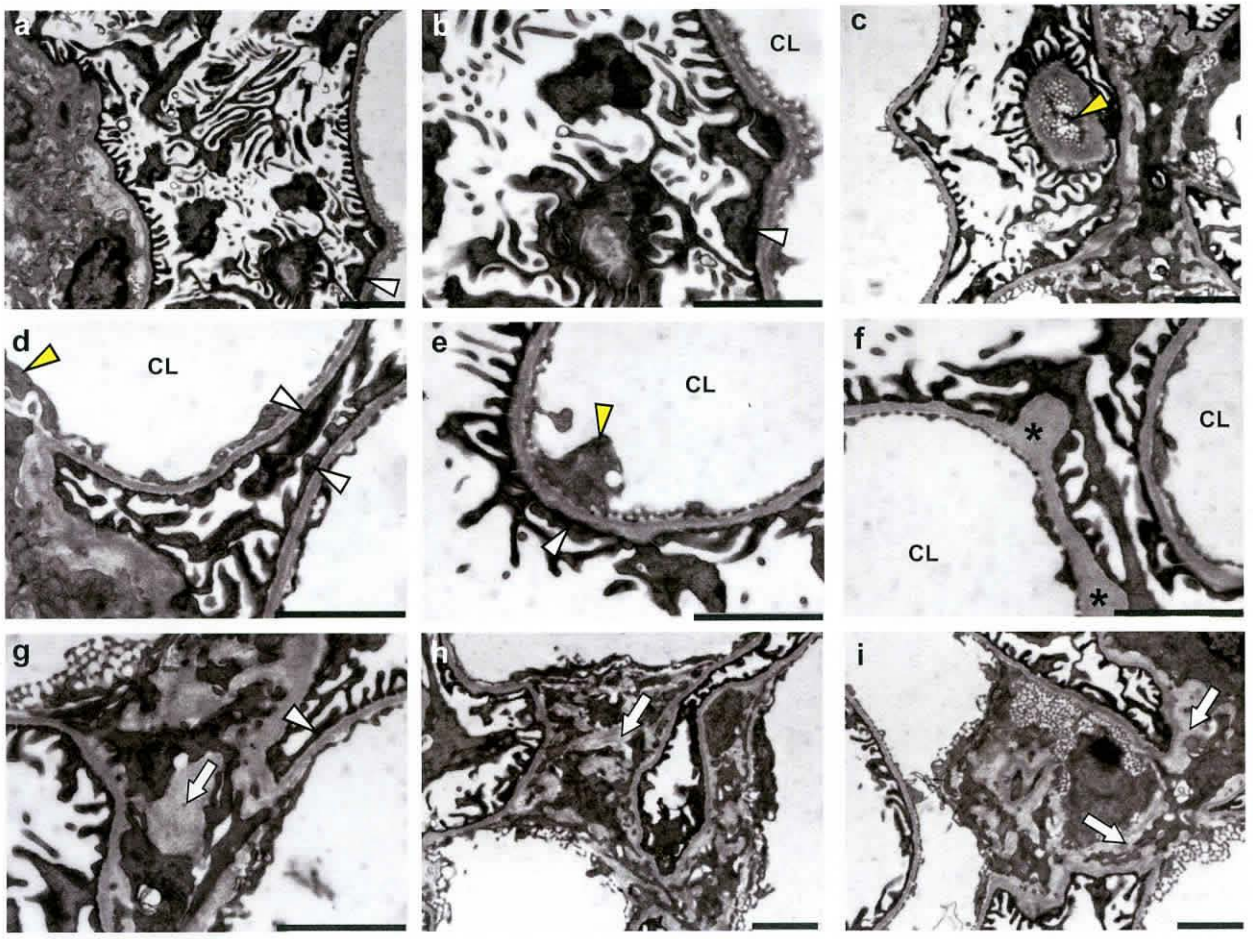

Figure 2 | Transmission electron microscopic findings in the transforming growth factor β1–induced kidney fibrosis model. Fixation, handling, and removal of the kidneys from mice were performed as described in the methods. (**a,b**) Microvillous transformation and (**a,b,d,e,g**) foot process effacement (white arrowheads) of podocytes, (**c–e**) decreased glomerular capillary endothelial fenestration (yellow arrowheads), (**f**) thickening of the glomerular basement membrane (asterisks), and (**h,i**) increased mesangial matrix deposition (white arrows) are present. CL, capillary lumen. To optimize viewing of this image, please see the online version of this article at www.kidney-international.org.

was no significant difference in the level of plasminogen activator inhibitor-1 (Supplementary Figure S8A). The levels of C5a in plasma, urine, and kidney tissue (630.1 vs. 1075.0 pg/mg/protein) and the plasma soluble podocin were significantly decreased in TGFβ1-TG mice treated with rhTM compared with in TGFβ1-TG mice treated with SAL (Supplementary Figure S8B). The level of podocin in urine was higher in the TGFβ1-TG/SAL group than in the WT/SAL and TGFβ1-TG/rhTM groups (Supplementary Figure S9A–C).

rhTM ameliorates renal function

The levels of L-fatty acid binding protein (197.0 vs. 313.4 pg/ml), kidney injury molecule 1 (299.9 vs. 596.2 pg/ml), blood urea nitrogen (12.9 vs 34.8 mg/dl), creatinine (0.5 vs. 1.4 mg/dl), and the albumin-creatinine ratio were significantly decreased in TGFβ1-TG mice with renal fibrosis treated with rhTM compared with in their untreated TG counterparts (Figure 5). The urine total protein and the total protein-creatinine ratio were also decreased in TGFβ1-TG mice treated with rhTM compared with in their untreated counterparts (Figure 5).

rhTM reduces apoptosis of glomerular cells

Terminal deoxynucleotidyl transferase–mediated dUTP nick end-labeling staining showed significantly decreased number of apoptotic cells in glomeruli from TGFβ1-TG mice treated with rhTM compared with in glomeruli from TGFβ1-TG mice treated with SAL (Supplementary Figure S10A and B). Cleavage of caspase-3 was also significantly reduced in kidney tissues from TGFβ1-TG mice treated with rhTM compared with in kidney tissues from TGFβ1-TG mice treated with SAL (Supplementary Figure S10C). The kidney tissues from TGFβ1-TG mice treated with rhTM, compared with those from TGFβ1-TG treated with SAL, showed significant elevation in mRNA levels of B-cell lymphoma 2 (Bcl-2), B-cell lymphoma—Q7 extra large (Bcl-XL), baculoviral inhibitor or apoptosis

FLA 5.6.0 DTD ■ KINT2156_proof ■ 12 August 2020 ■ 9:15 pm ■ ce

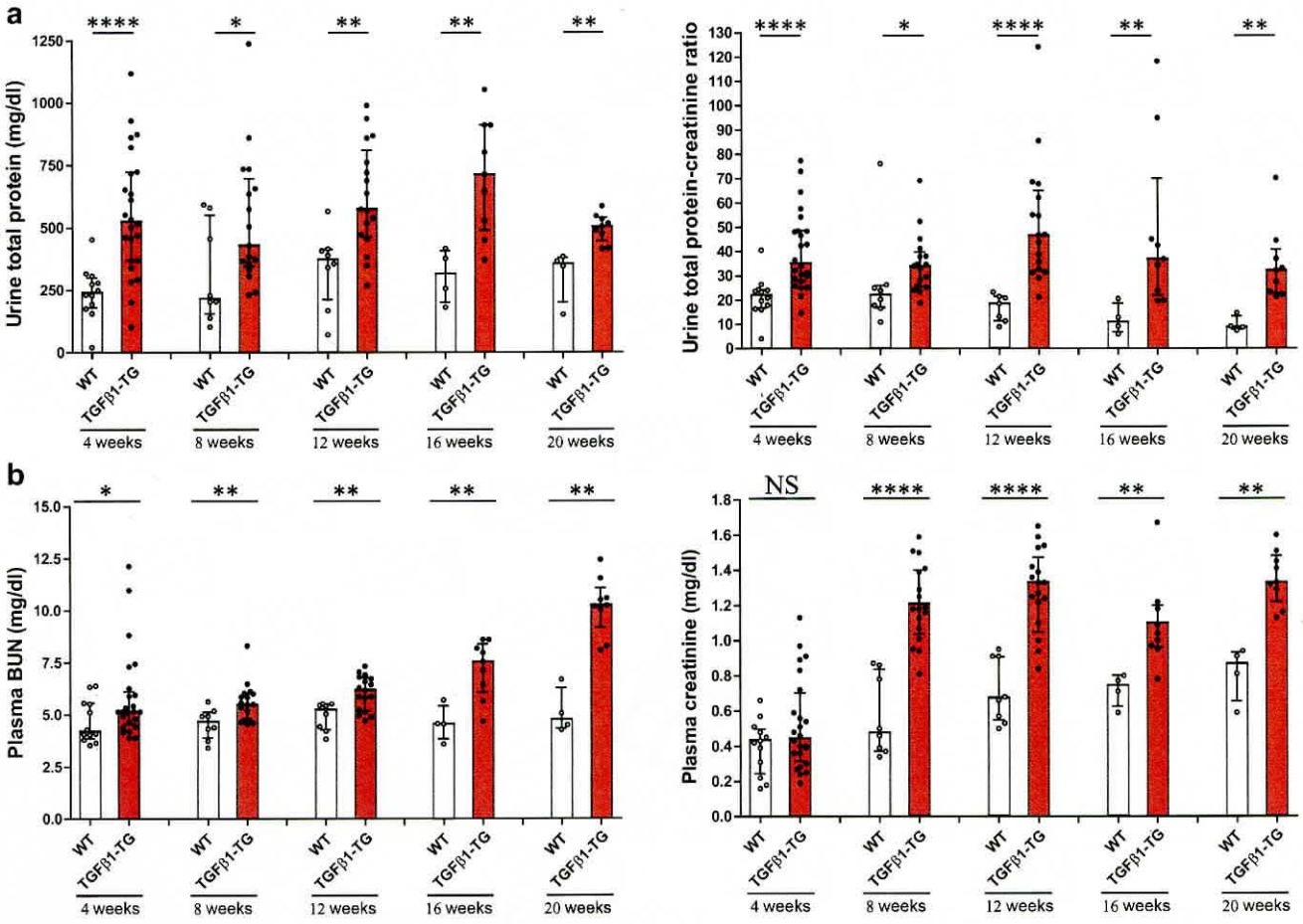

Figure 3 | The human transforming growth factor β1 (TGFβ1) transgenic (TG) mouse has renal dysfunction. (**a**) Total protein and (**b**) blood urea nitrogen (BUN) were measured by colorimetric methods and creatinine by an enzymatic method. The number of mice for plasma and urine evaluation: for wild-type (WT) mice, $n = 12$ at 4 weeks, $n = 7$ at 8 and 12 weeks, and $n = 4$ at 16 and 20 weeks; for TG mice, $n = 24$ at 4 weeks, $n = 17$ at 8 and 12 weeks, and $n = 9$ at 16 and 20 weeks. Data are expressed as median ± interquartile range. Statistical analysis by Mann-Whitney U test. $^*P < 0.05$, $^{**}P < 0.01$, $^{****}P < 0.0001$.

repeat-containing 5 (BIRC5, also known as survivin), and BIRC6 (apollon) with increased Bcl-2–Bax ratio (Supplementary Figure S11).

rhTM inhibits apoptosis of podocytes

Pretreatment of podocytes with rhTM significantly decreased apoptosis of podocytes cultured in the presence of TGFβ1 as assessed by the number of cells in subG1 phase (3.2% vs. 5.2%), terminal deoxynucleotidyl transferase–mediated dUTP nick end-labeling–positive cells (1.0 vs. 5.4 cells/field) and the degree of caspase-3 cleavage (0.9 vs. 1.1 ratio) (Figure 6a–e). Screening of antiapoptotic factors in cultured podocytes showed that rhTM significantly increases the mRNA expression of the antiapoptotic factor Bcl-2 compared with expression in untreated cells (Supplementary Figure S12). The mRNA expression of the antiapoptotic factor BIRC5 also increased in cells treated with rhTM compared with expression in untreated cells (Supplementary Figure S12). The mRNA expression of the proapoptotic factor Bax was significantly reduced by rhTM treatment compared with no treatment (Supplementary Figure S12). Treatment with rhTM also significantly inhibited the expression of annexin V and terminal deoxynucleotidyl transferase–mediated dUTP nick end-labeling staining in podocytes cultured in the presence of hydrogen peroxide (Supplementary Figure S13A–E) and under high glucose condition (Supplementary Figure S14A–E) further confirming the antiapoptotic property of rhTM on podocytes. Exploration of the antiapoptotic protein kinase B (Akt) pathway[25] showed that rhTM enhanced the phosphorylation of Akt in human primary podocytes cultured in the presence of hydrogen peroxide or TGFβ1 (Supplementary Figure S15A and B). We then isolated podocytes from each group of mice and evaluated Akt phosphorylation by Western blotting. There was significantly enhanced phosphorylation of Akt in podocytes isolated from the TGFβ1-TG/rhTM group compared with podocytes from the untreated group (1.1 vs. 0.7 ratio) (Supplementary Figure S16A and B).

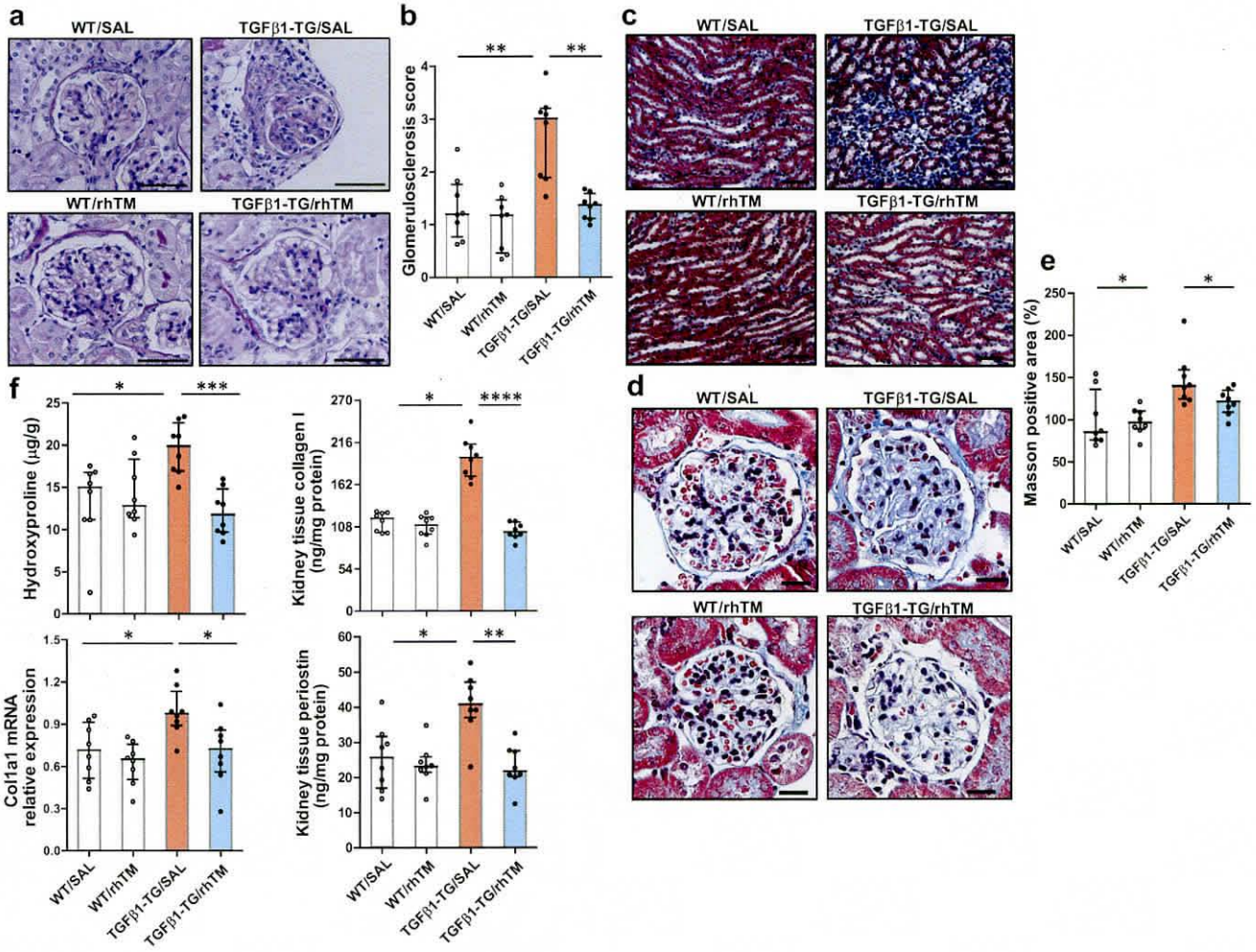

Figure 4 | Recombinant human thrombomodulin (rhTM) inhibits glomerulosclerosis and tubulointerstitial fibrosis. Sections of renal tissue were stained (**a,b**) with periodic acid–Schiff and (**c,d**) with Masson trichrome and (**e**) then quantified using a scoring system or the WinROOF imaging software. (**e**) The mean value of the wild-type (WT)/saline (SAL) group was taken as 100%. Statistical analysis by Mann-Whitney *U* test. (**f**) The tissue hydroxyproline content was measured by a colorimetric method, concentration of collagen I-α1 (Col1a1) and periostin by enzyme immunoassay and mRNA expression by reverse transcriptase polymerase chain reaction. Statistical analysis by Kruskal-Wallis analysis of variance and corrected Dunn test. $n = 8$ in each group. Bars = (**a,c**) 50 μm and (**d**) 20 μm. Data are expressed as median ± interquartile range. $^{*}P < 0.05$, $^{**}P < 0.01$, $^{***}P < 0.001$, $^{****}P < 0.0001$. TG, transgenic; TGFβ1, transforming growth factor β1. To optimize viewing of this image, please see the online version of this article at www.kidney-international.org.

GPR15 mediation

Previous studies reported that TM activate intracellular pathways by interacting with fibroblast growth factor receptor 1 (FGFR1) and G-protein coupled receptor 15 (GPR15).[26,27] Podocytes express FGFR1[28] but whether they express GPR15 is unclear. Here we isolated podocytes from each group of mice and showed that podocytes also express GPR15 (Supplementary Figure S17A–E). We found that podocytes from a healthy control and a patient with glomerulosclerosis also express GPR15 (Supplementary Figure S18). To clarify whether FGFR1 or GPR15 mediates the rhTM inhibitory activity on apoptosis of podocytes, we evaluated the anti-apoptotic activity of rhTM in TGFβ1-treated podocytes in the presence of FGFR1 inhibitor or after transfecting the cells with small, interfering RNA (siRNA) against FGFR1 or GPR15. Pretreatment of podocytes with FGFR1 inhibitor (Supplementary Figure S19A and B) or FGFR1 siRNA (13.2% vs. 7.9%) (Figure 7a and b) was unable to abolish the inhibitory activity of rhTM on apoptosis of podocytes. However, transfection of cells with GPR15 siRNA completely abolished the inhibitory activity of rhTM (14.6% vs. 13.8%) on apoptosis of podocytes (Figure 7a–c).

rhTM inhibits EMT of podocytes

There was a significantly increased area with positive staining for podocin and α-smooth muscle actin (α-SMA) (1.4% vs. 11.2%) in TGFβ1-TG/SAL mice compared with in TGFβ1-TG/rhTM mice (Figure 8a and b). We then cultured *in vitro* primary human podocytes, pretreated with rhTM before adding TGFβ1 protein to the culture medium. The fibroblast-

FLA 5.6.0 DTD ■ KINT2156_proof ■ 12 August 2020 ■ 9:15 pm ■ ce

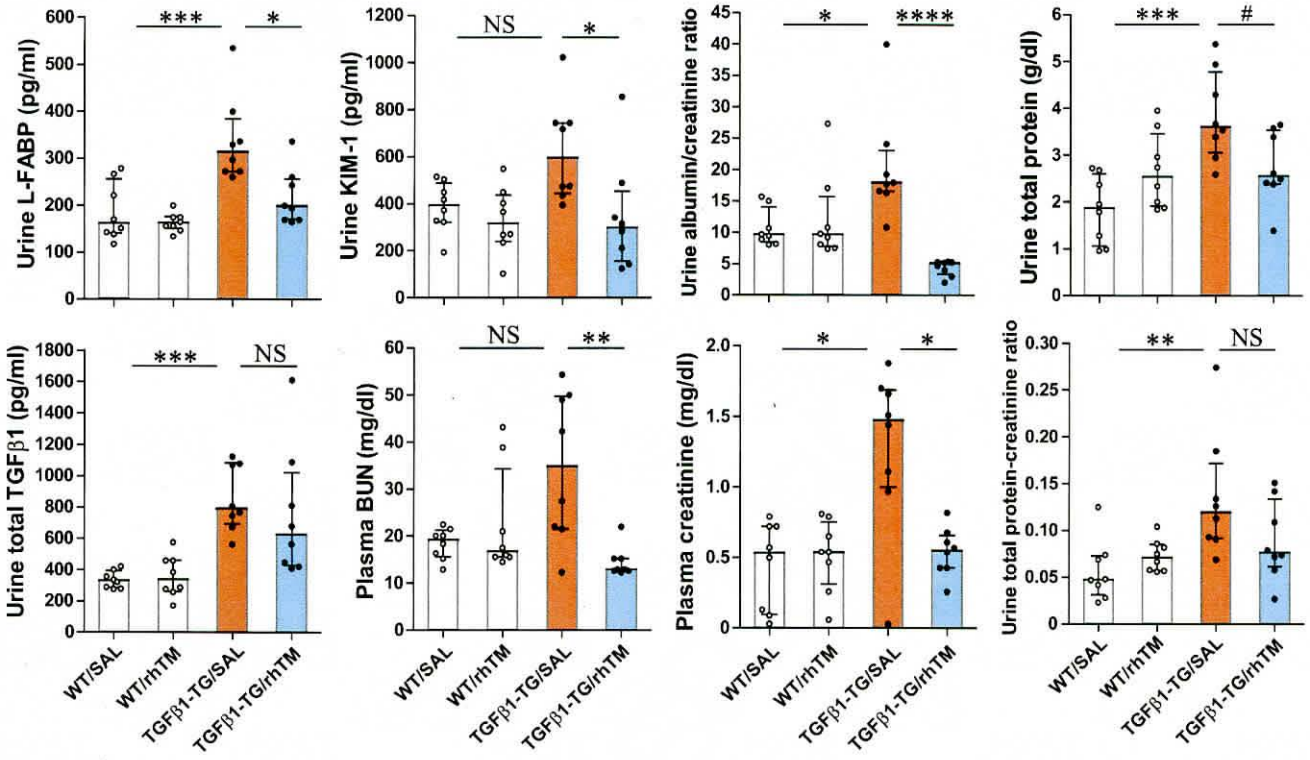

Figure 5 | Recombinant human thrombomodulin (rhTM) ameliorates kidney injury and renal dysfunction. Creatinine was measured by an enzymatic method, total protein by colorimetric method, blood urea nitrogen (BUN) and albumin, kidney injury molecule 1 (KIM-1), L-fatty acid binding protein (L-FABP), and total transforming growth factor β1 (TGFβ1) by enzyme immune assay. $n = 8$ in each group. Data are expressed as median ± interquartile range. Statistical analysis by Kruskal-Wallis analysis of variance and uncorrected Dunn test. $^{*}P < 0.05$, $^{**}P < 0.01$, $^{***}P < 0.001$, $^{****}P < 0.0001$, $^{\#}P = 0.1$, $^{\#}P = 0.06$. NS, not significant; SAL, saline; TG, transgenic; WT, wild type. Q17

like morphology and enhanced expression of α-SMA were suppressed in podocytes treated with rhTM compared with in untreated cells (Supplementary Figure S20A). In addition, rhTM inhibited the mRNA expression of fibronectin and vimentin, although it enhanced the mRNA expression of E-cadherin in podocytes compared with expression in untreated cells (Supplementary Figure S20B). SMAD family member 2 (Smad2) and Smad3 play a critical role in TGFβ1-mediated epithelial-mesenchymal transition (EMT).[29] Treatment with rhTM significantly suppressed the activation of Smad2 and Smad3 in TGFβ1-TG mice compared with in untreated TG mice (Figure 8c) and in human podocytes cultured in the presence of TGFβ1 (Supplementary Figure S20C).[29] TG mice treated with rhTM (TGFβ1-TG/rhTM) also show less expression of α-SMA (3.7% vs. 17.2%) in tubular epithelial cells compared with in their untreated counterparts (Supplementary Figure S21A and B).

GPR15 mediates the inhibitory activity of rhTM on EMT

Transfection of podocytes with FGFR1 siRNA was unable to abolish the inhibitory activity of rhTM on the relative mRNA expressions of both collagen I-α1 and α-SMA in TGFβ1-treated podocytes (Supplementary Figure S22). However, transfection of cells with GPR15 siRNA significantly abolished the inhibitory activity of rhTM on the relative mRNA expressions of both collagen I-α1 and α-SMA in TGFβ1-treated podocytes (Supplementary Figure S22).

DISCUSSION

TGFβ1 and injury of glomerular cells

The common consequence of disorders causing CKD is renal fibrosis.[8,30,31] TGFβ1 is the common driver of fibrogenesis in the kidneys associated with CKD caused by diseases including DM, arterial hypertension, and autoimmune disorders.[10] Cells from the glomerulus and tubulointerstitial spaces can secrete the latent forms of TGFβ1 that, when excessively activated during tissue injury, may lead to renal scarring.[32] As TGFβ1 can stimulate its own secretion, the fibrotic process generally becomes a vicious cycle.[8] An early event in the pathogenic process of TGFβ1-mediated kidney fibrosis is injury of podocytes and glomerular endothelial cells.[33–35] The plasma level of soluble TM is a marker of endothelial injury. Consistent with the role of TGFβ1 in renal cell injury, here we found a significant correlation of active TGFβ1 with soluble TM, soluble podocin, and creatinine in plasma from patients with DM. Crosstalk between glomerular endothelial cells and podocytes during renal injury leads to local expression of proteases causing glomerular basement membrane

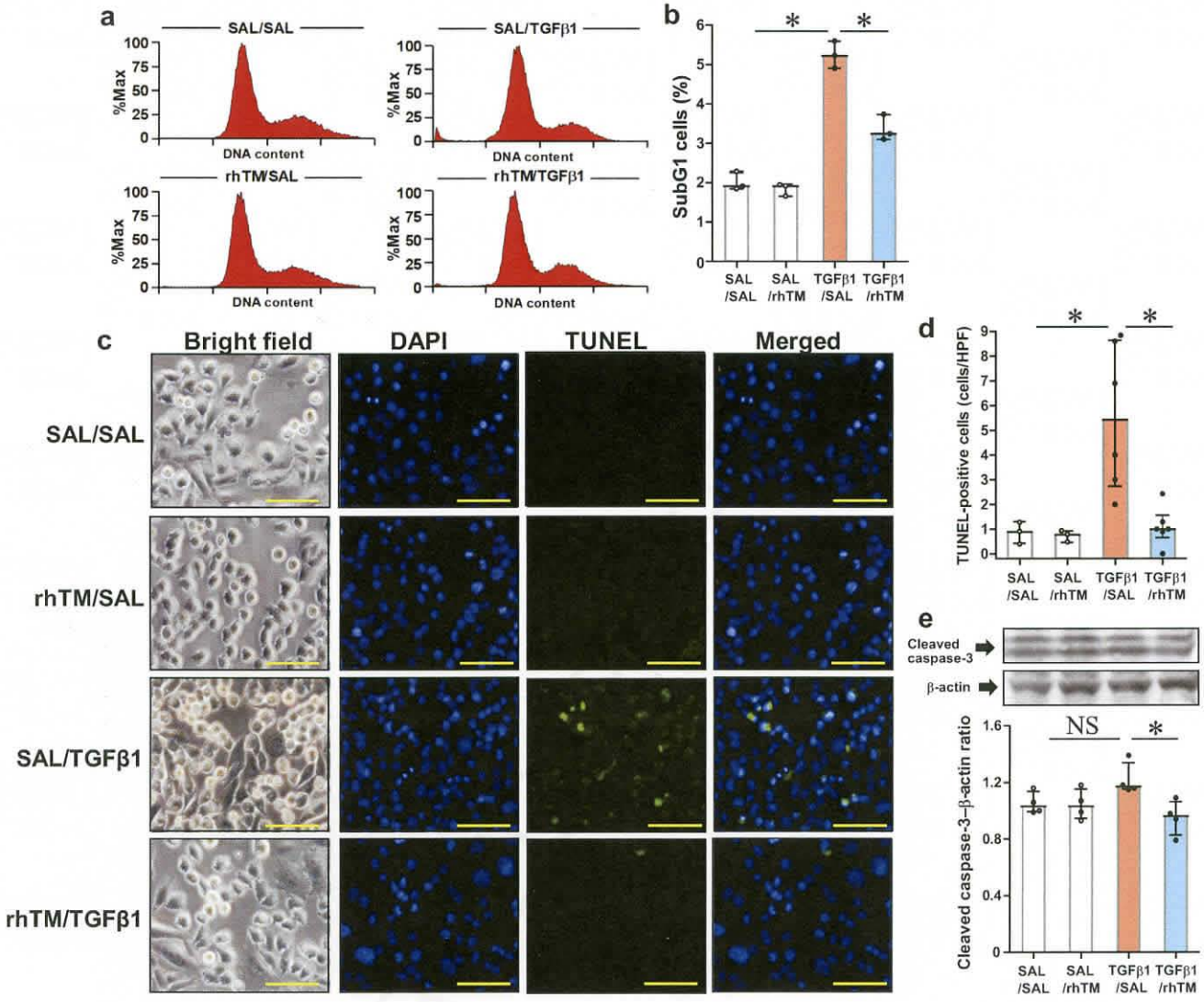

Figure 6 | Recombinant human thrombomodulin (rhTM) suppresses apoptosis of podocytes induced by transforming growth factor β1 (TGFβ1). (**a**) rhTM was added to the culture medium of podocytes 1 hour before inducing apoptosis with 10 ng/ml TGFβ1 for 48 hours. (**b**) The percentage of cells in subG1 phase was detected by flow cytometry. (**a,b**) $n = 3$ in each group. (**c,d**) The number of cells with DNA fragmentation was measured by terminal deoxynucleotidyl transferase–mediated dUTP nick end-labeling (TUNEL) analysis ($n = 3$ in saline [SAL]/SAL and rhTM/SAL groups; $n = 6$ in SAL/TGFβ1 and rhTM/TGFβ1 groups), and (**e**) the degree of caspase-3 cleavage was measured by Western blotting ($n = 4$ in each group). Bars = 100 μm. Data are expressed as median ± interquartile range. Statistical analysis by Mann-Whitney *U* test. *$P < 0.05$. DAPI, 4′,6-diamidino-2-phenylindole; HPF, high-powered field; %Max, maximum percentage; NS, not significant. To optimize viewing of this image, please see the online version of this article at www.kidney-international.org.

degradation.[34–36] This may explain the detection of soluble podocin and its significant correlation with soluble TM in our patients with DM.

Podocyte-specific human TGFβ1 overexpression-associated kidney fibrosis

A drug that can counteract the effect of TGFβ1 would be ideal to block renal fibrosis. Here we have generated a TG mouse overexpressing the human *TGFβ1* gene in the glomerulus that develops spontaneous and progressive glomerular sclerosis and tubulointerstitial fibrosis with renal failure as early as 4 weeks after birth. The model shows advanced glomerulopathy with injury of podocytes and glomerular endothelial cells; glomerular basement membrane thickening and mesangial expansion with interstitial scarring; increased markers of kidney tissue injury and renal dysfunction; and increased TGFβ1 in plasma, renal tissue, and urine. The increase in urinary excretion of proteins, TGFβ1, and activation of the complement system may explain the concurrent development of interstitial scarring in our present model.[37–40] Further experiments revealed increased apoptotic cells and activation of Smad proteins in kidney tissue from untreated TGFβ1-TG

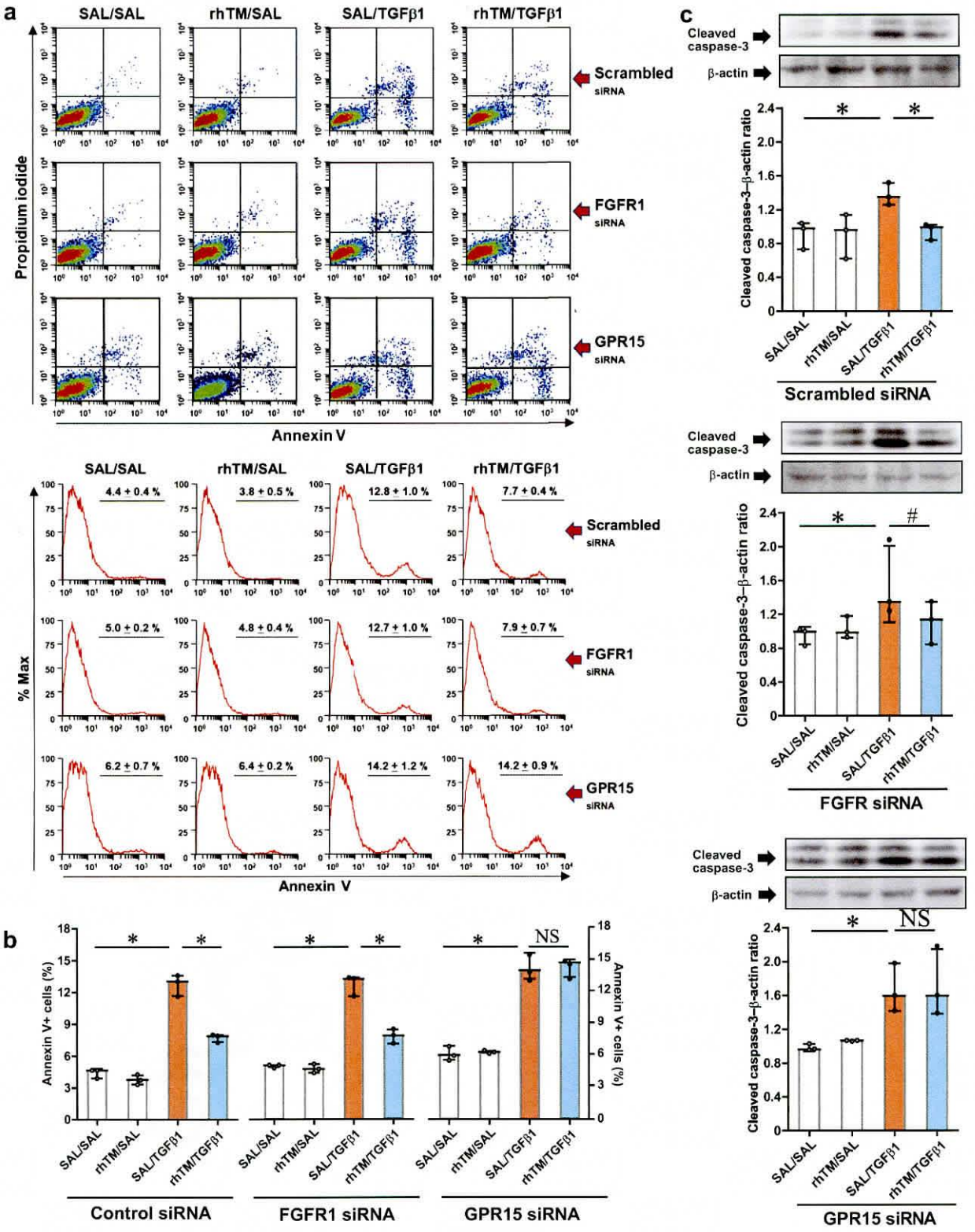

Figure 7 | G-protein coupled receptor (GPR15) mediates inhibition of apoptosis recombinant human thrombomodulin (rhTM) in podocytes. Human primary podocyte cells were transfected with fibroblast growth factor receptor 1 (FGFR1) small, interfering RNA (siRNA), GPR15 siRNA, or scrambled siRNA for 48 hours, and then rhTM was added to the cell culture 1 hour before treating with transforming growth factor β1 (TGFβ1). Apoptotic cells were (**a**) assessed by flow cytometry and (**b**) then quantified. (**c**) Cell lysates were prepared for Western blotting. $n = 3$ in each group. Data are expressed as median ± interquartile range. Statistical analysis by Mann-Whitney *U* test. $^{*}P < 0.05$, $^{\#}P = 0.1$. SAL, saline.

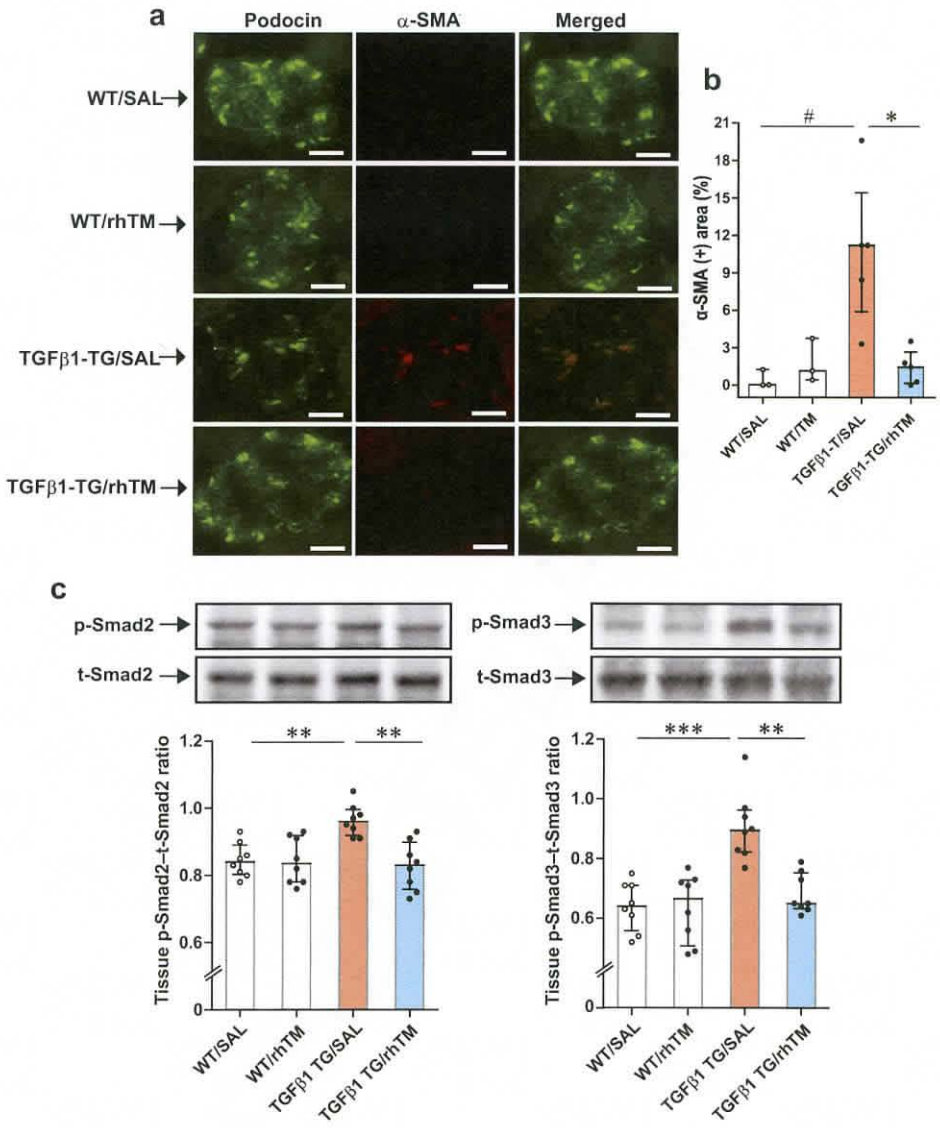

Figure 8 | Inhibition of epithelial-mesenchymal transition by recombinant human thrombomodulin (rhTM). (**a**) Podocin and α-smooth muscle actin (α-SMA) were stained as described in the methods. (**b**) The area positive for α-SMA staining was quantified by the WinROOF image processing software. $n = 3$ in wild-type (WT)/saline (SAL) and WT/rhTM groups and $n = 5$ in transforming growth factor-β1–transgenic (TGFβ1-TG)/SAL and TGFβ1-TG/rhTM groups. (**c**) Total (t) and phosphorylated (p) SMAD family member (Smad) proteins were evaluated by Western blotting. $n = 8$ in each group. Data are expressed as median ± interquartile range. Statistical analysis by Kruskal-Wallis analysis of variance and corrected Dunn test. $^{*}P < 0.05$, $^{**}P < 0.01$, $^{***}P < 0.001$, $^{\#}P = 0.08$. To optimize viewing of this image, please see the online version of this article at www.kidney-international.org.

mice compared with from WT mice. Overall, these findings point to this novel TGFβ1-TG mouse as a suitable model for drug discovery in kidney fibrosis.

rhTM ameliorates kidney fibrosis

We have shown that rhTM ameliorates pulmonary fibrosis developed in mice overexpressing human TGFβ1 in the lungs by suppressing alveolar epithelial cell apoptosis.[41] Clinical trials have also demonstrated amelioration of idiopathic pulmonary fibrosis after rhTM treatment.[42,43] These previous observations suggest the potential of rhTM for organ fibrosis therapy. We hypothesized that rhTM would be effective in TGFβ1-associated kidney fibrosis. To test this hypothesis, we treated kidney-specific TGFβ1-TG mice with rhTM.[44] Administration of rhTM for 4 weeks significantly attenuated injury, dysfunction, and fibrosis of the kidneys. Mice treated with rhTM showed low urinary levels of total protein, albumin, TGFβ1, C5a, and reduced renal levels of profibrotic cytokines, C5a and HMGB1.[45] Therapy with rhTM also inhibited both apoptosis and EMT of podocytes. However, rhTM exerted no effect on thrombin antithrombin complex, a coagulation activation marker, although it increased the generation of APC, an

anticoagulant factor with anti-inflammatory and antiapoptotic activity.[23] It is worth noting that thrombin, the procoagulant enzyme, may paradoxically promote anticoagulation under low-grade prothrombotic states by forming the TM/thrombin complex, which increases the generation of the anticoagulant APC. However, thrombin works mainly as a procoagulant under excessive prothrombotic states (e.g., sepsis).[46] This dual and paradoxical effect of thrombin may explain the apparent inefficacy of rhTM to inhibit coagulation activation in our model, which is in a low-grade prothrombotic state. Overall, these observations suggest that rhTM ameliorates progressive fibrosis and dysfunction of the kidneys by prolonging the survival of or preventing EMT of glomerular cells and by suppressing inflammation, complement activation, and growth factor activity directly or indirectly via activation of the protein C pathway and reduction of HMGB1 expression. Improvement of diabetic nephropathy in mice with increased circulating TM lectin-like domain and disease deterioration in mice lacking the lectin-like domain support the beneficial effect of rhTM on renal fibrosis.[20,21]

Inhibition of podocyte apoptosis

Podocytes play critical roles in the maintenance of the glomerular filtration barrier and the formation of the slit diaphragm to prevent the loss of essential circulating proteins.[47] Renal injury caused by reactive oxygen species, high glucose, or inflammatory mediators including TGFβ1 induces apoptosis of podocytes leading to podocyte depletion that may eventually end up causing renal dysfunction.[47] After binding and activating the serine/threonine kinase transmembrane heteromeric type I and type II receptor complex, TGFβ1 emits intracellular signals through the Smad family of transcription factors or through Smad-independent signaling pathways.[48] Activation of the Smad-dependent pathway occurs when activated TGFβ1 receptor phosphorylates Smad2 and Smad3, which with Smad4 translocate to the nucleus.[49] The Smad2/Smad3/Smad4 complex stimulates the transcription of proapoptotic factors and reduces that of antiapoptotic factors leading to cell apoptosis.[49] Consistent with this, we found high renal level of the proapoptotic factor Bax and low level of the antiapoptotic factors Bcl2 and Bcl-XL in TGFβ1-TG mice. TM can inhibit apoptosis of different cell types.[21,41,49] Consistent with this, here we found that rhTM inhibits apoptosis of podocytes induced by hydrogen peroxide, high glucose, or TGFβ1, and this finding may explain the beneficial effect of rhTM in CKD. In addition, rhTM tilted the balance toward inhibition of apoptosis by reducing the expression of Bax, by increasing the expression of Bcl2, Bcl-XL, BIRC5, and BIRC6, and by increasing the activation of the Akt pathway in kidney tissues. Overall, these observations suggest that rhTM stimulates podocyte survival by favoring Akt activation and antiapoptotic factor expression.

Inhibition of EMT

EMT of podocytes also contributes to renal fibrosis. Podocytes undergoing EMT release extracellular matrix proteins that accumulate and deposit during TGFβ1-associated renal fibrogenesis.[50] TGFβ1 promotes EMT through receptor-mediated activation of the Smad2/Smad3/Smad4 complex. Phosphorylated Smad3 promotes EMT by stimulating the transcription of matrix proteins and by reducing the expression of epithelial markers.[51] Consistent with this, we found increased EMT of podocytes in TGFβ1-TG mice and podocytes cultured in the presence of TGFβ1 or under oxidant or high glucose condition. Previous reports suggested that rhTM suppresses EMT.[52,53] Here we found that rhTM inhibits EMT of podocytes and tubulointerstitial epithelial cells in TGFβ1-TG mice. Inhibition of Smad protein activation appears to be the mechanism of the beneficial effect of rhTM on EMT because TGFβ1-TG mice and primary podocytes treated with rhTM depicted significantly reduced phosphorylation of Smad2 and Smad3 compared with untreated conditions. These findings support the inhibitory activity of TM on EMT.

Receptor mediation in rhTM protective activity

Previous studies have shown that GPR15 or FGFR1 mediates the cytoprotective activity of TM.[26,27,54] We tested whether these receptors mediate the protective activity of rhTM against apoptosis and EMT. While downregulation of GPR15 protein by siRNA completely abolished the TGFβ1-mediated apoptosis of podocytes by rhTM, neither FGFR1 siRNA nor its inhibitor abolished it, suggesting that GPR15 mediates the rhTM protective activity. There was enhanced phosphorylation of Akt in cultured podocytes and podocytes isolated from TGFβ1-TG mice after treatment with rhTM, suggesting the involvement of the intracellular Akt pathway. A work showing that rhTM activates the Akt pathway in endothelial cells supports this finding.[55] Activation of the Akt signaling pathway may further potentiate the rhTM effect by increasing the GPR15 surface expression.[56] These observations indicate that rhTM protects podocytes from apoptosis in our TGFβ1-TG mice by activating the GPR15/Akt axis leading to enhanced expression of antiapoptotic factors and decreased expression of proapoptotic factors.[57] On the other hand, previous studies demonstrated that the anaphylatoxins C3a and C5a through their GPRs may contribute to CKD by injuring podocytes, and that APC may inhibit podocyte apoptosis and kidney fibrosis via its endothelial protein C receptor and protease-activated receptor 1.[23,58–61] Here, we found that rhTM inhibits the complement system and increases the generation of APC. Therefore, apart from the activation of the GPR15/Akt pathway, inhibition of complement factors and increased activation of protein C and its receptors may also explain the beneficial effects of rhTM in our TGFβ1-associated kidney fibrosis model.

In addition, downregulation of GPR15 but not that of FGFR1 blocked the inhibitory effect of rhTM on EMT, suggesting that GPR15 also mediates this rhTM protective activity. Inhibition of Smad proteins is involved in EMT suppression because treatment with rhTM inhibited the phosphorylation of both Smad2 and Smad3 in TGFβ1-TG

mice and cultured podocytes. However, the precise mechanism of Smad protein inhibition via GPR15 is unclear. Some evidence shows that the Akt pathway may crosstalk with and regulate the Smad signaling pathway,[62–64] and that Akt can prevent phosphorylation of Smad3 by directly interacting with unphosphorylated Smad3 to sequester it outside the nucleus leading to inhibition of transcription and EMT.[62–64] Based on these reports, it is conceivable that Akt activated after rhTM binding to GPR15 sequesters unphosphorylated Smad3 leading to podocyte EMT inhibition. It is worth noting that this Akt-mediated beneficial effect is observed only in nonmalignant cells.[65–67] In malignant cells, interaction of TGFβ1 with its receptors may directly activate the phosphoinositide 3-kinase/Akt/Snail pathway and cause EMT.[65–67] Overall, the results of our study support the role of GPR15 as the receptor mediating the beneficial effects of rhTM on podocytes.

Conclusion

In summary, here we report for the first time a novel transgenic TG mouse overexpressing the full-length of human *TGFβ1* gene specifically in glomeruli that develops spontaneous and progressive glomerular sclerosis, tubulointerstitial fibrosis and renal failure, and amelioration of established kidney fibrosis/renal failure by rhTM interaction with GPR15 that inhibits apoptosis and mesenchymal transition of podocytes.

METHODS

Generation of the TGFβ1 BAC TG mouse

TGFβ1-BAC-TG mouse expressing the full-length human *TGFβ1* gene under the mouse podocin promoter control was generated by pronuclear injection into 392 C57BL/6J mouse embryos (CLEA Japan, Inc., Tokyo, Japan). We assessed the TG founders and germ line transmission of the BAC TG construct by Southern blotting.

Experimental animals

The TGFβ1-TG mice were bred for more than 10 generations under C57BL/6 background before using in the experiments. WT littermates were used as the control animals. All animals were maintained in a specific pathogen-free environment and subjected to a 12-hour light-dark cycle at an ambient temperature and humidity ranging between 22 °C and 26 °C and 40% and 70%, and with *ad libitum* access to food and water in the animal house of Mie University.

Ethical statement

The Recombinant DNA Experiment Safety Committee (approval no. I-629; date: September 19, 2013) and the Committee on Animal Investigation of Mie University (approval no. 27-4; date: August 19, 2015) approved the protocols of the study. All animal procedures were performed in accordance with the institutional guidelines of Mie University and following the internationally approved principles of laboratory animal care published by the National Institute of Health (https://olaw.nih.gov/).

For the clinical investigation, written informed consent was given by all patients and healthy subjects, and the study protocol was approved by the Ethics Committee for Clinical Investigation of Mie University (approval nos. 107 and 2194).

Experimental design

For characterization of the kidney fibrosis model, we allocated male TGFβ1-TG mice ($n = 24$) and male WT mice ($n = 12$) 4 weeks of age and weighing 20 to 23 g into 3 groups with 8 TGFβ1-TG mice and 4 WT mice in each group. Mice from each WT and TGFβ1-TG group were euthanized on weeks 0, 8, or 16 to collect samples of urine, blood, and kidney for assessing changes in fibrosis and renal function parameters over time.

To evaluate the therapeutic effectiveness of rhTM (rhTM was kindly provided by Asahi Kasei Pharma Corporation, Tokyo, Japan) in renal fibrosis, TGFβ1-TG mice ($n = 8$) or WT littermates ($n = 8$) were treated with rhTM (3 mg/kg) by i.p. injection, 3 times a week during the 4 weeks before the mice were killed. TGFβ1-TG mice ($n = 8$) or WT littermates ($n = 8$) receiving an equal amount of physiological SAL by i.p. injection were used as negative control mice.

The protocol of the present study followed the Animal Research: Reporting of *In Vivo* Experiments (ARRIVE) guidelines for animal investigation. Mice were randomized, and researchers who measured parameters were blinded to treatment groups.

Biochemical analysis

The concentrations of total protein (BCA protein assay kit; Pierce, Rockford, IL), TGFβ1 (R&D System, Minneapolis, MN), monocyte chemoattractant protein-1 (BD Biosciences Pharmingen, San Diego, CA), thrombin antithrombin complex (Cedarlane Laboratories, Hornby, Ontario, Canada) were measured using commercial enzyme immunoassay kits following the manufacturer's instructions.

Cell culture

The human podocyte primary cells were purchased from CELPROGEN (Torrance, CA). Human podocyte primary cells were cultured in Dulbecco's modified Eagle's medium in a humidified, 5% CO_2 atmosphere at 37 °C. Medium was supplemented with 10% heat-inactivated fetal bovine serum (Bio Whittaker, Walkersville, MD), 100 IU/ml penicillin, 100 μg/ml streptomycin, and L-glutamine.

Statistical analysis

Data are expressed as median ± interquartile range. The statistical difference between variables was calculated by Kruskal-Wallis analysis of variance with *post hoc* analysis using the Dunn test. Mann-Whitney *U* test was used to evaluate differences between 2 groups. Statistical analyses were done using the GraphPad Prism version 8.0.1 (GraphPad Software, San Diego, CA). Statistical significance was considered as $P < 0.05$.

DISCLOSURE

ECG, CND-G, and YY have a patent on the TGFβ1-TG mouse with renal fibrosis used in the present study. CND-G and YY received a grant from the Ministry of Education, Culture, Sports, Science, and Technology of Japan for the present study. ECG, TY, CND-G, and MT received a grant from Shionogi Pharmaceuticals. All the other authors declared no competing interests.

ACKNOWLEDGMENTS

This research was supported in part by grants from the Ministry of Education, Culture, Sports, Science, and Technology of Japan (Kakenhi no. 17K09824 for YY; Kakenhi no. 17K08442 for CND-G), and in part by a grant from Shionogi Pharmaceuticals. The funders had no role in study design, data analysis, decision to publish, or preparation of the manuscript.

Part of this work was published in abstract form.

AUTHOR CONTRIBUTIONS

AT prepared the disease model and wrote the first draft of the manuscript. TY, KN, TT, RI, and CND-G prepared the disease models and measured parameters. AM and SW performed the transmission microscopic study. MT, YO, and AU measured parameters and performed the *in vitro* experiments. YT, LQ, TK, and VFD provided intellectual contribution. YY and ECG corrected the manuscript draft and designed the study.

SUPPLEMENTARY MATERIAL

Supplementary File (PDF)

Supplementary Materials and Methods.

Table S1. Characteristics of the subjects.

Table S2. Primers for RT-PCR of mouse tissues.

Table S3. Primers for RT-PCR of human podocytes.

Figure S1. Soluble thrombomodulin fragments correlate with TGFβ1 and creatinine in patients with DM.

Figure S2. Human TGFβ1–bacterial artificial chromosome (BAC) construct.

Figure S3. Founder mice expressing the full-length of human *TGFβ1* gene.

Figure S4. Characterization of the glomerulus-specific transforming growth factor β1 transgenic mouse.

Figure S5. The human TGFβ1 transgenic mouse has increased markers of kidney injury.

Figure S6. Therapy with recombinant human thrombomodulin (rhTM) reduces foot process effacement of podocytes and thickening of glomerular basement membrane.

Figure S7. TGFβ1 transgenic mice treated with recombinant human thrombomodulin (rhTM) have low concentration of profibrotic factors and HMGB1 in renal tissue.

Figure S8. Therapy with recombinant human thrombomodulin (rhTM) increases generation of activated protein C, inhibits the complement system, decreased circulating soluble podocin, although exerts no effect on the coagulation system in TGFβ1 transgenic mouse.

Figure S9. Therapy with recombinant human thrombomodulin (rhTM) reduces the urine concentration of podocin.

Figure S10. Therapy with recombinant human thrombomodulin (rhTM) reduces apoptosis of glomerular cells.

Figure S11. Treatment of TGFβ1-overexpression associated kidney fibrosis with recombinant human thrombomodulin (rhTM) inhibits apoptosis in renal tissue.

Figure S12. Recombinant human thrombomodulin (rhTM) increases the expression of antiapoptotic factors in podocytes.

Figure S13. Recombinant human thrombomodulin (rhTM) suppresses apoptosis of podocytes induced by hydrogen peroxide.

Figure S14. Recombinant human thrombomodulin (rhTM) suppresses apoptosis of podocytes induced by high glucose level.

Figure S15. Recombinant human thrombomodulin (rhTM) increases the activation of the Akt pathways in podocytes.

Figure S16. Therapy with recombinant human thrombomodulin (rhTM) increases Akt phosphorylation in podocytes from TGFβ1-TG mice.

Figure S17. Podocytes from each treatment group of mice express GPR15 mRNA.

Figure S18. Staining of GPR15 in podocytes from a healthy individual and a patient with focal segmental glomerulosclerosis.

Figure S19. Fibroblast growth factor receptor-1 is not involved in the inhibitory activity of recombinant human thrombomodulin (rhTM) in podocytes.

Figure S20. Recombinant human thrombomodulin (rhTM) inhibits epithelial-mesenchymal transition of podocytes.

Figure S21. Therapy with recombinant human thrombomodulin (rhTM) inhibits the expression of α-smooth muscle actin in renal tubules.

Figure S22. G-protein coupled receptor (GPR15) mediates the inhibitory activity of recombinant human thrombomodulin (rhTM) on epithelial-mesenchymal transition of podocytes.

Supplementary References.

REFERENCES

1. Webster AC, Nagler EV, Morton RL, et al. Chronic kidney disease. *Lancet*. 2017;389:1238–1252.
2. Bello AK, Levin A, Tonelli M, et al. Assessment of global kidney health care status. *JAMA*. 2017;317:1864–1881.
3. Levin A, Tonelli M, Bonventre J, et al. Global kidney health 2017 and beyond: a roadmap for closing gaps in care, research, and policy. *Lancet*. 2017;390:1888–1917.
4. Ackland P. Prevalence, detection, evaluation and management of chronic kidney disease. *BMJ*. 2014;348:f7688.
5. Turner JM, Bauer C, Abramowitz MK, et al. Treatment of chronic kidney disease. *Kidney Int*. 2012;81:351–362.
6. Breyer MD, Susztak K. The next generation of therapeutics for chronic kidney disease. *Nat Rev Drug Discov*. 2016;15:568–588.
7. Liu Y. Renal fibrosis: new insights into the pathogenesis and therapeutics. *Kidney Int*. 2006;69:213–217.
8. Liu Y. Cellular and molecular mechanisms of renal fibrosis. *Nat Rev Nephrol*. 2011;7:684–696.
9. Xavier S, Vasko R, Matsumoto K, et al. Curtailing endothelial TGF-beta signaling is sufficient to reduce endothelial-mesenchymal transition and fibrosis in CKD. *J Am Soc Nephrol*. 2015;26:817–829.
10. Higgins SP, Tang Y, Higgins CE, et al. TGF-beta1/p53 signaling in renal fibrogenesis. *Cell Signal*. 2018;43:1–10.
11. Conway EM. Thrombomodulin and its role in inflammation. *Semin Immunopathol*. 2012;34:107–125.
12. Martin FA, Murphy RP, Cummins PM. Thrombomodulin and the vascular endothelium: insights into functional, regulatory, and therapeutic aspects. *Am J Physiol Heart Circ Physiol*. 2013;304:H1585–H1597.
13. Morser J. Thrombomodulin links coagulation to inflammation and immunity. *Curr Drug Targets*. 2012;13:421–431.
14. Roeen Z, Toda M, D'Alessandro-Gabazza CN, et al. Thrombomodulin inhibits the activation of eosinophils and mast cells. *Cell Immunol*. 2015;293:34–40.
15. Takagi T, Taguchi O, Toda M, et al. Inhibition of allergic bronchial asthma by thrombomodulin is mediated by dendritic cells. *Am J Respir Crit Care Med*. 2011;183:31–42.
16. Tateishi K, Imaoka M, Matsushita M. Dual modulating functions of thrombomodulin in the alternative complement pathway. *Biosci Trends*. 2016;10:231–234.
17. Toda M, D'Alessandro-Gabazza CN, Takagi T, et al. Thrombomodulin modulates dendritic cells via both antagonism of high mobility group protein B1 and an independent mechanism. *Allergol Int*. 2014;63:57–66.
18. Van de Wouwer M, Plaisance S, De Vriese A, et al. The lectin-like domain of thrombomodulin interferes with complement activation and protects against arthritis. *J Thromb Haemost*. 2006;4:1813–1824.
19. Sharfuddin AA, Sandoval RM, Berg DT, et al. Soluble thrombomodulin protects ischemic kidneys. *J Am Soc Nephrol*. 2009;20:524–534.
20. Wang H, Vinnikov I, Shahzad K, et al. The lectin-like domain of thrombomodulin ameliorates diabetic glomerulopathy via complement inhibition. *Thromb Haemost*. 2012;108:1141–1153.
21. Yang SM, Ka SM, Wu HL, et al. Thrombomodulin domain 1 ameliorates diabetic nephropathy in mice via anti-NF-kappaB/NLRP3 inflammasome-mediated inflammation, enhancement of NRF2 antioxidant activity and inhibition of apoptosis. *Diabetologia*. 2014;57:424–434.
22. Ohlin AK, Larsson K, Hansson M. Soluble thrombomodulin activity and soluble thrombomodulin antigen in plasma. *J Thromb Haemost*. 2005;3:976–982.
23. Gil-Bernabe P, D'Alessandro-Gabazza CN, Toda M, et al. Exogenous activated protein C inhibits the progression of diabetic nephropathy. *J Thromb Haemost*. 2012;10:337–346.
24. Yasuma T, Yano Y, D'Alessandro-Gabazza CN, et al. Amelioration of diabetes by protein S. *Diabetes*. 2016;65:1940–1951.
25. Havasi A, Borkan SC. Apoptosis and acute kidney injury. *Kidney Int*. 2011;80:29–40.

26. Kuo CH, Sung MC, Chen PK, et al. FGFR1 mediates recombinant thrombomodulin domain-induced angiogenesis. *Cardiovasc Res.* 2015;105:107–117.
27. Pan B, Wang X, Kojima S, et al. The fifth epidermal growth factor like region of thrombomodulin alleviates LPS-induced sepsis through interacting with GPR15. *Thromb Haemost.* 2017;117:570–579.
28. Lu Y, Ye Y, Bao W, et al. Genome-wide identification of genes essential for podocyte cytoskeletons based on single-cell RNA sequencing. *Kidney Int.* 2017;92:1119–1129.
29. Vigolo E, Marko L, Hinze C, et al. Canonical BMP signaling in tubular cells mediates recovery after acute kidney injury. *Kidney Int.* 2019;95:108–122.
30. Nangaku M. Chronic hypoxia and tubulointerstitial injury: a final common pathway to end-stage renal failure. *J Am Soc Nephrol.* 2006;17:17–25.
31. Thomas R, Kanso A, Sedor JR. Chronic kidney disease and its complications. *Prim Care.* 2008;35:329–344, vii.
32. Mozes MM, Bottinger EP, Jacot TA, et al. Renal expression of fibrotic matrix proteins and of transforming growth factor-beta (TGF-beta) isoforms in TGF-beta transgenic mice. *J Am Soc Nephrol.* 1999;10:271–280.
33. Arif E, Solanki AK, Srivastava P, et al. The motor protein Myo1c regulates transforming growth factor-beta-signaling and fibrosis in podocytes. *Kidney Int.* 2019;96:139–158.
34. Ebefors K, Wiener RJ, Yu L, et al. Endothelin receptor-A mediates degradation of the glomerular endothelial surface layer via pathologic crosstalk between activated podocytes and glomerular endothelial cells. *Kidney Int.* 2019;96:957–970.
35. Fu J, Lee K, Chuang PY, et al. Glomerular endothelial cell injury and cross talk in diabetic kidney disease. *Am J Physiol Renal Physiol.* 2015;308:F287–F297.
36. Masum MA, Ichii O, Elewa YHA, et al. Modified scanning electron microscopy reveals pathological crosstalk between endothelial cells and podocytes in a murine model of membranoproliferative glomerulonephritis. *Sci Rep.* 2018;8:10276.
37. Abbate M, Zoja C, Rottoli D, et al. Proximal tubular cells promote fibrogenesis by TGF-beta1-mediated induction of peritubular myofibroblasts. *Kidney Int.* 2002;61:2066–2077.
38. Liu BC, Tang TT, Lv LL, et al. Renal tubule injury: a driving force toward chronic kidney disease. *Kidney Int.* 2018;93:568–579.
39. Loeffler I, Wolf G. Transforming growth factor-beta and the progression of renal disease. *Nephrol Dial Transplant.* 2014;29(suppl 1):i37–i45.
40. Murakami K, Takemura T, Hino S, et al. Urinary transforming growth factor-beta in patients with glomerular diseases. *Pediatr Nephrol.* 1997;11:334–336.
41. Fujiwara K, Kobayashi T, Fujimoto H, et al. Inhibition of cell apoptosis and amelioration of pulmonary fibrosis by thrombomodulin. *Am J Pathol.* 2017;187:2312–2322.
42. Kataoka K, Taniguchi H, Kondoh Y, et al. Recombinant human thrombomodulin in acute exacerbation of idiopathic pulmonary fibrosis. *Chest.* 2015;148:436–443.
43. Tsushima K, Yamaguchi K, Yokoyama T, et al. Thrombomodulin for acute exacerbations of idiopathic pulmonary fibrosis: a proof of concept study. *Pulm Pharmacol Ther.* 2014;29:233–240.
44. Umemura Y, Yamakawa K. Optimal patient selection for anticoagulant therapy in sepsis: an evidence-based proposal from Japan. *J Thromb Haemost.* 2018;16:462–464.
45. Chen Q, Guan X, Zuo X, et al. The role of high mobility group box 1 (HMGB1) in the pathogenesis of kidney diseases. *Acta Pharm Sin B.* 2016;6:183–188.
46. Miyake Y, D'Alessandro-Gabazza CN, Takagi T, et al. Dose-dependent differential effects of thrombin in allergic bronchial asthma. *J Thromb Haemost.* 2013;11:1903–1915.
47. Assady S, Wanner N, Skorecki KL, et al. New insights into podocyte biology in glomerular health and disease. *J Am Soc Nephrol.* 2017;28:1707–1715.
48. Derynck R, Zhang YE. Smad-dependent and Smad-independent pathways in TGF-beta family signalling. *Nature.* 2003;425:577–584.
49. Schuster N, Krieglstein K. Mechanisms of TGF-beta-mediated apoptosis. *Cell Tissue Res.* 2002;307:1–14.
50. Greka A, Mundel P. Cell biology and pathology of podocytes. *Annu Rev Physiol.* 2012;74:299–323.
51. Isaka Y. Targeting TGF-beta signaling in kidney fibrosis. *Int J Mol Sci.* 2018;19:2532.
52. Chang YJ, Cheng YW, Lin RK, et al. Thrombomodulin influences the survival of patients with non-metastatic colorectal cancer through epithelial-to-mesenchymal transition (EMT). *PLoS One.* 2016;11:e0160550.
53. Zheng N, Huo Z, Zhang B, et al. Thrombomodulin reduces tumorigenic and metastatic potential of lung cancer cells by up-regulation of E-cadherin and down-regulation of N-cadherin expression. *Biochem Biophys Res Commun.* 2016;476:252–259.
54. Pan B, Wang X, Nishioka C, et al. G-protein coupled receptor 15 mediates angiogenesis and cytoprotective function of thrombomodulin. *Sci Rep.* 2017;7:692.
55. Chen PS, Wang KC, Chao TH, et al. Recombinant thrombomodulin exerts anti-autophagic action in endothelial cells and provides anti-atherosclerosis effect in apolipoprotein E deficient mice. *Sci Rep.* 2017;7:3284.
56. Chung JJ, Okamoto Y, Coblitz B, et al. PI3K/Akt signalling-mediated protein surface expression sensed by 14-3-3 interacting motif. *FEBS J.* 2009;276:5547–5558.
57. Sanchez-Capelo A. Dual role for TGF-beta1 in apoptosis. *Cytokine Growth Factor Rev.* 2005;16:15–34.
58. Griffin JH, Zlokovic BV, Mosnier LO. Activated protein C, protease activated receptor 1, and neuroprotection. *Blood.* 2018;132:159–169.
59. Isermann B, Vinnikov IA, Madhusudhan T, et al. Activated protein C protects against diabetic nephropathy by inhibiting endothelial and podocyte apoptosis. *Nat Med.* 2007;13:1349–1358.
60. Klos A, Tenner AJ, Johswich KO, et al. The role of the anaphylatoxins in health and disease. *Mol Immunol.* 2009;46:2753–2766.
61. Morigi M, Perico L, Corna D, et al. C3a receptor blockade protects podocytes from injury in diabetic nephropathy. *JCI Insight.* 2020;5:e131849.
62. Conery AR, Cao Y, Thompson EA, et al. Akt interacts directly with Smad3 to regulate the sensitivity to TGF-beta induced apoptosis. *Nat Cell Biol.* 2004;6:366–372.
63. Derynck R, Muthusamy BP, Saeteurn KY. Signaling pathway cooperation in TGF-beta-induced epithelial-mesenchymal transition. *Curr Opin Cell Biol.* 2014;31:56–66.
64. Remy I, Montmarquette A, Michnick SW. PKB/Akt modulates TGF-beta signalling through a direct interaction with Smad3. *Nat Cell Biol.* 2004;6:358–365.
65. Hamidi A, Song J, Thakur N, et al. TGF-beta promotes PI3K-AKT signaling and prostate cancer cell migration through the TRAF6-mediated ubiquitylation of p85alpha. *Sci Signal.* 2017;10:eaal4186.
66. Peng Z, Weber JC, Han Z, et al. Dichotomy effects of Akt signaling in breast cancer. *Mol Cancer.* 2012;11:61.
67. Zhou F, Geng J, Xu S, et al. FAM83A signaling induces epithelial-mesenchymal transition by the PI3K/AKT/Snail pathway in NSCLC. *Aging (Albany NY).* 2019;11:6069–6088.

Supplementary Material

Thrombomodulin Ameliorates Transforming Growth Factorβ1-mediated Chronic Kidney Disease via the G-Protein Coupled Receptor 15/Akt Signal Pathway

Atsuro Takeshita, Taro Yasuma, Kota Nishihama, Corina N. D' Alessandro-Gabazza, Masaaki Toda, Toshiaki Totoki, Yuko Okano, Akihiro Uchida, Ryo Inoue, Liqiang Qin, Shujie Wang, Valeria Fridman D'Alessandro, Tetsu Kobayashi, Yoshiyuki Takei, Akira Mizoguchi, Yutaka Yano, Esteban C. Gabazza.

Supplementary Material and Methods

Subjects

Blood samples were collected from 48 patients with diabetes mellitus (DM) with controlled glycemia for determination of soluble TM and active TGFβ1 plasma levels. The diagnosis of DM was based on the criteria of the American Diabetes Association.[1] The presence of nephropathy was based on the Criteria reported by the Diabetic Nephropathy Research Group of the Ministry of Health, Labor and Welfare of Japan.[2] Data obtained from 26 healthy volunteers served as controls. **Supplementary Table S1** shows the demography and laboratory data of the subjects.

Preparation of a TGFβ1 bacterial artificial chromosome (BAC) transgenic construct

RP23-5701, a mouse podocin BAC clone, was selected from the C57BL/6J Mouse BAC Library by searching the mouse BAC ends database at the National Center for Biotechnology Information (NCBI). The sequence analysis showed that the BAC clone contains the whole 17 kb of mouse podocin genomic sequence, 69 kb of the 5'-flanking and 139 kb of the 3'-flanking genomic DNA. On the other hand, RP11-638N16, a human TGFβ1 BAC clone, was selected from the human BAC Library by BLAST search of the GenBank database at NCBI. The sequence analysis of the BAC end showed that the BAC clone contains the whole 23 kb of human TGFβ1 genomic sequence, and additionally, a 57 kb of the 5'-flanking and 115 kb of the 3'-flanking genomic DNA. The BAC clones were obtained from the BACPAC Resources Center at the Children's Hospital Oakland Research Institute (CHORI, Oakland, CA).

A mouse-podocin/human-TGFβ1 BAC transgenic construct that contains the full length coding exons and an intervening intron of human TGFβ1 was prepared by BAC *recombination* genetic engineering. The Red/ET Counter Selection BAC Modification Kit (Gene Bridges, Heidelberg, Germany) was used to transfer the human TGFβ1 gene from the human BAC clone to the mouse podocin BAC clone following a methods previously described.[3] Briefly, a rpsL-kan counter selection cassette flanked by sequences of an intervening intron of the human TGFβ1 gene was amplified by PCR. The amplified rpsL-kan counter selection cassette was inserted into the TGFβ1 gene from the human BAC clone by Red/ET recombination. The TGFβ1 gene was subcloned into plasmid SacB-pBluescript by Red/ET recombination using both end sequences of the human TGFβ1 gene as

homology arms. The human TGFβ1 gene fragment was flanked by nucleotides from the mouse podocin gene untranslated regions, adjacent to the start codon (5' end) and the stop codon (3' end). To generate the chimeric podocin-TGFβ1 BAC clone, the human TGFβ1 gene fragment was transferred to the mouse podocin gene in the mouse BAC clone by Red/ET recombination. The rpsL-neo cassette in the intron of human TGFβ1 gene was then removed and the BAC modification was sequenced for confirmation. To purify the podocin-TGFβ1 BAC transgenic construct we extracted it from the cultured *E. coli*, linearized, separated by pulsed field gel electrophoresis, extracted from the gel by electroelution and finally dialyzed before using for microinjection.

Generation of the TGFβ1 BAC TG mouse

TGFβ1 BAC TG mouse expressing the full-length human TGFβ1 gene under the control of the mouse podocin promoter control was generated by pronuclear injection into 392 C57BL/6J mouse embryos (CLEA Japan, Inc., Tokyo, Japan) before transfer to pseudopregnant mice. We assessed the TG founders and germ line transmission of the BAC TG construct by Southern blotting of PstI-digested tail DNA probed by the [32P]-labeled intron 1 fragment of the human TGFβ1 gene. Eight of 52 progeny contained the transgene from which a colony was derived.

Sample collection and histopathological evaluation

The animals were euthanized by intraperitoneal injection of an overdose of pentobarbital sodium on day 29 after the start of the experiment and samples were collected for biochemical analysis and tissue staining. Blood was collected by closed-chest heart puncture into tubes containing 10 U/ml heparin as anticoagulant. Urine was collected using metabolic cages. After flushing the systemic circulation with physiological saline, we dissected each kidney, separated and weighed. The left kidney was stored at -80˚C until analysis and the right kidney was fixed in 10% paraformaldehyde, dehydrated, embedded in paraffin, and cut into 3-μm thick sections to stain with hematoxylin/eosin (H&E), periodic acid-Schiff (PAS) or Masson's trichrome. Glomerular sclerosis was assessed based on the extent of glomerular PAS staining following a previously reported method.[4] We used an Olympus BX53 microscope with a digital camera attachment Olympus DP73 (Tokyo, Japan) to capture the images from resected kidneys. To evaluate glomerular sclerosis, we randomly selected 25 glomerular per mouse, and scored according to PAS positive area as follows: score 0: normal

glomeruli, score 1: mild mesangial thickness (PAS positive area < 25%), score 2: moderate segmental sclerosis (PAS positive area 25-50%), score 3: severe segmental sclerosis (PAS positive area 50-75%), score 4: global sclerosis (PAS positive area≧75%). We defined the average score from 25 glomeruli as the glomerular sclerosis score. Six investigators scored with blind condition. Renal fibrosis was estimated by Masson's trichrome staining. Ten images of kidney cortex per mouse were randomly obtained. The ratio of Masson's trichrome positive area/total kidney cortex area was calculated using WinROOF image processing software (Minani Corp., Fukui, Japan).

Biochemical analysis

The concentrations of activated protein C/αantitrypsin complex was measured as described before.[5] Plasma and urine creatinine levels were measured by enzymatic method and blood urea nitrogen by colorimetric method (NCal^{TM} NIST-Calibrated kit; Arbor Assays, Ann Arbor, MI) according to the manufacturer's instructions. Urinary liver-type fatty acid binding protein (L-FABP), a marker of nephropathy severity, and kidney injury molecule 1 (KIM-1), a marker of tubular damage, were measured using commercial enzyme immunoassay kits (R&D). The concentration of plasminogen activator inhibitor-1 was measured as previously described.[6] The concentration of podocin was measured using commercial immunoassay kits from Cloud-Cone Corporation (Katy, TX) following the manufacturer's instructions. The clinical parameters in patients with DM were measured by routine and standard methods at the Central Clinical Laboratory of Mie University Hospital.

Transmission electron microscopy

Under profound anesthesia with pentobarbital we performed transcardial perfusion of the mice using a cacodylate-buffered solution containing 2 mM $CaCl_2$, 4% paraformaldehyde, and 2.5% glutaraldehyde at room temperature for 5 min as described.[7] The kidneys we then removed and post-fixed in the same cacodylate-buffered solution at 4 ºC. Tissue sections were prepared and further processed for observation with a transmission electron microscope (JEM-1010, JEOL, Tokyo, Japan) as previously described.[7, 8] The width of the podocuyte foot process and glomerular basement membrane thickening was measured as described.[9]

Isolation of podocytes from each treatment group of mice

After euthanasia by an overdose of pentobarbital, the kidneys were dissected, minced in small

pieces and incubated in 2 mg/ml collagenase solution at 37ºC for 40 min. After passing the through a 100-µm cell strainer, the preparation was treated with an ammonium-chloride-potassium solution to remove red blood cells. Following separation by centrifugation, the pellet was re-suspended in a solution containing 0.5 mg collagenase, 0.5 mg/ml dispase II, 0.075% trypsin, incubated at 37ºC for 20 min and passed through a 25-µm cell strainer. The cell suspension was treated with 2.5 µg anti-CD31 antibody and CD31-positive endothelial cells were removed using CD31 microbeads and MACS system (Miltenyi Biotec, Rhine-Westphalia, Germany). CD31-negativee cells were treated with 10 µg rabbit anti-nephrin and then nephrin-positive cells were collected using anti-rabbit IgG microbeads and a MACS system (Miltenyi Biotec).

Evaluation of epithelial-mesenchymal transition

Podocytes were cultured up to subconfluency, treated with 200 nM rhTM for 1h before adding 10 ng/ml TGFβ1 and culture for 48h. The cells were then fixed with 4% paraformaldehyde for 10 min at room temperature and stained with rabbit anti-NPHS-2 (Abcam, Cambridge, UK), and mouse anti ACTA2 (Santa Cruz Biotechnology, Santa Cruz, CA) followed by treatment with the secondary antibodies AF594 anti-rabbit IgG (Invitrogen) and AF488 anti-mouse IgG (Invitrogen). After washing, the sections were counterstained with 4,6-diamidino-2-phenylindole (DAPI) and mounted using a fluorescence mounting medium. In a separate experiment, human podocytes were cultured up to subconfluency, starved overnight and then treated with 10 ng/ml TGFβ1 1h before adding 200 nM rhTM to the culture medium. Culture cells were harvested 48 after treatment with rhTM to evaluate mesenchymal markers.

Evaluation of apoptosis

Apoptosis of primary human podocyte cells was analyzed by flow cytometry (BD Biosciences, Oxford, UK) after staining with FITC-annexin V (BD Pharmingen) and propidium iodide. DNA content/cell cycle analysis was also analyzed by flow cytometry after treating the cells with propidium iodide. To evaluate the anti-apoptotic activity of rhTM, cultured podocytes were pre-treated with 200 nM rhTM for 1h before adding 10 ng/ml TGFβ1 or control (saline) and continuing the culture for 48h. The effect of rhTM on apoptosis of podocytes was also evaluated by culturing them in the presence of 1 mM H_2O_2 or 30 mM glucose for 24h after pre-treating the cells with 200 nM rhTM for 1h. The

mRNA expression of the inhibitor of baculoviral inhibitor of apoptosis repeat-containing (BIRC) 3/inhibitor of apoptosis (IAP) and B-cell lymphoma 2 (Bcl-2) family of regulator proteins were evaluated by reverse transcriptase PCR. DNA fragmentation was evaluated by the terminal deoxynucleotidyl transferase dUTP Nick-End Labeling (TUNEL) method at the Biopathology institute Corporation using Alexa Fluor 594 goat anti-rabbit IgG and slow-fade gold-antifade reagent with 4',6-diamidino-2-phenylindole (DAPI).

Evaluating mediation of fibroblast growth factor receptor-1 (FGFR1) and G-protein coupled receptor 15 (GPR15) in TM activity

Human primary podocyte cells were transfected with 33 nmol of FGFR1 siRNA, GPR15 siRNA or scrambled siRNA for 48h, and then 200 nM rhTM was added to the cell culture 1h before treating with 10 ng/ml TGFβ1. Apoptotic cells were assessed by flow cytometry and epithelial-mesenchymal transition by immunohistochemistry and reverse transcriptase polymerase chain reaction (RT-PCR) after 48h. In a separate experiment, human primary podocyte cells were treated with 200 nM rhTM and with 1 μM PD-161570, a FGFR1 inhibitor, and then apoptotic cells were assessed by flow cytometry after 48h.

Western blotting

Western blotting was performed following standard methods using antibodies against phosphorylated Akt, total Akt, cleaved form of caspase-3 and β-actin from Cell Signaling (Danvers, MA) and antibody against podocin Abcam Incorporation (Cambridge, MA).

Immunofluorescence staining

Immunostaining was performed using commercially available rabbit polyclonal anti-podocin (NPHS2; abcam, Cambridge, UK), monoclonal anti-αsmooth muscle actin (αSMA; cone # 1A4; R&D System, Minneapolis, MN), rabbit polyclonal anti-phosphorylated-Akt (Cell Signaling, Danvers, MA) and rabbit polyclonal anti-GPR15 (Aviva Systems Biology, San Diego, CA) antibodies at MorphoTechnology Incorporation (Sapporo, Japan).

software (Mitani Corp., Fukui, Japan).

Immunohistochemical staining of GPR15 in human kidney samples

Staining of GPR15 was performed at MorphoTechnology Corporation (Sapporo, Hokkaido, Japan).

Commercially available paraffinized preparations of human kidney tissues from a healthy control and from a patient with chronic glomerulosclerosis were purchased from OriGene (Rockville, MD). The samples were deparaffinized with xylene and re-hydrated using ethanol series and Tris-buffered saline. The samples were treated with 0.3% H_2O_2 in methanol for 30 min for blocking endogenous peroxidase and then blocked. After washing with Tris-buffered saline, GPR15 was stained using rabbit polyclonal anti-GPR15 antibody (Aviva Systems Biology Corporation, San Diego, CA) and horseradish peroxidase-labelled mouse anti-rabbit IgG antibody following to standard methods.

Analysis of gene expression

The total RNA from renal tissues or cell lysates extracted by Trizol Reagent (Invitrogen, Carlsbad, CA) was reverse transcribed using oligo-dT primers to amplify DNA by PCR using the Superscript Preamplification system kit (Invitrogen). The Applied Biosystem Step One Real-Time PCR System, Taqman master mix and SYBR green were used for quantitative amplification. Primer sequences are described in **Supplementary Table S1 and Supplementary Table S2**. Gene expression was normalized by the GAPDH transcription level.

Supplementary Table S1. Characteristics of the subjects.

Variables	Nephropathy (-)	Nephropathy (+)	*P values
No of subjects	32	16	
Sex (Male/Female)	16/16	7/9	
Type of diabetes (1/2/others)	9/21/2	0/16/0	
Age (year-old)	57.0(48.3-71.0)	57.0(47.0-70.5)	0.4978
Diabetes duration (years)	10.0(3.0-21.8)	22.5(6.3-26.5)	0.0637
Systolic blood pressure (mmHg)	119.0(113.3-134.0)	138.5(114.3-165.3)	0.0219
Diastolic blood pressure (mmHg)	66.0(57.0-83.3)	75.5(68.5-81.8)	0.0586
Hemoglobin A1c (%)	9.2(7.7-10.1)	9.9(8.7-13.3)	0.0405
Fasting blood glucose (mg/dl)	114.0(95.5-145.5)	177(136.0-223.8)	<0.0001
Creatinine (mg/dL)	0.5(0.5-0.7)	0.8(0.6-1.1)	0.0067
eGFR (ml/min/1.73m^2)	89.5(79.6-105.3)	61.8(48.4-94.2)	0.0065
Urine microalbumin (mg/gCre)	12.0(4.9-16.9)	586.9(118.7-1534.0)	<0.0001
Total cholesterol (mg/dl)	182.0(162.5-196.0)	198.0(167.8-230.3)	0.0824

Data are the median ± interquartile range. eGFR, estimated glomerular filtration rate.

*Statistical analysis by Mann-Whitney U test.

Supplemental Table S2. Primers for RT-PCR of mouse tissues

	Sequence (5' -> 3')	Tm	Reference	Location	Product size
BIRC1a (NAIP1)					
Sense	TGCCCAGTATATCCAAGGCTAT	60.2	NM_008670	708-729	116 bp
Antisense	AGACGCTGTCGTTGCAGTAAG	62.6		823-803	
BIRC1b (NAIP2)					
Sense	AGCTTGGTGTCTGTTCTCTGT	61	NP_001119654	1204-1224	180 bp
Antisense	GCGGAAAGTAGCTTTGGTGTAG	61.2		1383-1362	
BIRC2 (c-IAP1)					
Sense	TGTGGCCTGATGTTGGATAAC	60	NM_007465	256-276	164 bp
Antisense	GGTGACGAATGTGCAAATCTACT	60.9		419-397	
BIRC3 (c-IAP2)					
Sense	ACGCAGCAATCGTGCATTTTG	62.9	NM_007464	1073-1093	181 bp
Antisense	CCTATAACGAGGTCACTGACGG	61.6		1253-1232	
BIRC4 (x-IAP)					
Sense	CGAGCTGGGTTTCTTTATACCG	60.7	NM_009688	145-166	126 bp
Antisense	GCAATTTGGGGATATTCTCCTGT	60.4		270-248	
BIRC5 (Survivin)					
Sense	GAGGCTGGCTTCATCCACTG	62.6	NM_009689	118-137	250 bp
Antisense	CTTTTTGCTTGTTGTTGGTCTCC	60.7		367-345	
BIRC6 (Apollon)					
Sense	ACAGATTGTCTTACCTCTTGCCC	61.9	NM_007566	695-717	120 bp
Antisense	GCCACGAAGTGAAGGTCTCC	62.5		814-795	
BIRC7 (ml-IAP)					
Sense	AGCCTCCTTCTACGACTGG	60.1	NM_001163247	291-309	245 bp
Antisense	GCAAAGGGGTGTAGGTCTGG	62.2		535-516	
Podocin					
Sense	AAGCTGAGGCACAAAGACAGG	64	NM-130456	848-868	416 bp
Antisense	CTATTTGGCAACCAAACAAGTG	62		1263-1242	
Bcl-2					
Sense	AGCTGCACCTGACGCCCTT	69.6	NM_009741	1754-1772	192 bp
Antisense	GTTCAGGTACTCAGTCATCCAC	60.1		1947-1926	
Bcl-xL					
Sense	AGGTTCCTAAGCTTCGCAATTC	64.4	NM_001289716	128-149	248 bp
Antisense	TGTTTAGCGATTCTCTTCCAGG	64.2		375-354	
Bax					
Sense	CGGCGAATTGGAGATGAACTG	68.7	NM_007527	313-333	161 bp
Antisense	GCAAAGTAGAAGAGGGCAACC	63.8		473-453	
Col1a1					
Sense	TAAGGGTCCCCAATGGTGAGA	67.4	NM007742	107-127	203 bp
Antisense	GGGTCCCTCGACTCCTACAT	64.2		309-290	
mTGFβ1					
Sense	ACTCCACGTGGAAATCAACGG	64	NM-011577	693-713	414 bp
Antisense	TAGTAGACGATGGGCAGTGG	62		1106-868	
GPR15					
Sense	AACGCGGCAACCGAAGATT	62.9	NM_001162955	182-200	105 bp
Antisense	GAGAGGCTTCCTTATCCATCCA	60.7		286-265	
Nephrin					
Sense	CTCTGGCGGAGAAGACTGAGG	67.6	NM_019459.2	3381-3401	370 bp
Antisense	CAGGCCAGCGAAGGTCATAGG	69.9		3750-3730	
WT-1					
Sense	AGCACGGTCACTTTCGACG	62.6	NM_144783	652-670	85 bp
Antisense	GTTTGAAGGAATGGTTGGGGAA	60.7		736-715	
GAPDH					
Sense	TGGCCTTCCGTGTTCCTAC	61.3	NM_008084	686-704	178 bp
Antisense	GAGTTGCTGTTGAAGTCGCA	60.9		863-844	

BIRC1a,1b, 2, 3, 4, 5, 6, or 7: baculoviral iap repeat-containing 1a, 1b, 2, 3, 4, 5, 6, or 7; NAIP1, or 2: neuronal apoptosis inhibitory protein1, or 2; c-IAP1, or 2: cellular inhibitor of apoptosis protein 1, or 2; x-IAP: x-linked inhibitor of apoptosis protein; ml-IAP: melanoma inhibitor of apoptosis; TGFβ1: transforming growth factor-β1; GAPDH: glyceraldehyde 3-phosphate dehydrogenase.

Supplemental Table S3. Primers for RT-PCR of human podocytes

	Sequence (5' -> 3')	Tm	Reference	Location	Product size
BIRC1 (NAIP1)					
Sense	TACGAAGAACTACGGCTGGAC	61.2	NM_00453	829-849	180 bp
Antisense	GGTGTGATCGTCTAATGGGTCA	61.5		1008-987	
BIRC2 (c-IAP1)					
Sense	GTTCAGTGGTTCTTACTCCAGC	60.6	NM_001166	444-465	91 bp
Antisense	ACTGTAGGGGTTAGTCCTCGAT	61.4		534-513	
BIRC3 (c-IAP2)					
Sense	TTTCCGTGGCTCTTATTCAAACT	60.2	NM_001165	399-421	96 bp
Antisense	GCACAGTGGTAGGAACTTCTCAT	61.9		494-472	
BIRC4 (x-IAP)					
Sense	TATCAGACACCATATACCCGAGG	60.2	NM_001167	446-468	98 bp
Antisense	TGGGGTTAGGTGAGCATAGTC	60.7		543-523	
BIRC5 (Survivin)					
Sense	GAGGCTGGCTTCATCCACTG	62.6	NM_001012270	44-64	118 bp
Antisense	CTTTTTGCTTGTTGTTGGTCTCC	61.7		161-141	
BIRC6 (Apollon)					
Sense	TGCACAGTTTCCTTGTACGGA	62.6	NM_016252	1128-1148	207 bp
Antisense	GAGCTTGGGTCTCCTGATAGAA	60.6		1334-1313	
BIRC7 (ml-IAP)					
Sense	GCTCTGAGGAGTTGCGTCTG	62.5	NM_139317	254-273	245 bp
Antisense	CACACTGTGGACAAAGTCTCTT	60.1		498-477	
BIRC8 (ILP-2)					
Sense	GCGCTCAGAAAGACACTACAG	60.7	NM_033341	464-484	93 bp
Antisense	CCTCTTGCAGACGCCTTAGC	62.9		556-537	
Bcl-2					
Sense	GCCTTCTTTGAGTTCGGTGG	60.9	NM_000657	445-464	192 bp
Antisense	ATCTCCCGGTTGACGCTCT	62.7		497-479	
Bcl-xL					
Sense	AGGTTCCTAAGCTTCGCAATTC	64.4	NM_001289716	128-149	248 bp
Antisense	TGTTTAGCGATTCTCTTCCAGG	64.2		375-354	
Bax					
Sense	GACTGAATCGGAGATGGAGACC	61.6	NM_001191	120-141	179 bp
Antisense	CCAGCCCATGATGGTTCTGAT	61.9		298-279	
αSMA					
Sense	GTGTTGCCCCTGAAGAGCAT	62.5	NM_001613	290-309	364 bp
Antisense	GCTGGGACATTGAAAGTCTCA	60		398-378	
Col1a1					
Sense	AACCTGGATGCCATCAAACTC	65	NM_000088	3847-3867	287 bp
Antisense	TCCATGTAGGCCACGCTGTTC	69.3		4113-4133	
Fibronectin (FN1)					
Sense	CGGTGGCTGTCAGTCAAAG	60.7	NM_212482	125-143	130 bp
Antisense	AAACCTCGGCTTCCTCCATAA	60.9		254-234	
Vimentin (VIM)					
Sense	GAGAACTTTGCCGTTGAAGC	63.7	NM_003380	1507-1526	163 bp
Antisense	GCTTCCTGTAGGTGGTGGCAATC	69.6		1669-1655	
E-cadherin (CDH1)					
Sense	GTATCTTCCCCGCCCTGCCAATCC	75.9	NM_004360	2514-2537	765 bp
Antisense	CCTGGCCGATAGAATGAGACCCT	72.2		3278-3255	
Human TGFβ1					
Sense	AAGACTATCGACATGGAGCTGG	64.3	NM_001256799	108-128	444 bp
Antisense	GTATCGCCAGGAATTGTTGCTG	67.4		304-282	
GAPDH					
Sense	GGAGCGAGATCCCTCCAAAAT	61.6	NM_008084	686-704	197 bp
Antisense	GGCTGTTGTCATACTTCTCATGG	60.9		863-844	

BIRC1, 2, 3, 4, 5, 6, or 7: baculoviral iap repeat-containing 1, 2, 3, 4, 5, 6, or 7; NAIP1: neuronal apoptosis inhibitory protein1, or 2; c-IAP1, or 2: cellular inhibitor of apoptosis protein 1, or 2; x-IAP: x-linked inhibitor of apoptosis protein; ml-IAP: melanoma inhibitor of apoptosis; TGFβ1: transforming growth factor-β1; GAPDH: glyceraldehyde 3-phosphate dehydrogenase.

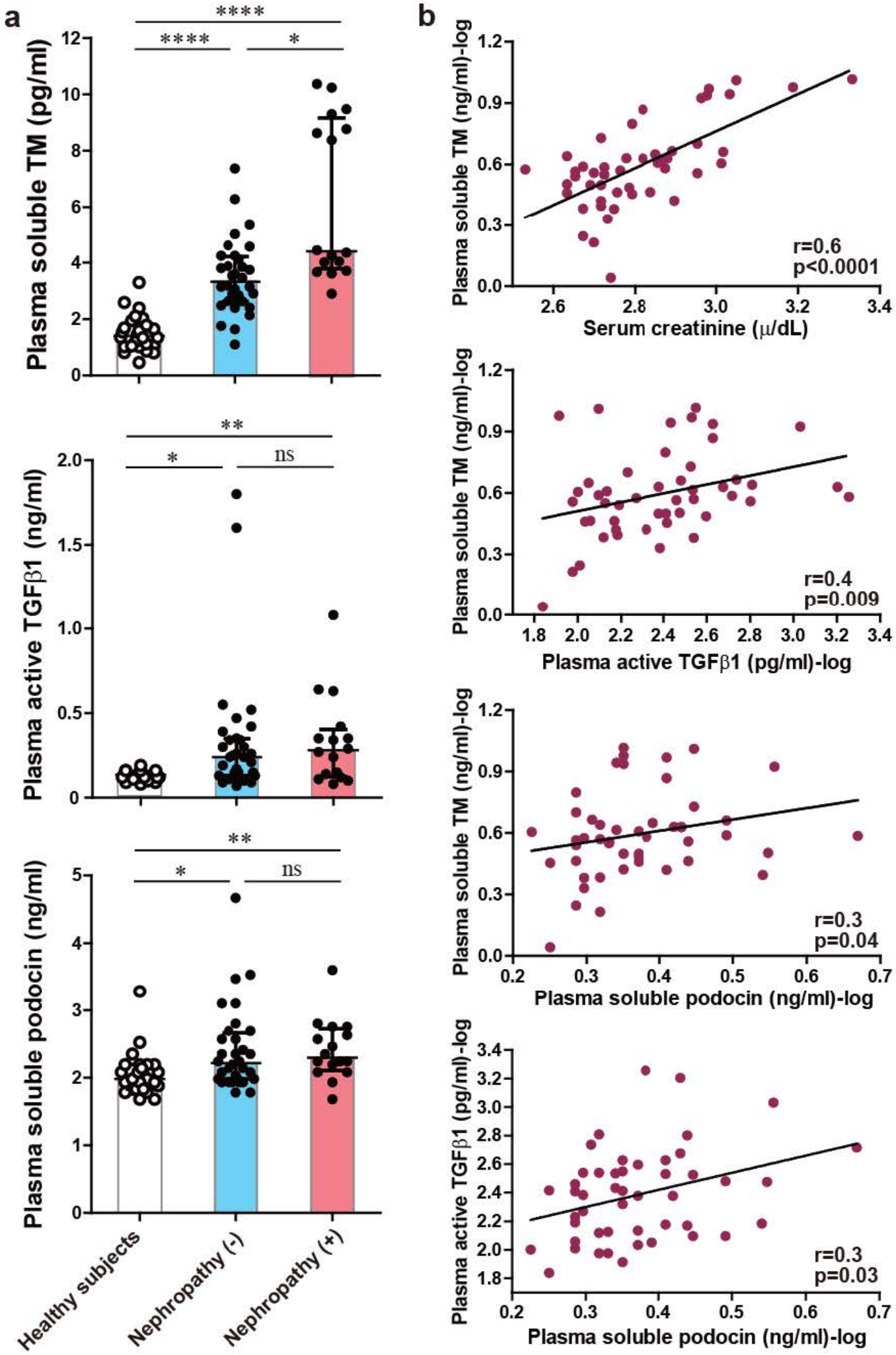
a
b
Plasma soluble TM (pg/ml)
Plasma active TGFβ1 (ng/ml)
Plasma soluble podocin (ng/ml)
****
****
*
**
*
ns
**
*
ns
Healthy subjects
Nephropathy (-)
Nephropathy (+)
Plasma soluble TM (ng/ml)-log
Serum creatinine (μ/dL)
r=0.6
p<0.0001
Plasma active TGFβ1 (pg/ml)-log
r=0.4
p=0.009
Plasma soluble podocin (ng/ml)-log
r=0.3
p=0.04
Plasma active TGFβ1 (pg/ml)-log
r=0.3
p=0.03

Supplementary Figure S1. Soluble thrombomodulin fragments correlate with TGFβ1 and creatinine in DM patients. The concentrations of soluble thrombomodulin fragment, active TGFβ1 and podocin were measured by enzyme immunoassay as described under material and methods. The concentration of creatinine was measured by an enzymatic method at the Central Clinical Laboratory of our institution. Data are expressed as the median ± interquartile range. Statistical analysis by Mann-Whitney U test and Spearman correlation. ns, not significant; TM, thrombomodulin. *p<0.05, **p<0.01, ****p<0.001.

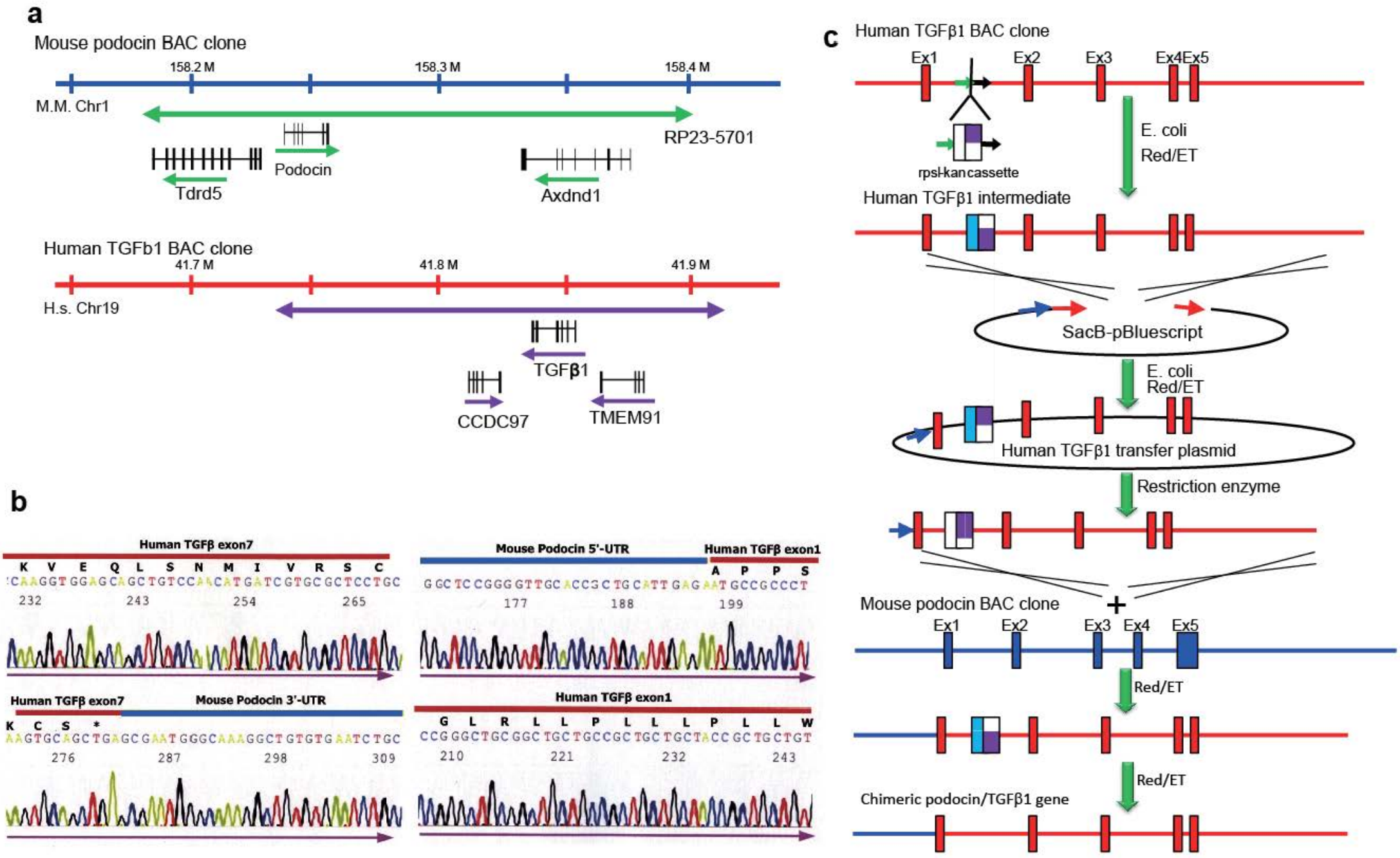
a
Mouse podocin BAC clone
158.2 M
158.3 M
158.4 M
M.M. Chr1
RP23-5701
Podocin
Tdrd5
Axdnd1
Human TGFb1 BAC clone
41.7 M
41.8 M
41.9 M
H.s. Chr19
TGFβ1
CCDC97
TMEM91
b
Human TGFβ exon7
K V E Q L S N M I V R S C
232
243
254
265
Mouse Podocin 5'-UTR
Human TGFβ exon1
A P P S
177
188
199
Human TGFβ exon7
Mouse Podocin 3'-UTR
K C S *
276
287
298
309
Human TGFβ exon1
G L R L L P L L L P L L W
210
221
232
243
c
Human TGFβ1 BAC clone
Ex1
Ex2
Ex3
Ex4Ex5
rpsl-kan cassette
E. coli
Red/ET
Human TGFβ1 intermediate
SacB-pBluescript
E. coli
Red/ET
Human TGFβ1 transfer plasmid
Restriction enzyme
Mouse podocin BAC clone
+
Ex1
Ex2
Ex3
Ex4
Ex5
Red/ET
Red/ET
Chimeric podocin/TGFβ1 gene

Supplementary Figure S2. Human TGFβ1–bacterial artificial chromosome (BAC) construct. (a) Structure of the mouse podocin and human TGFβ1 BAC clones. Both clones are composed of the full-length coding sequence and 5′- and 3′-flanking sequences. (b) Sequence of the BAC construct. (c) Diagram of the transgene construction. The coding region of mouse podocin was replaced by the human TGFβ1 sequence by Red/ET recombination. The chimeric podocin–TGFβ1 BAC transgenic construct contains a unique PstI (Pst1) to allow genotyping of transgenic mice. In (b) and (c), brown and red colors indicate human origin, and blue color indicates mouse origin. Ex, exon.

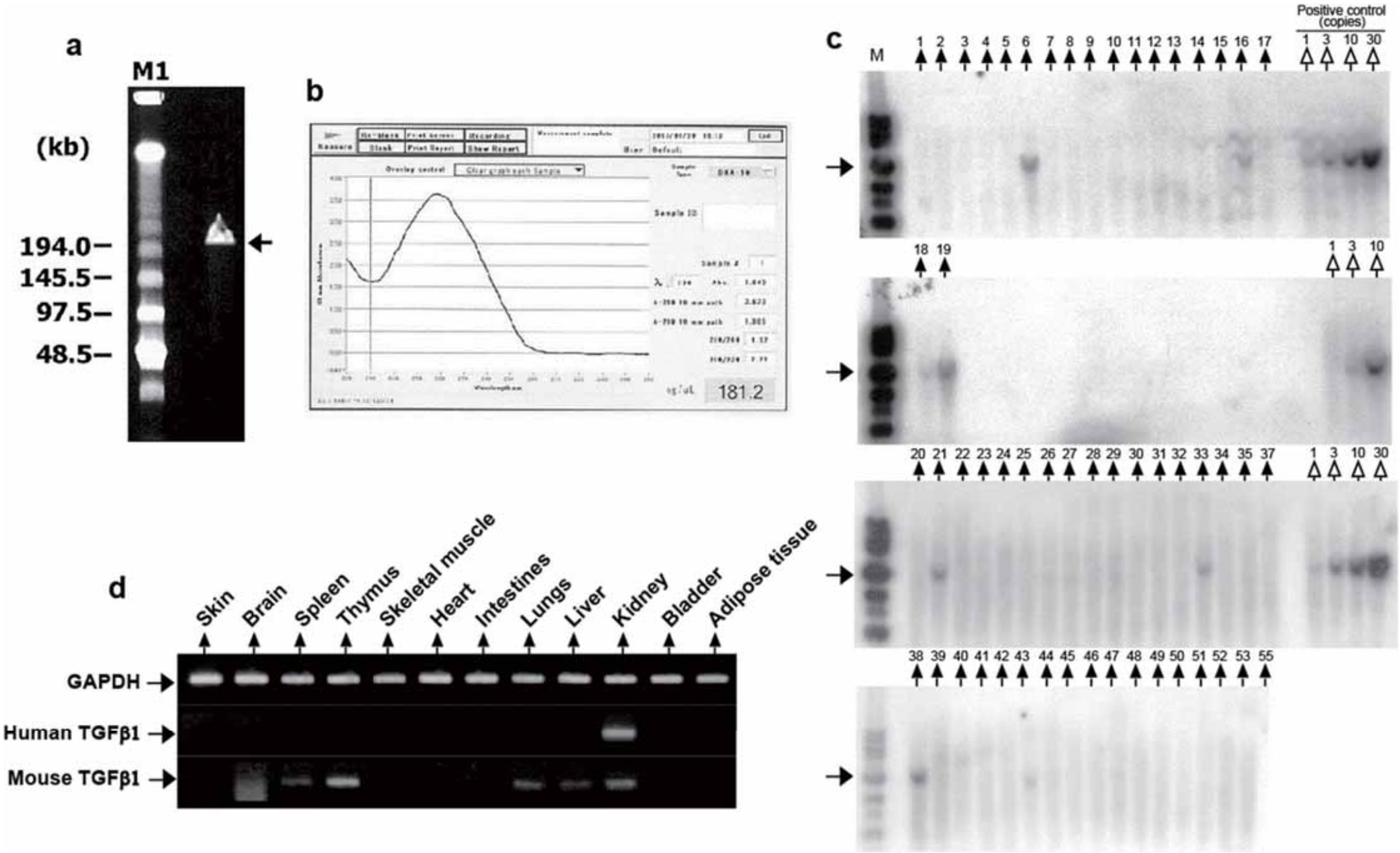
a
M1
(kb)
194.0
145.5
97.5
48.5
b
181.2
c
M
1 2 3 4 5 6 7 8 9 10 11 12 13 14 15 16 17
Positive control (copies)
1 3 10 30
18 19
1 3 10
20 21 22 23 24 25 26 27 28 29 30 31 32 33 34 35 37
1 3 10 30
38 39 40 41 42 43 44 45 46 47 48 49 50 51 52 53 55
d
Skin
Brain
Spleen
Thymus
Skeletal muscle
Heart
Intestines
Lungs
Liver
Kidney
Bladder
Adipose tissue
GAPDH
Human TGFβ1
Mouse TGFβ1

Supplementary Figure S3. Founder mice expressing the full-length of human TGFβ1 gene. (a), (b) The TGFβ1 bacterial artificial chromosome (BAC) transgenic construct was purified. The purified TGFβ1 BAC transgenic construct is almost 200 kb. Lane M indicates low range marker with the sizes marked. (c) The tail DNA from TGFβ1 BAC transgenic founder lines were analyzed by Southern blotting. The copy number of the transgenes was determined by comparing with the control for copy number intensity. (d) Genotyping by polymerase chain reaction (PCR) shows that the human TGFβ1 BAC TG mice express the transgene only in the kidneys.

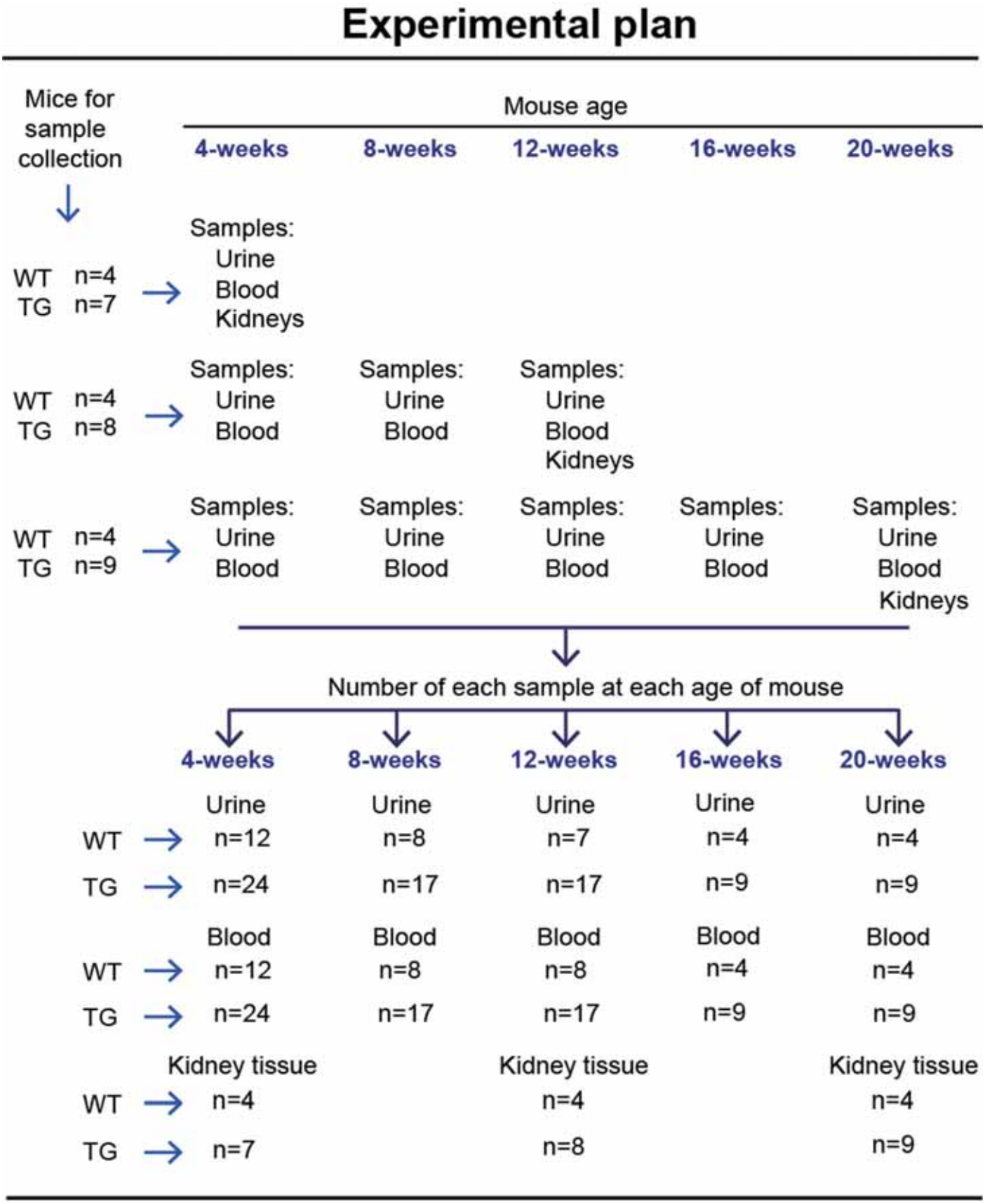

Supplementary Figure S4. Characterization of the glomerulus-specific transforming growth factorβ1 transgenic mouse. Several pathological and functional parameters of the kidneys were measured every 4 weeks for a period of 16 weeks. WT, wild type; TG, transforming growth factor β1 transgenic mouse.

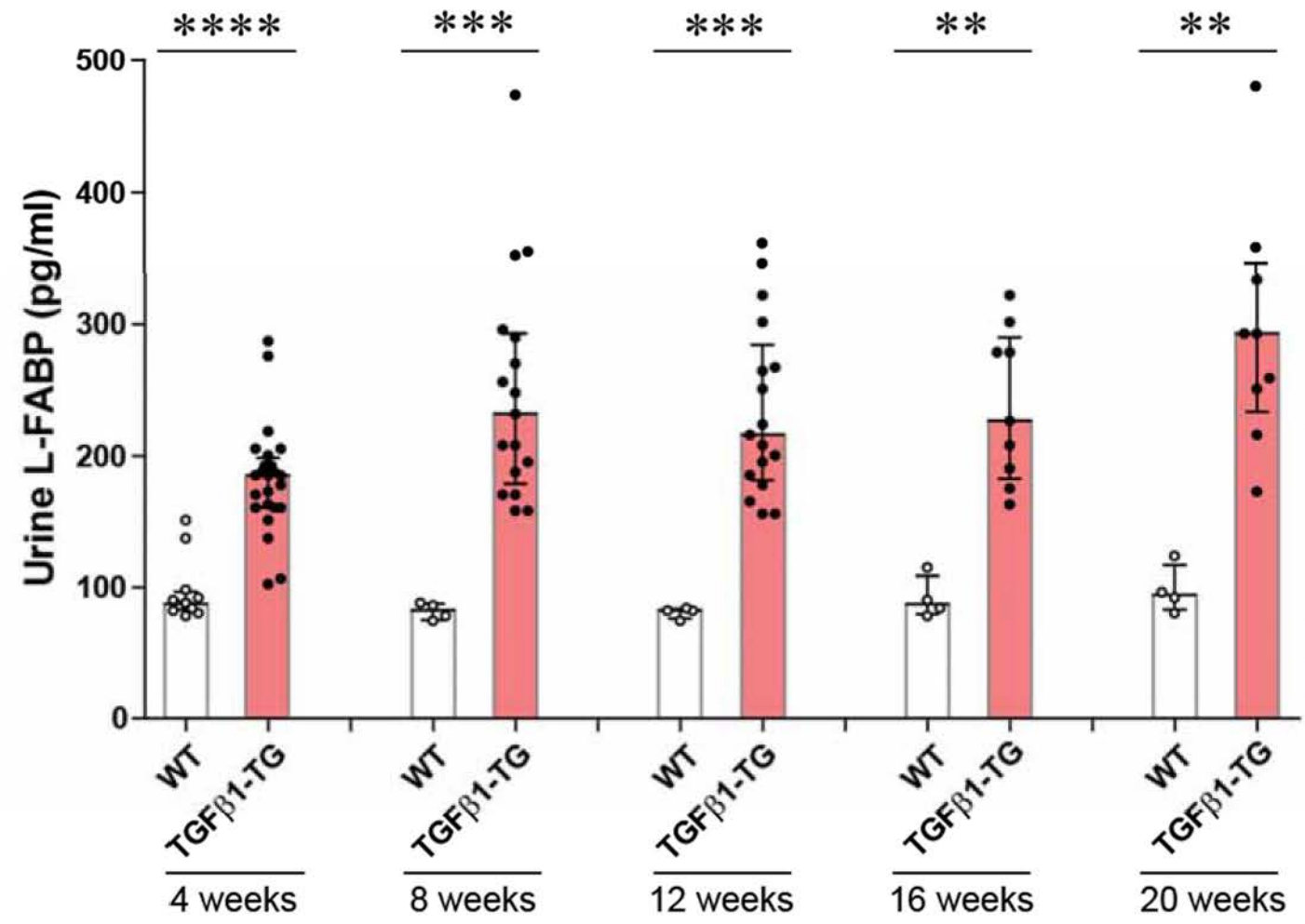
****
***
***
**
**
Urine L-FABP (pg/ml)
500
400
300
200
100
0
WT
TGFβ1-TG
4 weeks
8 weeks
12 weeks
16 weeks
20 weeks

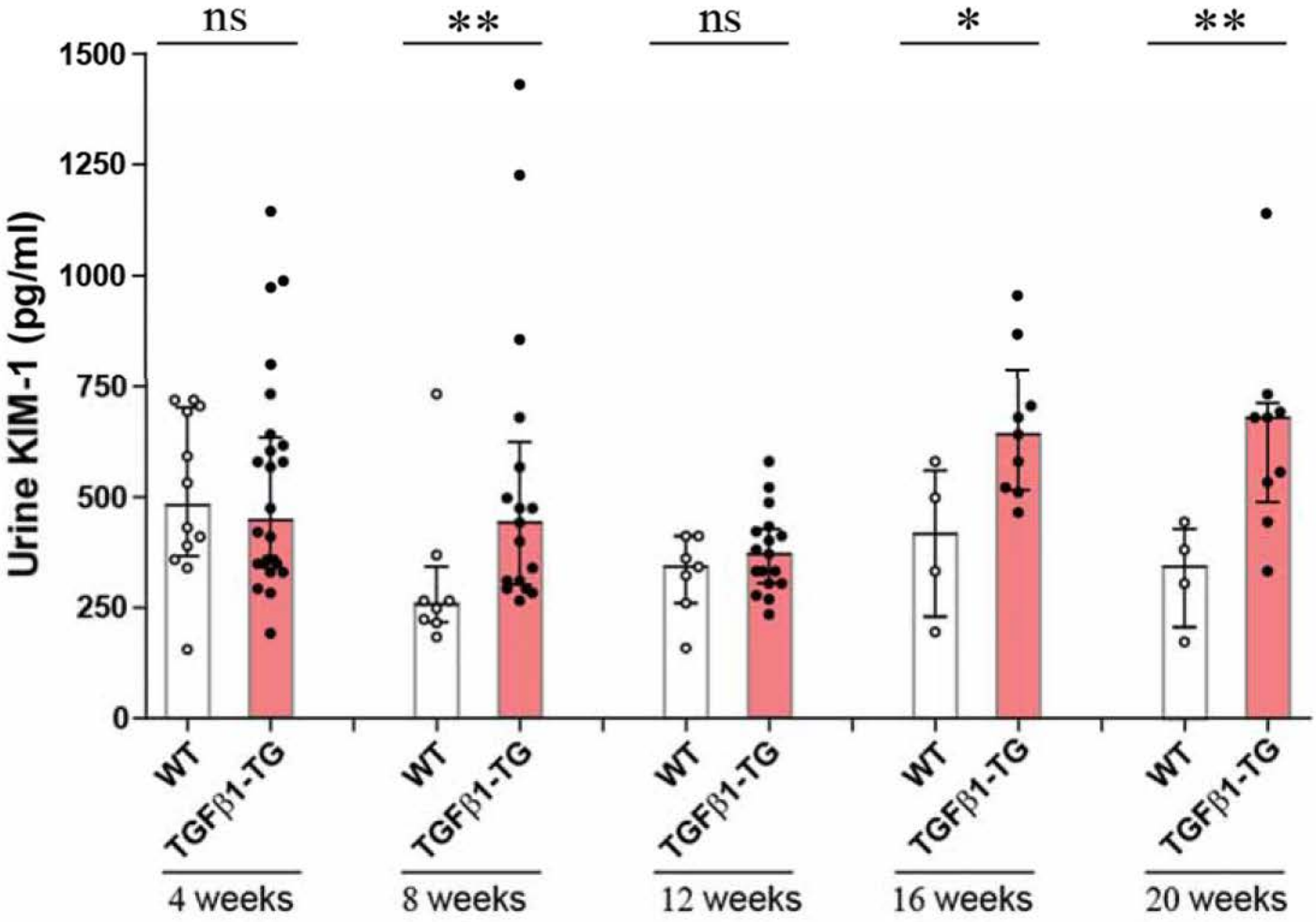
ns
**
ns
*
**
Urine KIM-1 (pg/ml)
1500
1250
1000
750
500
250
0
WT
TGFβ1-TG
4 weeks
8 weeks
12 weeks
16 weeks
20 weeks

Supplementary Figure S5. The human TGFβ1 transgenic mouse has increased markers of kidney injury. The concentration of liver-type fatty acid binding protein (L-FABP) and kidney injury molecule-1 (KIM-1) was measured by enzyme immune assay. Number of mice for measuring L-FABP: for WT mice n=12 in 4-weeks, n=4 in 8-weeks and 12-weeks, 16-weeks and 20-weeks mice; for TG mice n=24 in 4-weeks, n=17 in 8-weeks and 12-weeks, and n=9 in 16-weeks and 20-weeks mice. Number of mice for measuring KIM-1: for WT mice n=12 in 4-weeks, n=8 in 8-weeks, n=7 in 12-weeks, and n=4 in16-weeks and 20-weeks mice; for TG mice n=24 in 4-weeks, n=17 in 8-weeks and 12-weeks, and n=9 in 16-weeks and 20-weeks miceData are expressed as the median ± interquartile range. Statistical analysis by Mann-Whitney U test. WT, wild type mice, TGFβ1-TG, transforming growth factor-β1 transgenic mice; ns, not significant. *p<0.05, **p<0.01, ***p<0.001, ****p<0.0001.

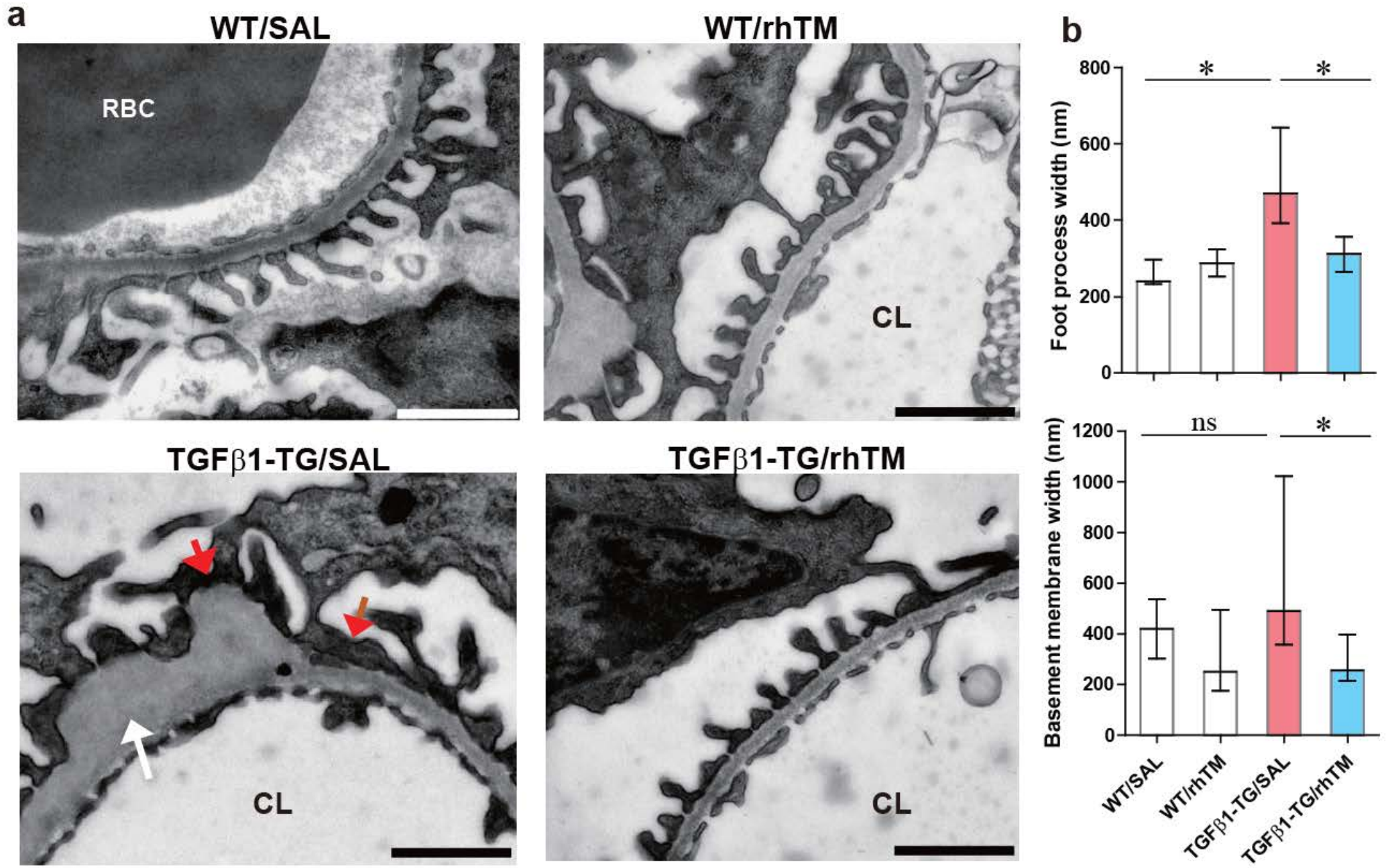
a
WT/SAL
RBC
WT/rhTM
CL
TGFβ1-TG/SAL
CL
TGFβ1-TG/rhTM
CL
b
Foot process width (nm)
800
600
400
200
0
*
*
Basement membrane width (nm)
1200
1000
800
600
400
200
0
ns
*
WT/SAL
WT/rhTM
TGFβ1-TG/SAL
TGFβ1-TG/rhTM

Supplementary Figure S6. Therapy with recombinant human thrombomodulin (rhTM) reduces foot process effacement of podocytes and thickening of glomerular basement membrane. Fixation, handling and removal of the kidneys from mice were performed as described under material and methods. (a) Red arrows indicate foot process effacement of podocytes, and white arrow thickening of glomerular basement membrane. (b) Foot process width and basement membrane width were quantified using WinROOF software. Scale bars indicate 1 µm. Data are expressed as the median ± interquartile range. Statistical analysis by Mann-Whitney U test. CL, capillary lumen; RBC, red blood cell, WT, wild type; TGFβ1-TG, transforming growth factor-β1 transgenic mouse. *$p<0.05$.

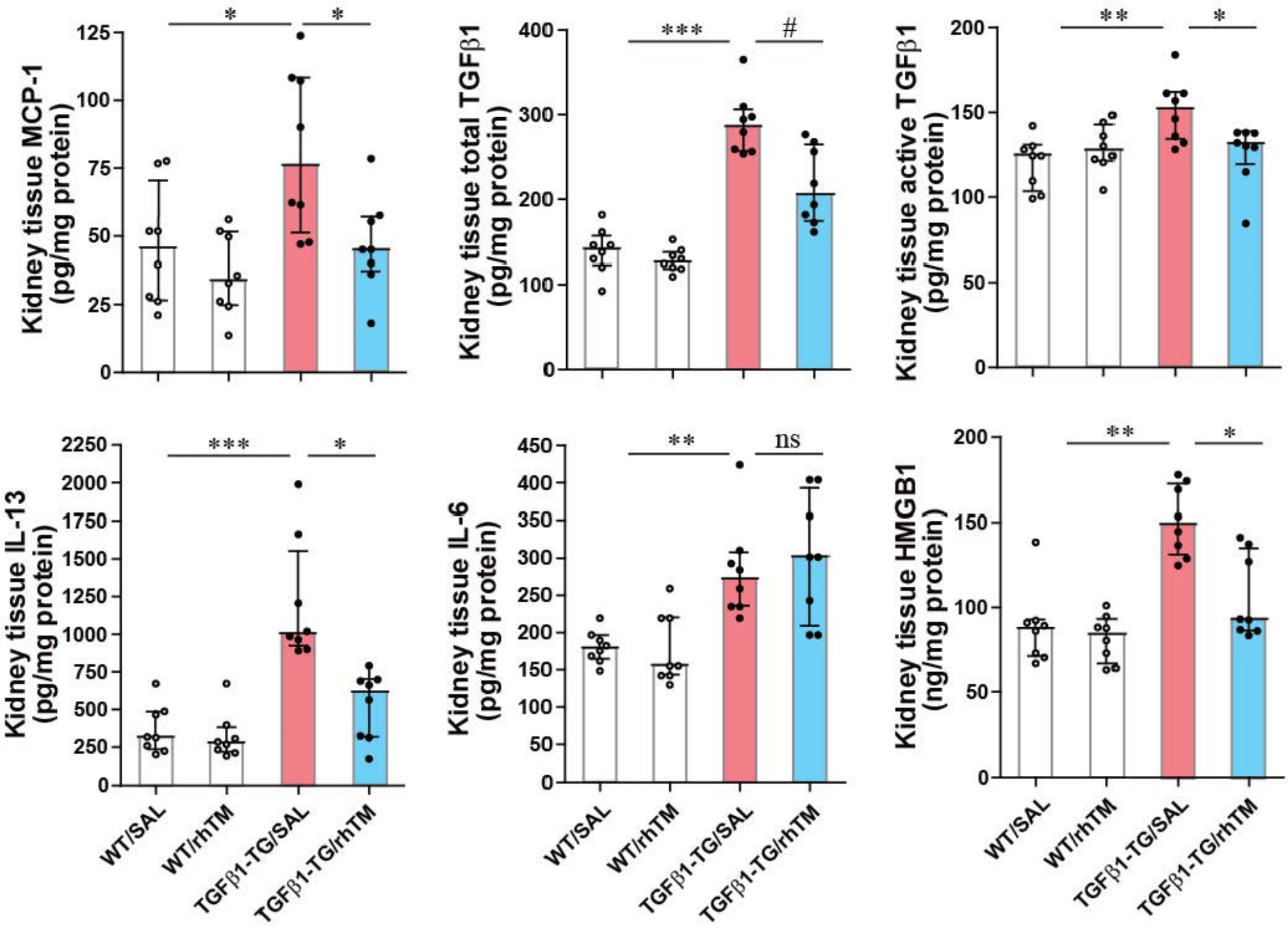
Kidney tissue MCP-1 (pg/mg protein)
125
100
75
50
25
0
*
*
Kidney tissue total TGFβ1 (pg/mg protein)
400
300
200
100
0
***
#
Kidney tissue active TGFβ1 (pg/mg protein)
200
150
100
50
0
**
*
Kidney tissue IL-13 (pg/mg protein)
2250
2000
1750
1500
1250
1000
750
500
250
0
***
*
Kidney tissue IL-6 (pg/mg protein)
450
400
350
300
250
200
150
100
50
0
**
ns
Kidney tissue HMGB1 (ng/mg protein)
200
150
100
50
0
**
*
WT/SAL
WT/rhTM
TGFβ1-TG/SAL
TGFβ1-TG/rhTM

Supplementary Figure S7. TGFβ1 transgenic mice treated with recombinant human thrombomodulin (rhTM) have low concentration of pro-fibrotic factors and HMGB1 in renal tissue. Monocyte chemoattractant protein-1 (MCP-1), interleukin-13 (IL-13), transforming growth factor-β1 (TGFβ1), IL-6 and high mobility group box-1 protein (HMGB1) were measured by enzyme immunoassays. N=8 in each group. Data are expressed as the median ± interquartile range. Statistical analysis by the Kruskal-Wallis analysis of variance with uncorrected Dunn's test. WT, wild type mice; TGFβ1-TG, transforming growth factor-β1 transgenic mice; ns, not significant; SAL, saline. HMGB1, high mobility group box 1 protein. *p<0.05, #p<0.1

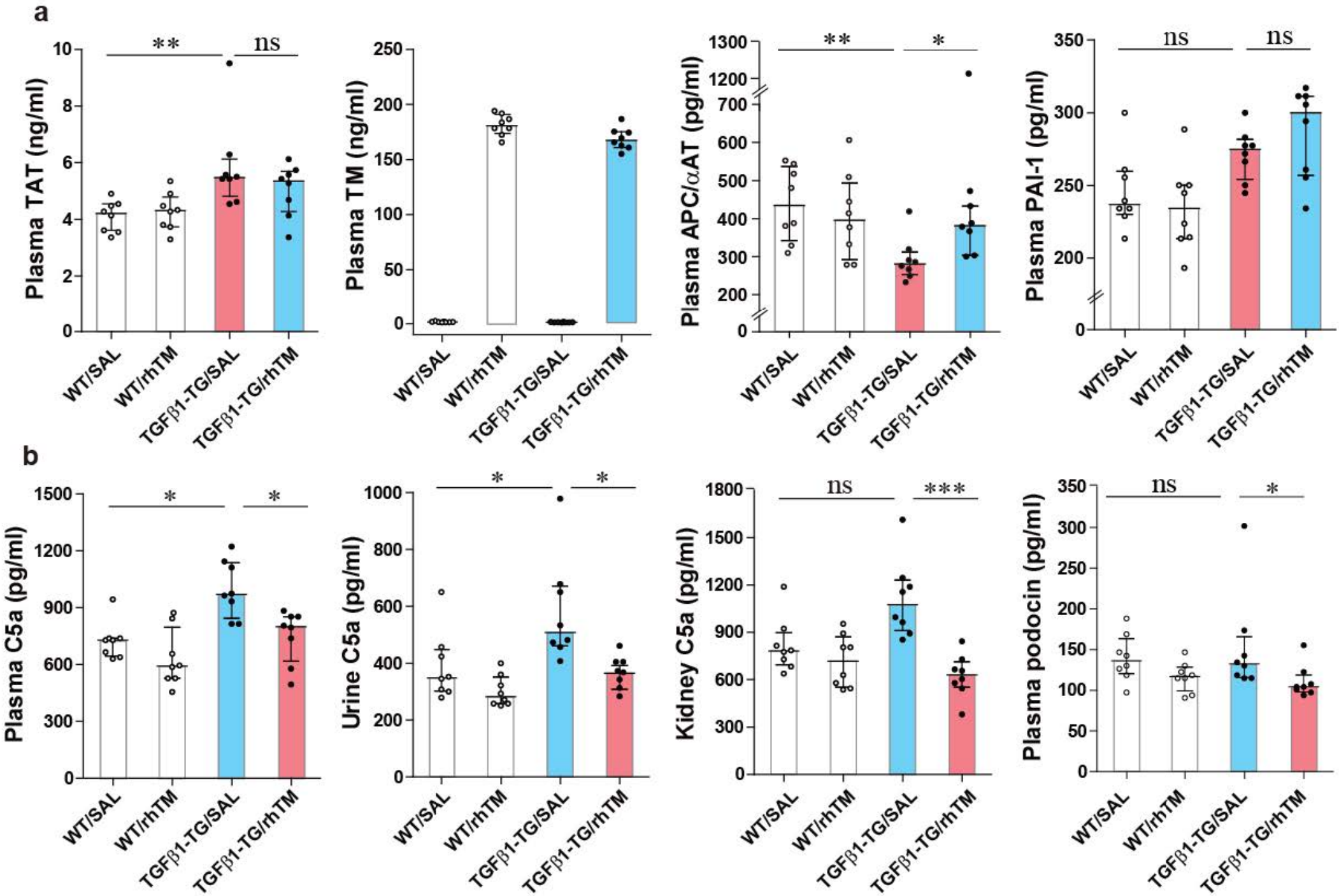
a
Plasma TAT (ng/ml)
**
ns
Plasma TM (ng/ml)
Plasma APC/αAT (pg/ml)
**
*
Plasma PAI-1 (pg/ml)
ns
ns
b
Plasma C5a (pg/ml)
*
*
Urine C5a (pg/ml)
*
*
Kidney C5a (pg/ml)
ns
***
Plasma podocin (pg/ml)
ns
*
WT/SAL
WT/rhTM
TGFβ1-TG/SAL
TGFβ1-TG/rhTM

Supplementary Figure S8. Therapy with recombinant human thrombomodulin (rhTM) increases generation of activated protein C, inhibits the complement system, decreased circulating soluble podocin, although exerts no effect on the coagulation system in TGFβ1 transgenic mouse. The levels of thrombin antithrombin (TAT), thrombomodulin, APC/αAT complex, C5a and podocin were evaluated by enzyme immunoassays. N=8 in each group. Data are expressed as the median ± interquartile range. Statistical analysis by the Kruskal-Wallis analysis of variance with corrected Dunn's test. WT, wild type mice; TGFβ1-TG, transforming growth factor-β1 transgenic mice; SAL, saline; ns, not significant; APC/αAT, activated protein C/αantitrypsin complex. *p<0.05.

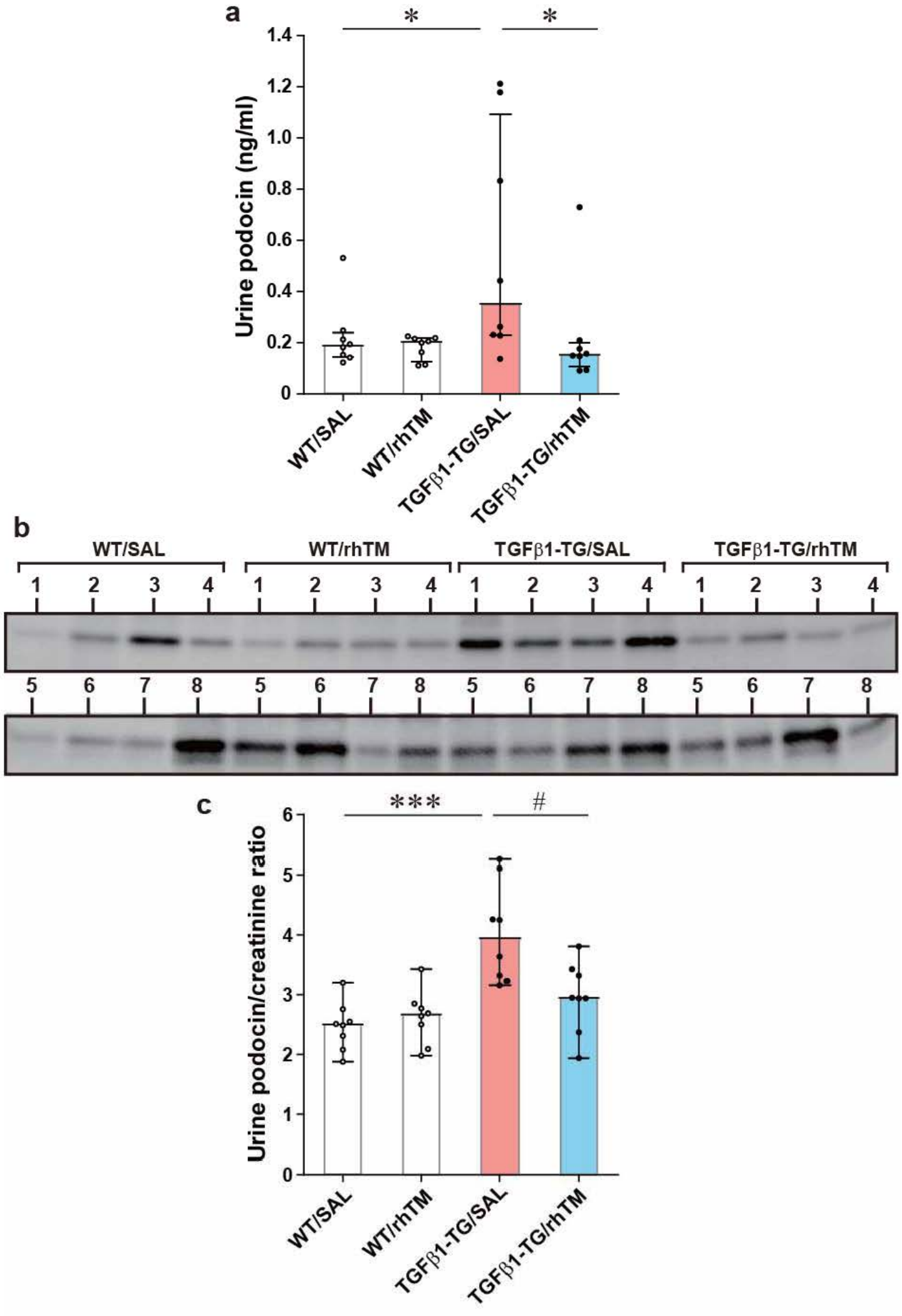
a
*
*
Urine podocin (ng/ml)
1.4
1.2
1.0
0.8
0.6
0.4
0.2
0
WT/SAL
WT/rhTM
TGFβ1-TG/SAL
TGFβ1-TG/rhTM
b
WT/SAL
WT/rhTM
TGFβ1-TG/SAL
TGFβ1-TG/rhTM
1 2 3 4 1 2 3 4 1 2 3 4 1 2 3 4
5 6 7 8 5 6 7 8 5 6 7 8 5 6 7 8
c
***
#
Urine podocin/creatinine ratio
6
5
4
3
2
1
0
WT/SAL
WT/rhTM
TGFβ1-TG/SAL
TGFβ1-TG/rhTM

Supplementary Figure S9. Therapy with recombinant human thrombomodulin (rhTM) reduces the urine concentration of podocin. Mice were treated by intraperitoneal administration of rhTM or saline before sacrifice. (a) Podocin was measured by enzyme immunoassay in urine in all mice of each group (n=8 in each group) as described under materials and methods. Data are expressed as the median ± interquartile range. Statistical analysis by the Kruskal-Wallis analysis of variance with corrected Dunn's test. (b,c) Western blotting of podocin was performed in n=8 of each group. Data are expressed as the median ± interquartile range. Statistical analysis by the Kruskal-Wallis analysis of variance with uncorrected Dunn's test. WT, wild type mice; TGFβ1-TG, transforming growth factor-β1 transgenic mice; ns, not significant; SAL, saline. *$p<0.05$, #$p<0.07$

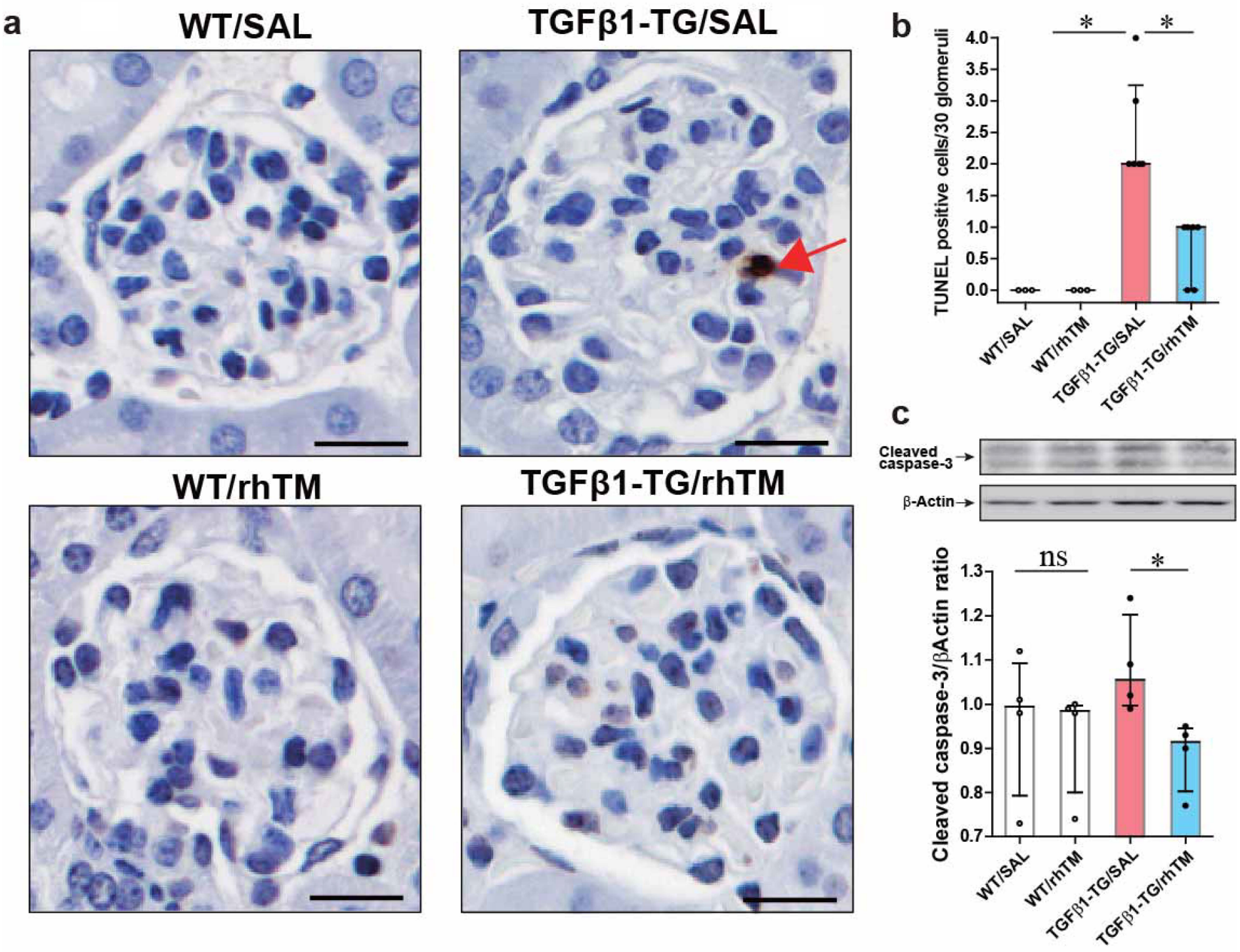
a
WT/SAL
TGFβ1-TG/SAL
WT/rhTM
TGFβ1-TG/rhTM
b
TUNEL positive cells/30 glomeruli
4.0
3.5
3.0
2.5
2.0
1.5
1.0
0.5
0.0
*
*
WT/SAL
WT/rhTM
TGFβ1-TG/SAL
TGFβ1-TG/rhTM
c
Cleaved caspase-3
β-Actin
Cleaved caspase-3/βActin ratio
1.3
1.2
1.1
1.0
0.9
0.8
0.7
ns
*
WT/SAL
WT/rhTM
TGFβ1-TG/SAL
TGFβ1-TG/rhTM

Supplementary Figure S10. Therapy with recombinant human thrombomodulin (rhTM) reduces apoptosis of glomerular cells. Mice were treated by intraperitoneal administration of rhTM or saline before sacrifice. WT/SAL (n=3) and TGFβ1-TG/SAL (n=6) groups received intraperitoneal saline; WT/rhTM (n=3) and TGFβ1-TG/rhTM (n=6) mice treated with intraperitoneal rhTM. Apoptosis in kidney specimens was evaluated by TUNEL method (a) and quantified by densitometry analysis (b). The cleaved form of caspase-3 was evaluated by Western blotting (c). Bar scale indicates 20 μm. Data are expressed as the median ± interquartile range. Statistical analysis by the Kruskal-Wallis analysis of variance with corrected Dunn's test. WT, wild type mice; TGFβ1-TG, transforming growth factor-β1 transgenic mice; ns, not significant; SAL, saline. *$p<0.05$.

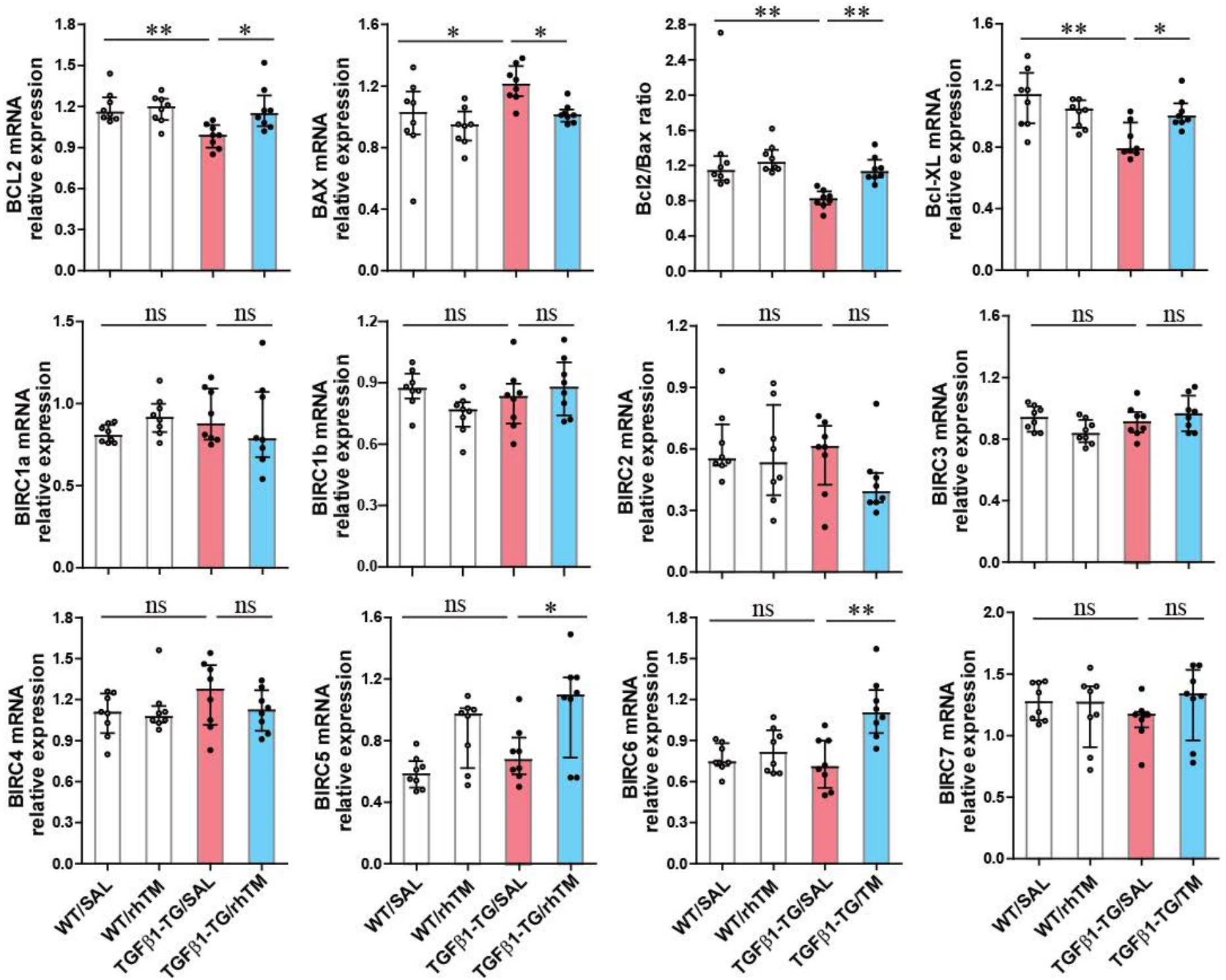
BCL2 mRNA relative expression
BAX mRNA relative expression
Bcl2/Bax ratio
Bcl-XL mRNA relative expression
BIRC1a mRNA relative expression
BIRC1b mRNA relative expression
BIRC2 mRNA relative expression
BIRC3 mRNA relative expression
BIRC4 mRNA relative expression
BIRC5 mRNA relative expression
BIRC6 mRNA relative expression
BIRC7 mRNA relative expression
ns
*
**
WT/SAL
WT/rhTM
TGFβ1-TG/SAL
TGFβ1-TG/rhTM
TGFβ1-TG/TM

Supplementary Figure S11. Treatment of TGFβ1-overexpression associated kidney fibrosis with recombinant human thrombomodulin (rhTM) inhibits apoptosis in renal tissue. The expression of pro-apoptotic and anti-apoptotic proteins were measured by RT-PCR. The expression of glyceraldehyde-3-phosphate dehydrogenase (GAPDH) was used for normalizing gene expression. N=8 in each group. Data are expressed as the median ± interquartile range. Statistical analysis by Kruskal-Wallis analysis of variance with uncorrected Dunn's test. WT, wild type mice; TGFβ1-TG, transforming growth factor-β1 transgenic mice; SAL, saline. BIRC1a,1b, 2, 3, 4, 5, 6, or 7: baculoviral inhibition of apoptosis repeat-containing 1a, 1b, 2, 3, 4, 5, 6, or 7; Bcl, B-cell leukemia/lymphoma protein; ns, not significant. *p<0.05, **p<0.01.

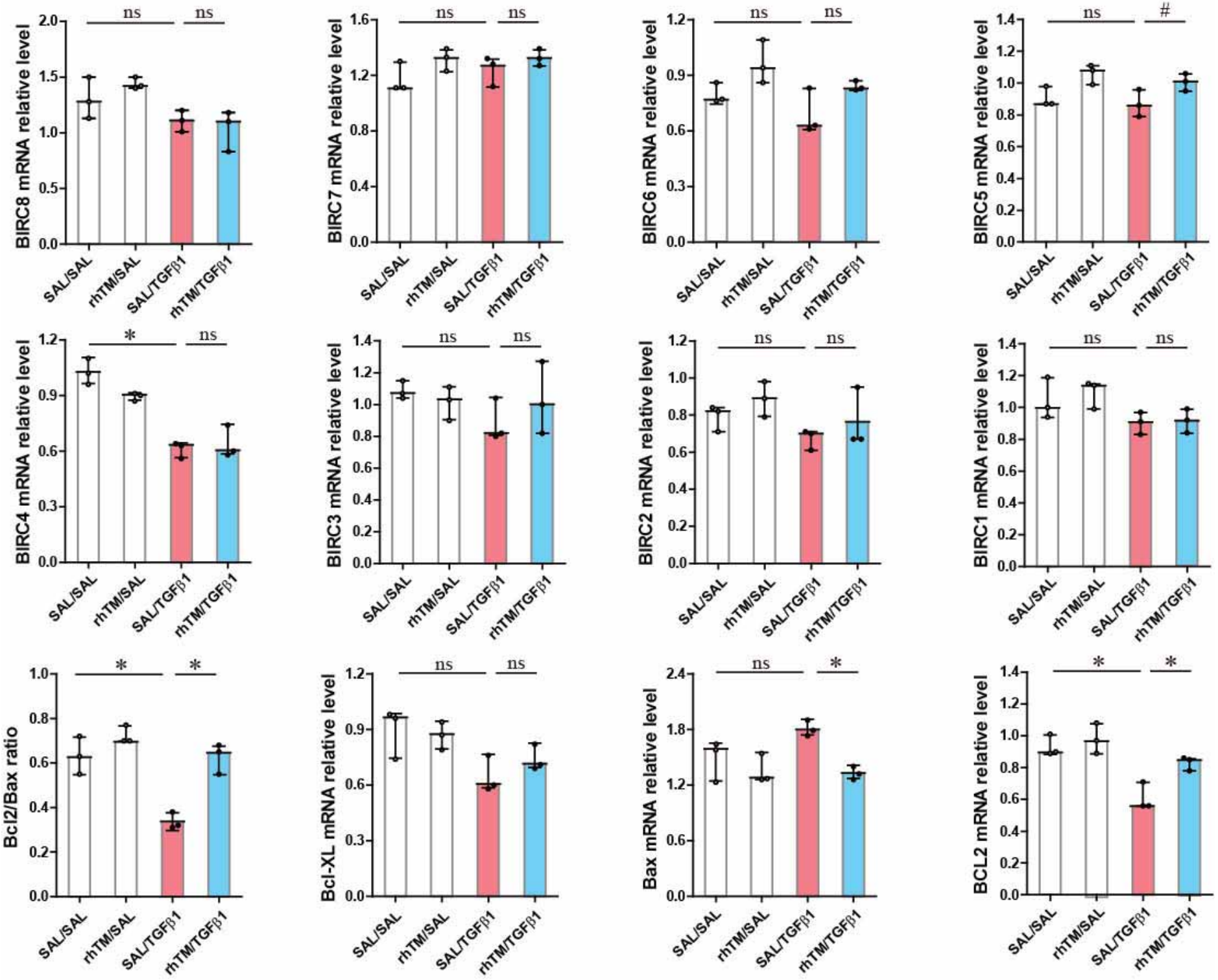
BIRC8 mRNA relative level
BIRC7 mRNA relative level
BIRC6 mRNA relative level
BIRC5 mRNA relative level
BIRC4 mRNA relative level
BIRC3 mRNA relative level
BIRC2 mRNA relative level
BIRC1 mRNA relative level
Bcl2/Bax ratio
Bcl-XL mRNA relative level
Bax mRNA relative level
BCL2 mRNA relative level
ns
*
#
SAL/SAL
rhTM/SAL
SAL/TGFβ1
rhTM/TGFβ1

Supplementary Figure S12. Recombinant human thrombomodulin (rhTM) increases the expression of anti-apoptotic factors in podocytes. Recombinant human thrombomodulin (200 nM) was added to the culture medium of podocytes before inducing apoptosis with TGFβ1 (10 ng/ml) for 48h.The expression of pro-apoptotic and anti-apoptotic proteins were measured by RT-PCR. The expression of glyceraldehyde-3-phosphate dehydrogenase (GAPDH) was used for normalizing gene expression. N=3 in each group. Data are expressed as the median ± interquartile range. Statistical analysis by Mann-Whitney U test. TGFβ1, transforming growth factor-β1; Sal, saline. BIRC1a,1b, 2, 3, 4, 5, 6, or 7: baculoviral inhibition of apoptosis repeat-containing 1a, 1b, 2, 3, 4, 5, 6, or 7; Bcl, B-cell leukemia/lymphoma protein; ns, not significant. *$p<0.05$, $^{\#}p=0.1$.

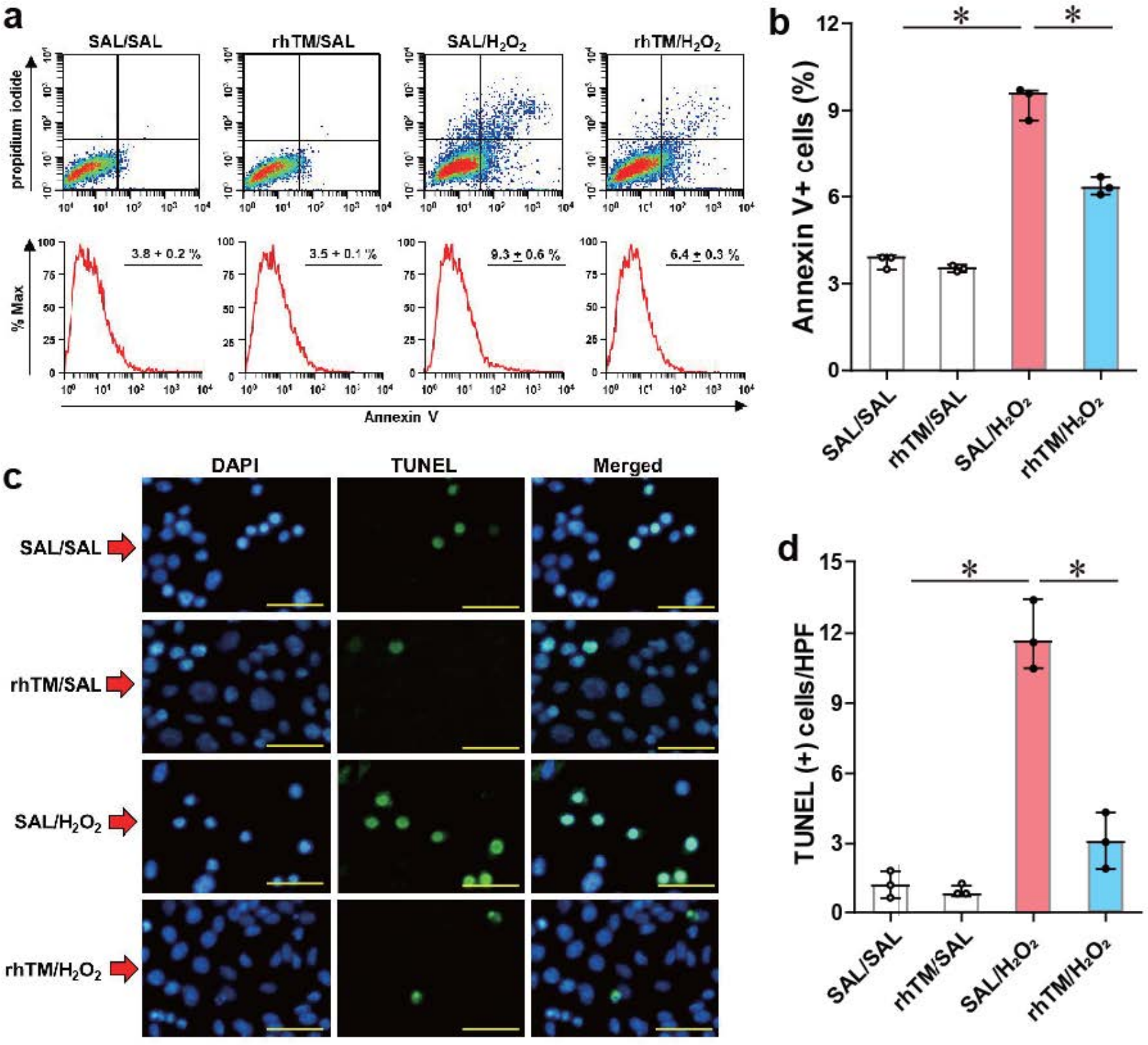
a
SAL/SAL
rhTM/SAL
SAL/H2O2
rhTM/H2O2
propidium iodide
% Max
3.8 ± 0.2 %
3.5 ± 0.1 %
9.3 ± 0.6 %
6.4 ± 0.3 %
Annexin V
b
Annexin V+ cells (%)
SAL/SAL
rhTM/SAL
SAL/H2O2
rhTM/H2O2
c
DAPI
TUNEL
Merged
SAL/SAL
rhTM/SAL
SAL/H2O2
rhTM/H2O2
d
TUNEL (+) cells/HPF
SAL/SAL
rhTM/SAL
SAL/H2O2
rhTM/H2O2

Supplementary Figure S13. Recombinant human thrombomodulin (rhTM) suppresses apoptosis of podocytes induced by hydrogen peroxide. Recombinant human thrombomodulin was added to the culture medium of podocytes 1h before inducing apoptosis with 1mM hydrogen peroxide for 24h. (a, b) The percentage of annexin V (+) cells was evaluated by flow cytometry. (c, d) The number of cells with DNA fragmentation was measured by TUNEL analysis and quantified. Scale bars indicate 100 μm. N=3 in each group. Data are expressed as the median ± interquartile range. Statistical analysis by Mann-Whitney U test. TGFβ1, transforming growth factor-β1; SAL, saline. *p<0.05.

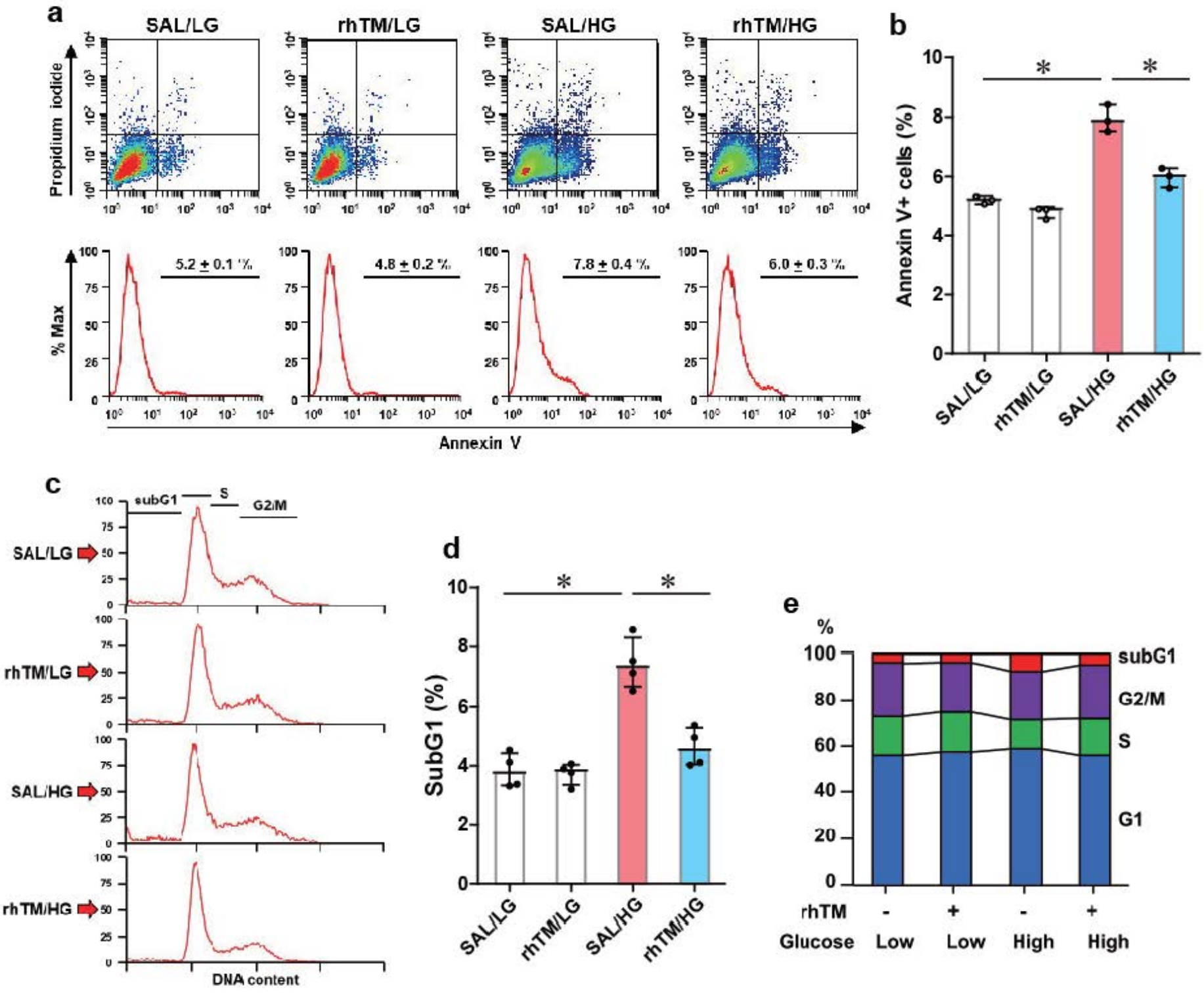
a
SAL/LG
rhTM/LG
SAL/HG
rhTM/HG
Propidium iodide
% Max
5.2 ± 0.1 %
4.8 ± 0.2 %
7.8 ± 0.4 %
6.0 ± 0.3 %
Annexin V
b
Annexin V+ cells (%)
SAL/LG
rhTM/LG
SAL/HG
rhTM/HG
c
subG1
S
G2/M
SAL/LG
rhTM/LG
SAL/HG
rhTM/HG
DNA content
d
SubG1 (%)
SAL/LG
rhTM/LG
SAL/HG
rhTM/HG
e
%
subG1
G2/M
S
G1
rhTM
Glucose
Low
High

Supplementary Figure S14. Recombinant human thrombomodulin (rhTM) suppresses apoptosis of podocytes induced by high glucose level. Recombinant human thrombomodulin (200 nM) was added to the culture medium of podocytes before inducing apoptosis with high concentration (30 mM) of glucose for 24h. The percentage of annexin V (+) cells (a, b; n=3 in each group), and the percentage of cells in subG1 phase (c, d, e; n=4 in each group) were evaluated by flow cytometry. Data are expressed as the median ± interquartile range. Statistical analysis by Mann-Whitney U test. HG, high glucose; LG, low glucose. *p<0.05.

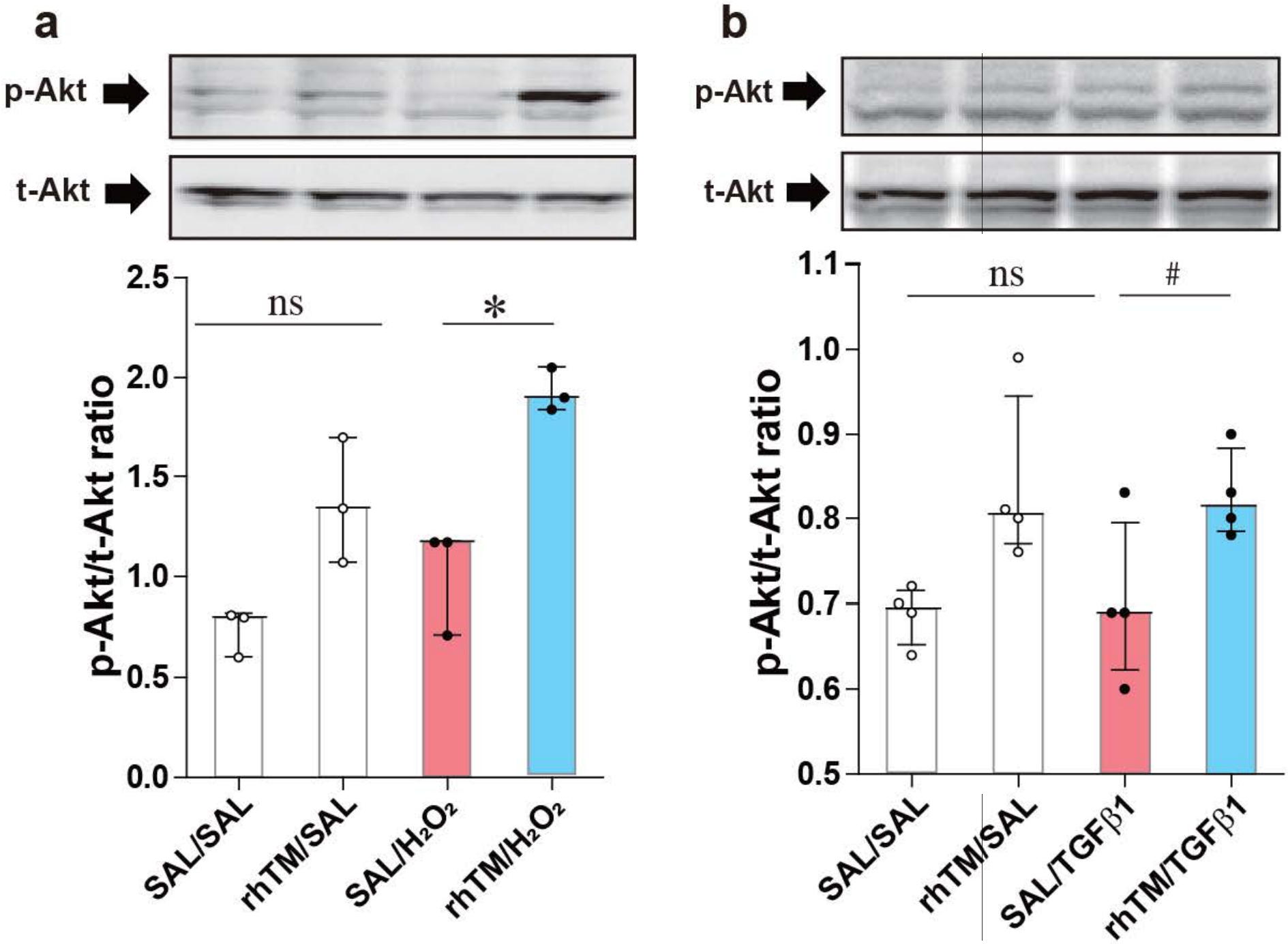
a
p-Akt
t-Akt
p-Akt/t-Akt ratio
2.5
2.0
1.5
1.0
0.5
0.0
ns
*
SAL/SAL
rhTM/SAL
SAL/H2O2
rhTM/H2O2
b
p-Akt
t-Akt
p-Akt/t-Akt ratio
1.1
1.0
0.9
0.8
0.7
0.6
0.5
ns
#
SAL/SAL
rhTM/SAL
SAL/TGFβ1
rhTM/TGFβ1

Supplementary Figure S15. Recombinant human thrombomodulin (rhTM) increases the activation of the Akt pathways in podocytes. Recombinant human thrombomodulin (200 nM) was added to the culture medium of podocytes before inducing apoptosis with 1mM hydrogen peroxide for 24h (a; n=3 in each group) or 10 ng/ml TGFβ1 for 48h (b; n=4 in each group).Total (t-Akt) and phosphorylated (p-Akt) Akt were evaluated by Western blotting. N=4 in each group. Data are expressed as the median ± interquartile range. Statistical analysis by the Kruskal-Wallis analysis of variance with uncorrected Dunn's test. ns, not significant; TGFβ1, transforming growth factor-β1. *$p<0.05$, $^{\#}p=0.057$.

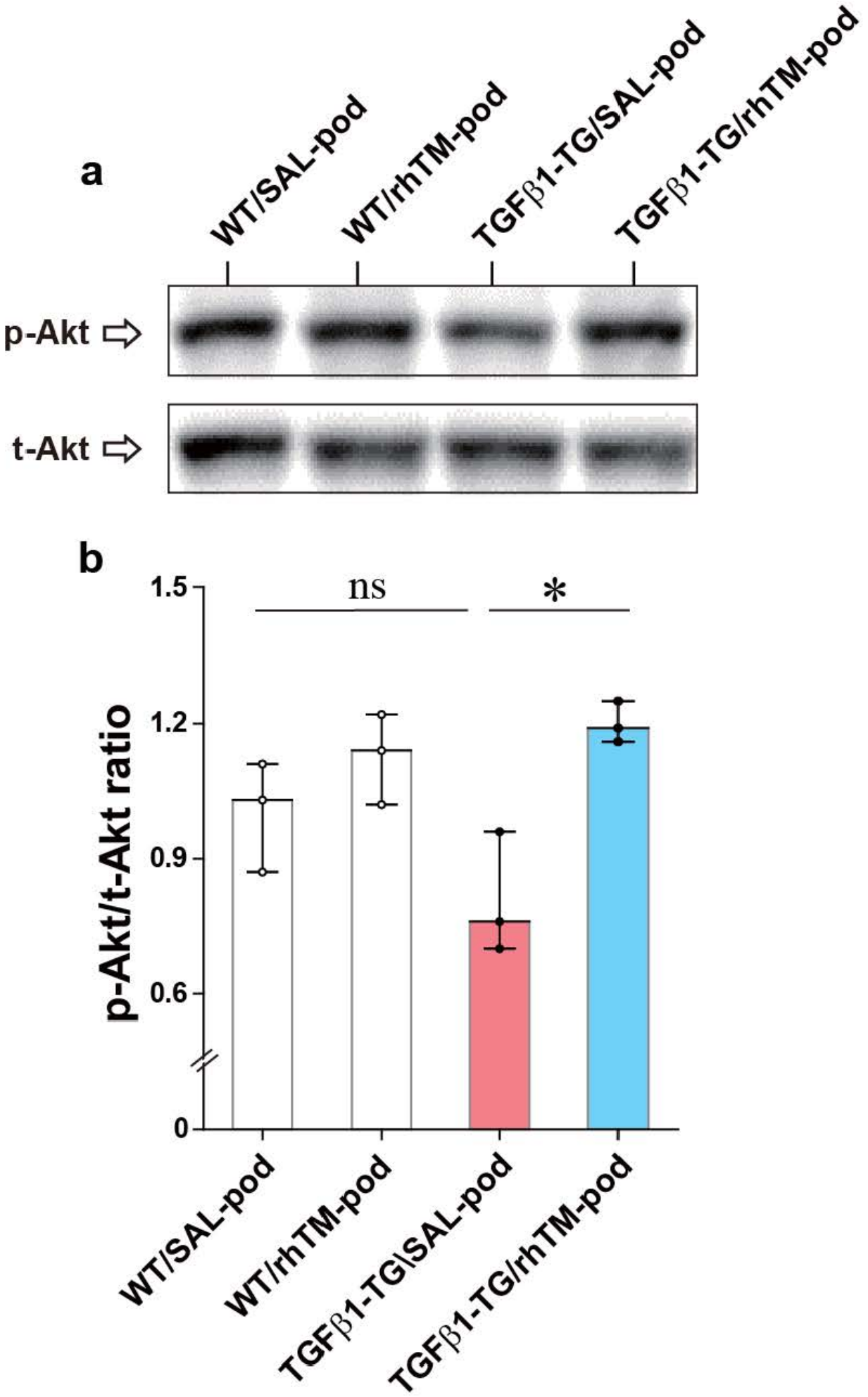
a
WT/SAL-pod
WT/rhTM-pod
TGFβ1-TG/SAL-pod
TGFβ1-TG/rhTM-pod
p-Akt
t-Akt
b
ns
*
p-Akt/t-Akt ratio
1.5
1.2
0.9
0.6
0
WT/SAL-pod
WT/rhTM-pod
TGFβ1-TG\SAL-pod
TGFβ1-TG/rhTM-pod

Supplementary Figure S16. Therapy with recombinant human thrombomodulin (rhTM) increases Akt phosphorylation in podocytes from TGFβ1-TG mice. Podocytes were isolated from one mouse of each treatment group of mice as described under materials and methods. Podocytes of each group was separated and total (t-Akt) and phosphorylated (p-Akt) Akt was evaluated by Western blotting. Statistical analysis by the Kruskal-Wallis analysis of variance with corrected Dunn's test. WT, wild type mice; TGFβ1-TG, transforming growth factor-β1 transgenic mice; ns, not significant; pod, podocytes. *$p<0.05$.

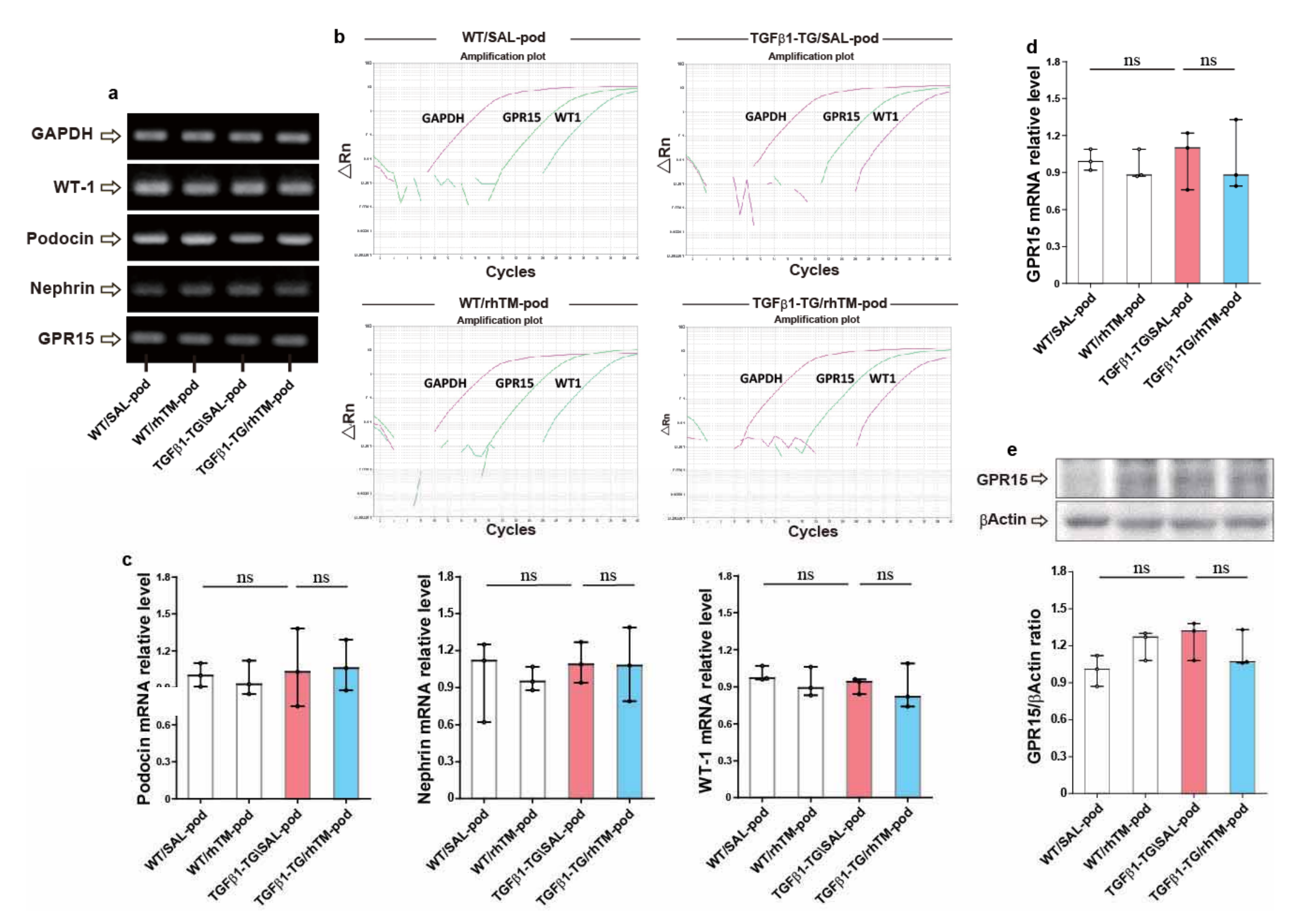
a
GAPDH
WT-1
Podocin
Nephrin
GPR15
WT/SAL-pod
WT/rhTM-pod
TGFβ1-TG\SAL-pod
TGFβ1-TG/rhTM-pod
b
WT/SAL-pod
Amplification plot
TGFβ1-TG/SAL-pod
Amplification plot
WT/rhTM-pod
Amplification plot
TGFβ1-TG/rhTM-pod
Amplification plot
GAPDH
GPR15
WT1
△Rn
Cycles
c
Podocin mRNA relative level
Nephrin mRNA relative level
WT-1 mRNA relative level
ns
d
GPR15 mRNA relative level
e
GPR15
βActin
GPR15/βActin ratio

Supplementary Figure S17. Podocytes from each treatment group of mice express GPR15 mRNA. Podocytes were isolated from mice of each treatment group (n=3) as described under materials and methods. Podocytes of each group was separated and the mRNA expression of markers of podocytes and GPR15 were evaluated by RT-PCR and Western blotting as described under materials and methods. Statistical analysis by the Kruskal-Wallis analysis of variance with corrected Dunn's test. WT, wild type mice; TGFβ1-TG, transforming growth factor-β1 transgenic mice; pod, podocytes; ns, not significant.

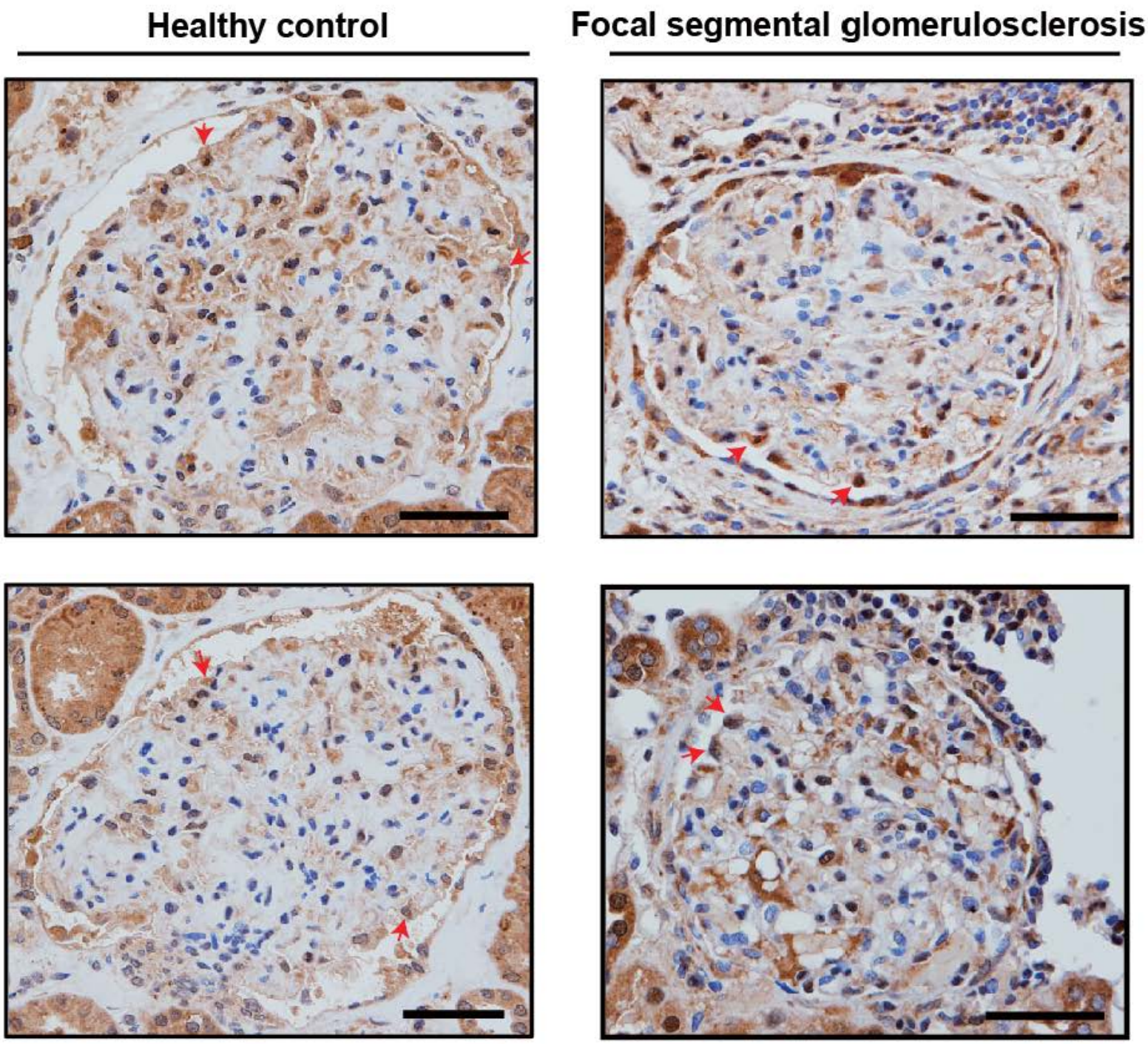
Healthy control
Focal segmental glomerulosclerosis

Supplementary Figure S18. Staining of GPR15 in podocytes from a healthy individual and a patient with focal segmental glomerulosclerosis. Staining of GPR15 was performed in human kidney tissues from a healthy control and from a patient with a focal segmental glomerulosclerosis using a rabbit polyclonal anti-GPR15 antibody and horseradish peroxidase labelled mouse anti-rabbit polyclonal antibody as described under materials and methods. Red arrows indicate podocytes stained positive for GPR15. Scale bars indicate 50 μm.

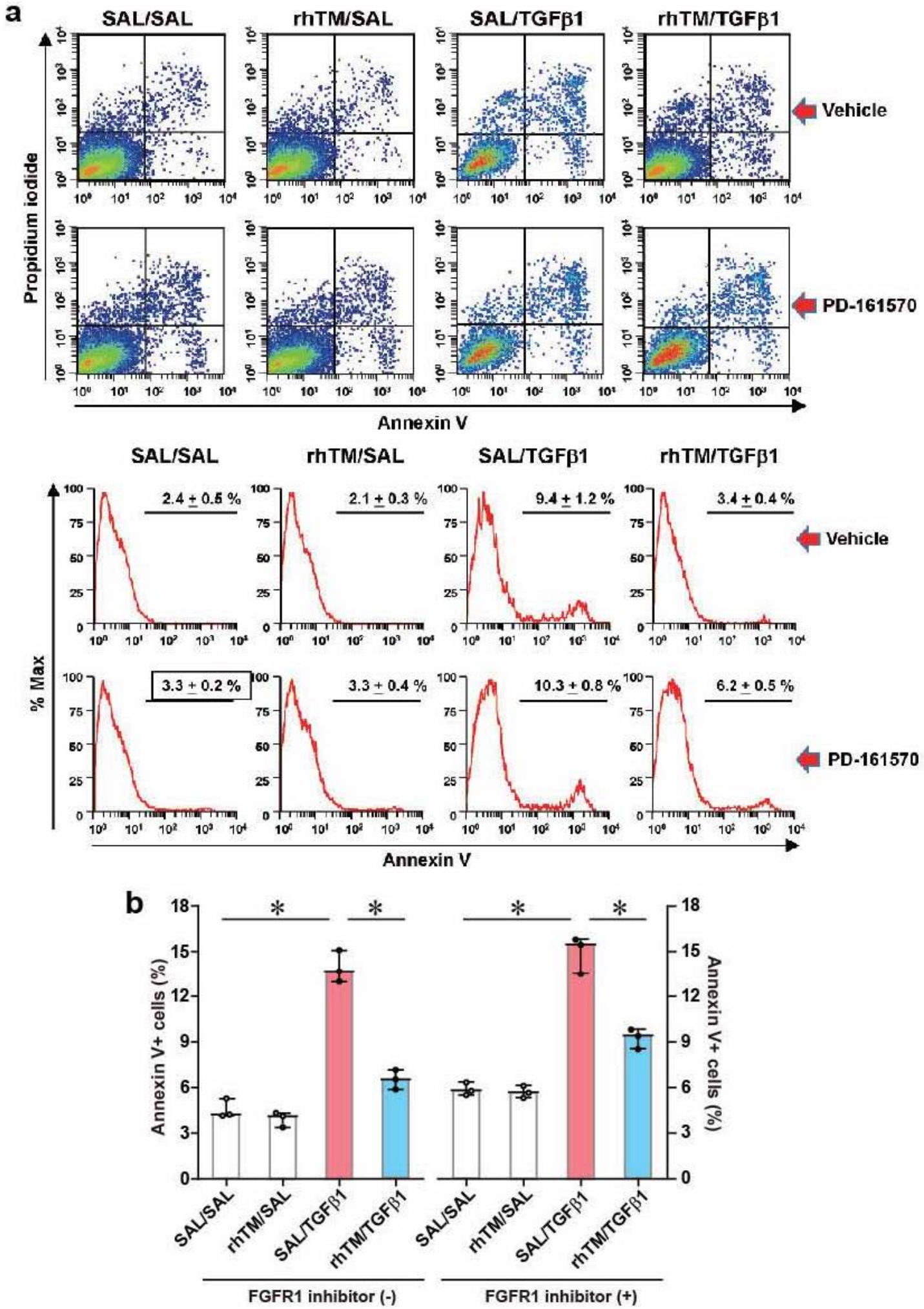
a
SAL/SAL
rhTM/SAL
SAL/TGFβ1
rhTM/TGFβ1
Vehicle
PD-161570
Propidium iodide
Annexin V
% Max
2.4 ± 0.5 %
2.1 ± 0.3 %
9.4 ± 1.2 %
3.4 ± 0.4 %
3.3 ± 0.2 %
3.3 ± 0.4 %
10.3 ± 0.8 %
6.2 ± 0.5 %
b
Annexin V+ cells (%)
FGFR1 inhibitor (-)
FGFR1 inhibitor (+)

Supplementary Figure S19. Fibroblast growth factor receptor-1 is not involved in the inhibitory activity of recombinant human thrombomodulin (rhTM) in podocytes. Human primary podocyte cells were treated with 200 nM rhTM and with 1 μM PD-161570, a fibroblast growth factor receptor-1 (FGFR1) inhibitor, and apoptotic cells were assessed by flow cytometry after 48h (a) and quantified (b). N=3 in each group. Data are expressed as the median ± interquartile range. Statistical analysis by Mann-Whitney U test. *$p<0.05$.

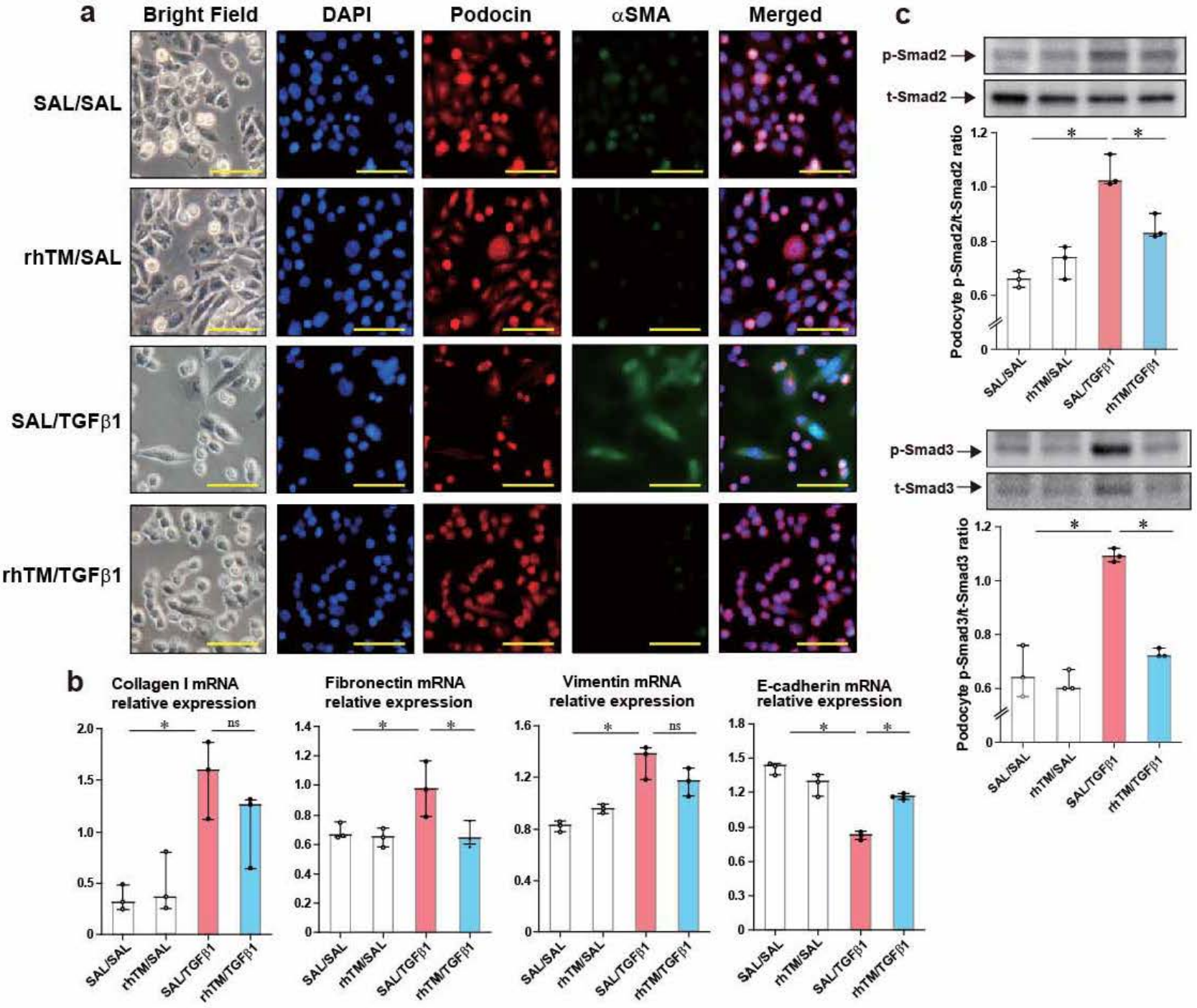
a
Bright Field
DAPI
Podocin
αSMA
Merged
SAL/SAL
rhTM/SAL
SAL/TGFβ1
rhTM/TGFβ1
b
Collagen I mRNA relative expression
Fibronectin mRNA relative expression
Vimentin mRNA relative expression
E-cadherin mRNA relative expression
SAL/SAL
rhTM/SAL
SAL/TGFβ1
rhTM/TGFβ1
c
p-Smad2
t-Smad2
Podocyte p-Smad2/t-Smad2 ratio
p-Smad3
t-Smad3
Podocyte p-Smad3/t-Smad3 ratio

Supplementary Figure S20. Recombinant human thrombomodulin (rhTM) inhibits epithelial-mesenchymal transition of podocytes. Recombinant human thrombomodulin (200 nM) was added to the culture medium of podocytes before treating with TGFβ1 and cultured for additional 48h. Epithelial-mesenchymal transition was evaluated by staining podocin and α-smooth muscle actin (αSMA) and by RT-PCR as described under material and methods. Phosphorylation of Smad proteins was evaluated by Western blotting. Data are expressed as the median ± interquartile range. Statistical analysis by Mann-Whitney U test. Scale bars indicate 100 μm. TGFβ1, transforming growth factor β1; SAL, saline; ns, not significant; DAPI, 4',6-diamidino-2-phenylindole. *p<0.05.

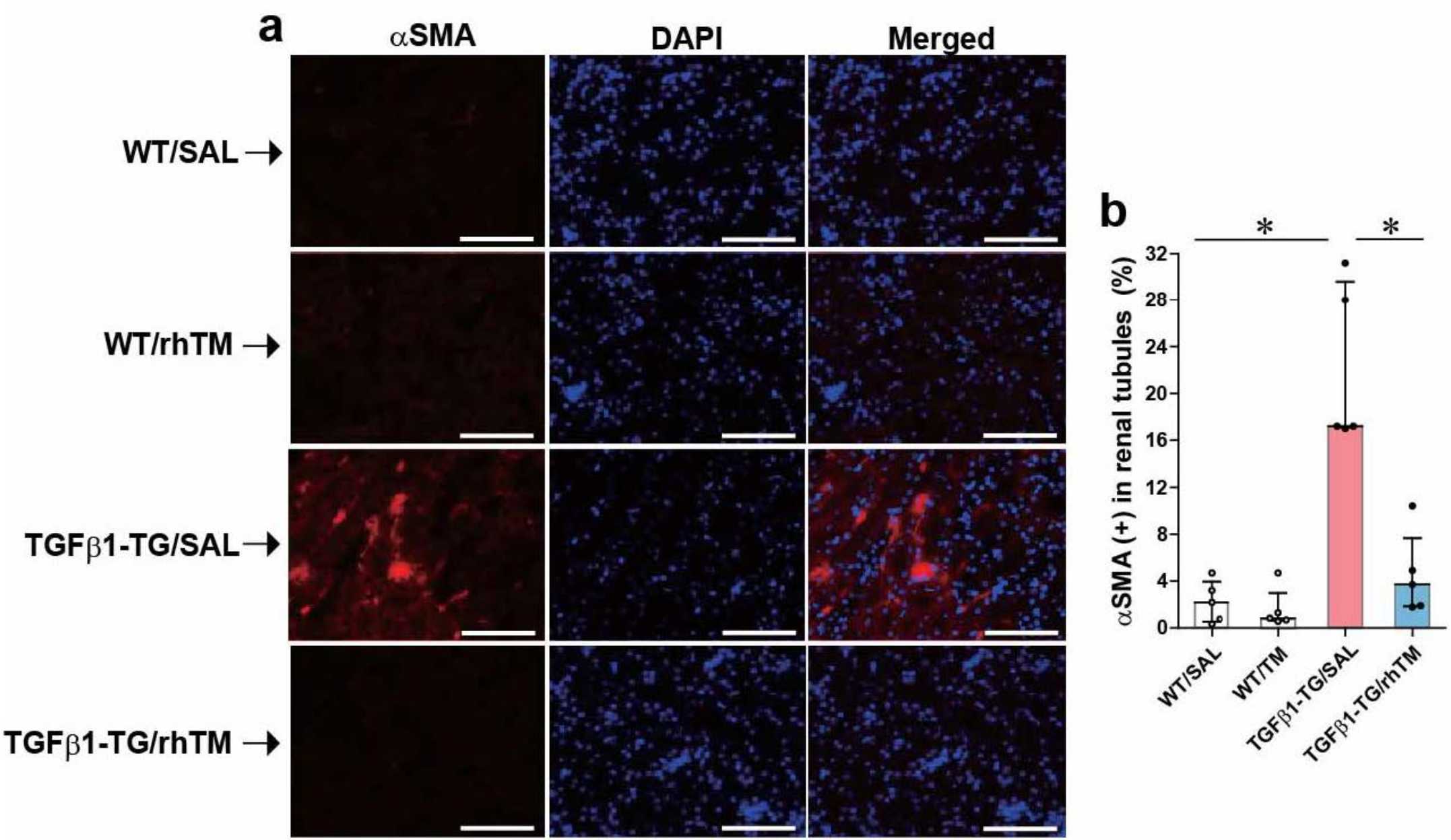
a
αSMA
DAPI
Merged
WT/SAL
WT/rhTM
TGFβ1-TG/SAL
TGFβ1-TG/rhTM
b
αSMA (+) in renal tubules (%)
32
28
24
20
16
12
8
4
0
*
*
WT/SAL
WT/TM
TGFβ1-TG/SAL
TGFβ1-TG/rhTM

Supplementary Figure S21. Therapy with recombinant human thrombomodulin (rhTM) inhibits the expression of α-smooth muscle actin in renal tubules. (a) α-smooth muscle actin were stained as described under material and methods. The area positive for αsmooth muscle actin staining was quantified by the WinROOF image processing software (b). N=5 in each group. Data are expressed as the median ± interquartile range. Statistical analysis by Mann-Whitney U test. TGFβ1, transforming growth factor-β1; SAL, saline; αSMA, α-smooth muscle actin. *p<0.05.

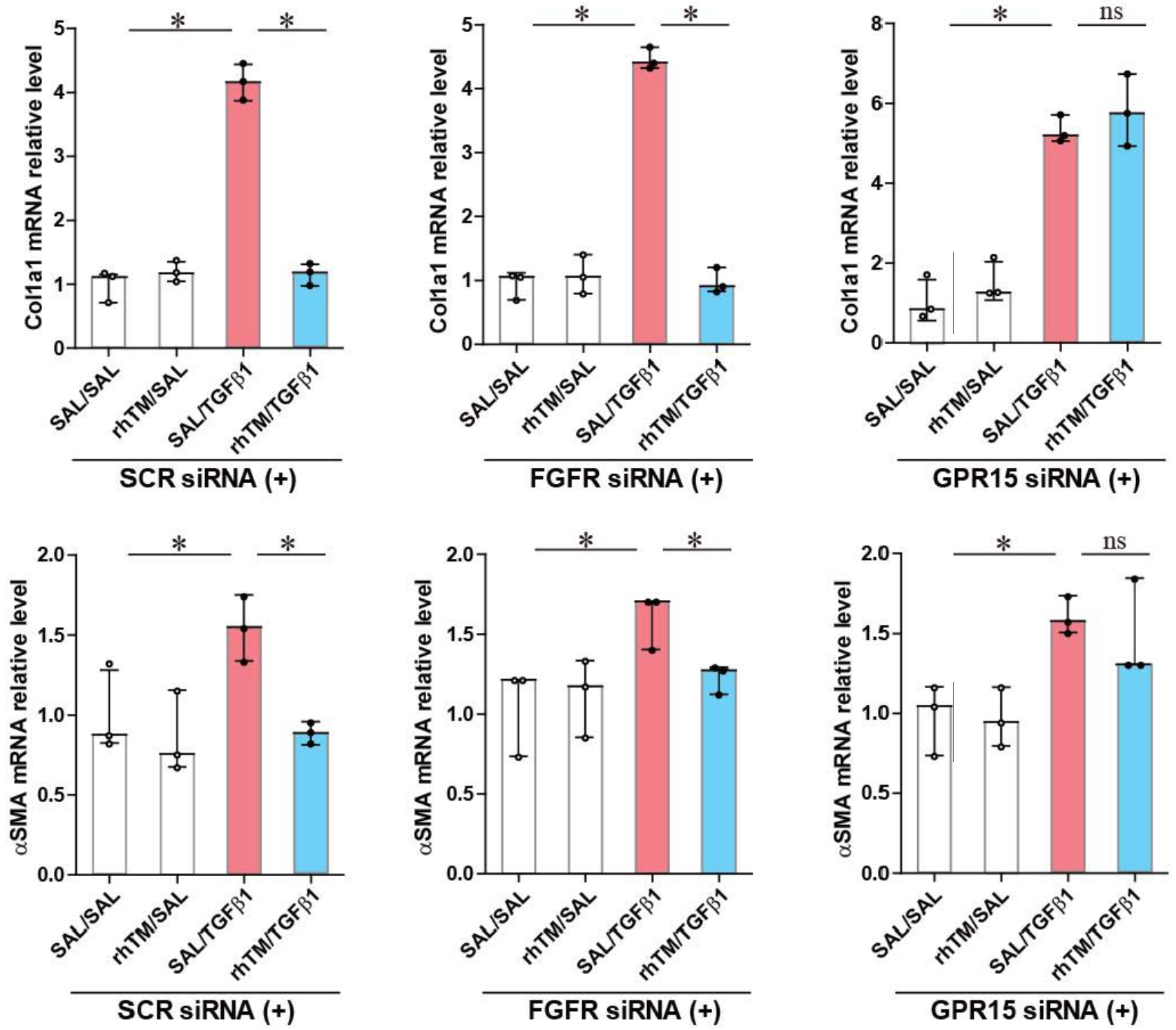
Col1a1 mRNA relative level
αSMA mRNA relative level
SAL/SAL
rhTM/SAL
SAL/TGFβ1
rhTM/TGFβ1
SCR siRNA (+)
FGFR siRNA (+)
GPR15 siRNA (+)
*
ns

Supplementary Figure S22. G-protein coupled receptor (GPR15) mediates the inhibitory activity of recombinant human thrombomodulin (rhTM) on epithelial-mesenchymal transition of podocytes. Human primary podocyte cells were transfected with fibroblast growth factor receptor 1 (FGFR1) siRNA, GPR15 siRNA or scrambled siRNA for 48h, and then rhTM was added to the cell culture 1h before treating with TGFβ1. Markers of epithelial-mesenchymal transition were evaluated by RT-PCR. N=3 in each group. Statistical analysis by Mann-Whitney U test. TGFβ1, transforming growth factor-β1; ns, not significant; SAL, saline. *$p<0.05$.

References

S1. American Diabetes A. 2. Classification and Diagnosis of Diabetes: Standards of Medical Care in Diabetes-2019. *Diabetes Care* 2019; **42:** S13-S28.

S2. Haneda M, Utsunomiya K, Koya D*, et al.* A new Classification of Diabetic Nephropathy 2014: a report from Joint Committee on Diabetic Nephropathy. *J Diabetes Investig* 2015; **6:** 242-246.

S3. Muyrers JP, Zhang Y, Benes V*, et al.* Point mutation of bacterial artificial chromosomes by ET recombination. *EMBO Rep* 2000; **1:** 239-243.

S4. Raij L, Azar S, Keane W. Mesangial immune injury, hypertension, and progressive glomerular damage in Dahl rats. *Kidney Int* 1984; **26:** 137-143.

S5. Watanabe R, Wada H, Sakakura M*, et al.* Plasma levels of activated protein C-protein C inhibitor complex in patients with hypercoagulable states. *Am J Hematol* 2000; **65:** 35-40.

S6. Fujiwara A, Taguchi O, Takagi T*, et al.* Role of thrombin-activatable fibrinolysis inhibitor in allergic bronchial asthma. *Lung* 2012; **190:** 189-198.

S7. Sai K, Wang S, Kaito A*, et al.* Multiple roles of afadin in the ultrastructural morphogenesis of mouse hippocampal mossy fiber synapses. *J Comp Neurol* 2017; **525:** 2719-2734.

S8. Wilke SA, Antonios JK, Bushong EA*, et al.* Deconstructing complexity: serial block-face electron microscopic analysis of the hippocampal mossy fiber synapse. *J Neurosci* 2013; **33:** 507-522.

S9. Zhong F, Wang W, Lee K*, et al.* Role of C/EBP-alpha in Adriamycin-induced podocyte injury. *Sci Rep* 2016; **6:** 33520.